

# **ANALYSIS OF HOLE QUALITY IN LASER DRILLING OF FRP COMPOSITE**

Thesis Submitted For the Award of the Degree of

**DOCTOR OF PHILOSOPHY**

**in**

**(MECHANICAL ENGINEERING)**

**By**

**KAUSHAL PRATAP SINGH**

**(REGISTRATION NO. 41800893)**

**Supervised By**

**Dr. ANKUR BAHL**

**Co-Supervised by**

**Dr. GIRISH DUTT GAUTAM**

**Co-Supervised by**

**Dr. GAVENDRA NORKEY**



**L**OVELY  
**P**ROFESSIONAL  
**U**NIVERSITY

*Transforming Education Transforming India*

---

**LOVELY PROFESSIONAL UNIVERSITY  
PUNJAB  
2023**



## **DECLARATION**

I, hereby declared that the presented work in the thesis entitled “**Analysis of hole quality in laser drilling of FRP composite**” in fulfillment of degree of **Doctor of Philosophy (Ph. D.)** is outcome of research work carried out by me under the supervision **Dr. Ankur Bahl** working as **Associate Professor**, in the **Department of Mechanical Engineering** of Lovely Professional University, Punjab, India. In keeping with general practice of reporting scientific observations, due acknowledgements have been made whenever work described here has been based on findings of other investigator. This work has not been submitted in part or full to any other University or Institute for the award of any degree.



**(Signature of Supervisor)**

Kaushal Pratap Singh

Registration No.: 41800893

Department of Mechanical Engineering

Lovely Professional University,

Punjab, India



## **CERTIFICATE**

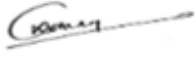
This is to certify that the work reported in the Ph. D. thesis entitled “**Analysis of hole quality in laser drilling of FRP composite**” submitted in fulfillment of the requirement for the reward of degree of **Doctor of Philosophy (Ph.D.)** in the **Department of Mechanical Engineering** is a research work carried out by **Kaushal Pratap Singh, (41800893)**, is bonafide record of his original work carried out under my supervision and that no part of thesis has been submitted for any other degree, diploma or equivalent course.

**(Signature of Supervisor)**

Dr. Ankur Bahl  
Associate Professor and Deputy Dean  
School of Mechanical Engineering  
Lovely Professional University, Jalandhar, Punjab, India

**(Signature of Co-Supervisor)**

Dr. Girish Dutt Gautam  
Associate Professor  
Department of Mechanical Engineering  
Mangalmay Institute of Technology And Management , Greater Noida, UP



**(Signature of Co-Supervisor)**

Dr. Gavendra Norkey

Assistant Professor

Department of Mechanical Engineering

Madhav Institute of Technology & Science, Gwalior, (MP)

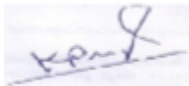
## Acknowledgement

My Ph.D. tenure is not only enjoyable but also painful experience. It's just like climbing a high peak step by step, accomplished with bitterness, hardships, frustration, encouragement and trust with so many people's help. Though it will not be enough to express my gratitude in words to all those people who helped me, I would still like to give my thanks to all these people. My first debt of gratitude must go to my supervisor **Dr. Ankur Bahl, Associate Professor and Deputy Dean, School of Mechanical Engineering, LPU, Jalandhar, Punjab**. He offered me so much advice, patiently supervising me and always guiding me in the right direction. His understanding, encouraging and personal guidance have provided a good basis for the present thesis. His wide knowledge and his logical way of thinking have been of great value for me.

I am deeply grateful to **Dr. Girish Dutt Gautam, Associate Professor, Department of Mechanical Engineering, Mangalmai Institute of Technology and Management, Greater Noida, Uttar Pradesh** and **Dr. Gavendra Norkey, Assistant Professor, Department of Mechanical Engineering, Madhav Institute of Technology & Science, Gwalior, Madhya Pradesh** for their detailed and constructive comments and for their important supports throughout this work. I have learned a lot from them.

I express my special thanks to **Dr. B.N. Upadhyay, SOF, Solid State Division of RRCAT (Raja Ramanna Centre for Advanced Technology), Indore (M.P)**.

My special gratitude is due to my father **Late Mr. R. P. Singh**, my mother **Mrs. Meera Singh** and my wife **Mrs. Priyanka Singh** and My Brother **Mr. Sanjay Singh** and my sister **Mrs. Madhuri Singh** for their unending support in the bad phase of my life. Their love provided me inspiration and was my driving force. I am heartily thankful to my hostel roommate Mr. Deepak Sati, a faculty of Department of Electronics & Communication, RVIT, Bijnor for his programming related help and moral support.



**(KAUSHAL PRATAP SINGH)**

## **Abstract**

In recent years, Kevlar and Basalt fibre-based composites are in increasingly high demand in various sectors particularly in defense, aerospace and automotive industries. Typical applications of these composites in the automobile and aerospace sectors need precise and dimensionally accurate machining. Laser drilling proves its suitability over conventional techniques during the processing of fiber reinforced polymer composites due to its unique characteristics such as material versatility and no tool wear etc. It also offers precise and accurate drilling in term of hole quality characteristics such as hole circularity, taper angle and Heat affected zone. In the present thesis, a pulsed Neodymium-Doped Yttrium Aluminium Garnet (Nd:YAG) laser system is used for drilling of fabricated Kevlar Fiber Reinforced Polymer (KFRP), Basalt Fiber Reinforced Polymer (BFRP) and their hybrid Kevlar-Basalt Fiber Reinforced Polymer (KBFRP) composite laminate. A range of experiments has been performed with varied values of three laser drilling parameters such as lamp current, pulse frequency and air pressure and key hole quality characteristics viz. top and bottom Hole Circularity (HC), Hole Taper (HT) and Heat Affected Zone (HAZ) have been considered as output performance measures. Experimentally observed data have been used to develop adequate mathematical models and statistical analysis. In order to improve the dimensional accuracy of the proposed composites during laser drilling, three different multi-response optimization techniques such as Taguchi technique, Response surface method (RSM) based on Box-Behnken Design (BBD) and Particle Swarm Optimization (PSO) technique have been employed. Validation experiments show that the proposed optimal value of parameters improved the overall hole quality for Kevlar, Basalt and their hybrid composite respectively. It is believed that the outcomes of this thesis can lead the researchers and modern industries to ensure a better quality of Fiber Reinforced Polymer (FRP) composites laser drilling products with the high precision and geometrical accuracy.

# CONTENTS

<b>Declaration by the Scholar</b>	<i>I</i>
<b>Supervisor’s Certificate</b>	<i>ii-iii</i>
<b>Acknowledgement</b>	<i>Iv</i>
<b>Abstract</b>	<i>V</i>
<b>Index</b>	<i>vi-ix</i>
<b>List of Figures</b>	<i>x-xii</i>
<b>List of Tables</b>	<i>xiii-xiv</i>
<b>List of Acronyms and Abbreviations</b>	<i>xv-xvii</i>
<b>CHAPTER 1</b>	
<b>1. Introduction</b>	<b>1-11</b>
1.1 Background	1-2
1.2 Laser	2
1.2.1 Background	2-3
1.2.2 Working Principle	3-4
1.2.3 Nd:YAG Laser System	4-5
1.3 Laser Beam Machining	5
1.4 Laser Beam Drilling (LBD)	5
1.4.1 Mechanism	5-6
1.4.2 Performance Characteristics	7
1.5 Fiber-Reinforced Polymer (FRP) Composites	7
1.5.1 Definition	8
1.5.2 Characteristics	7-8
1.5.3 Hybrid FRP Composites	9
1.6 Kevlar Fiber Reinforced Polymer (KFRP) Composites	9
1.7 Basalt Fiber Reinforced Polymer (BFRP) Composites	9-10
1.8 Objectives	10-11
1.9 Thesis structure	11

<b>CHAPTER 2</b>	12-18
<b>2. Literature Review</b>	12
2.1 Introduction	12
2.2 Machining of FRP Composites	12-13
2.3 Laser Beam Drilling of FRP Composites	13-15
2.3.1 Optimization in Laser Drilling of FRP Composites	15-17
2.4 Conclusions Drawn from Literature Survey	17
2.5 Summary	18
<b>CHAPTER 3</b>	19-32
<b>3. Materials, Methodology and Optimization Techniques</b>	19
3.1 Introduction	19
3.2 Materials	19-20
3.2.1 Composite Fabrication	21-23
3.3 Experimental Procedure	24
3.3.1 Laser System	24
3.3.2 Design of Experiments (DOE)	25
3.3.3 Hole Quality Measurement	27
3.4 Purpose of Optimization	28-29
3.5 Optimization Techniques	29
3.5.1 Taguchi Optimization (TO)	29
3.5.2 Response Surface Method (RSM)	30
3.5.3 Particle Swarm Optimization (PSO)	30-31
3.6 Summary	32
<b>CHAPTER 4</b>	33-47
<b>4. Parametric Optimization of Hole Quality Characteristics in Laser Drilling of Kevlar-29 Fiber Composite</b>	33-47
4.1 Introduction	33
4.2 Material, Experimentation and Measurement	34-38
4.2.1 Material	34



4.2.2	Experimentation & Analysis	34-38
4.3	Linear Model Analysis and validation	38-39
4.4	Optimization Techniques	39
4.4.1	Taguchi Optimization Technique	39
4.4.2	Result and Discussion for Hole circularity	39-43
4.4.3	Analysis of Variance (ANOVA) for Hole circularity	43
4.4.4	Result and Discussion for Hole Taper	46
4.4.5	Optimal Range of Process Parameter	46
4.5	Conclusion	46
4.6	Summary	47
<b>CHAPTER 5</b>		<b>48-57</b>
<b>5. Parametric Optimization of Hole Quality in Laser Drilling Kevlar/Basalt Hybrid FRP Composite</b>		<b>48-57</b>
5.1	Introduction	48
5.2	Material, Experimentation and Measurement	49-53
5.2.1	Material	49
5.2.2	Experimentation & Measurement	49-53
5.3	Optimization Technique	53-57
5.3.1	Taguchi Optimization Technique	53
5.3.2	Result and Discussion	53-56
5.3.3	Analysis of Variance (ANOVA)	57
5.4	Conclusion	57
5.5	Summary	57
<b>CHAPTER 6</b>		<b>58-76</b>
<b>Particle Swarm based Optimization of Hole Characteristics during Laser Drilling of BFRP</b>		<b>58-76</b>
6.1	Introduction	58
6.2	Material, Experimentation and Measurement	58-69
6.2.1	Material	58

6.2.2	Experimentation and Measurement	58-70
6.3	Optimization Technique	70-76
6.3.1	Particle Swarm Optimization Technique	70
6.3.2	Result and Discussion	70-76
6.4	Conclusion	76
6.5	Summary	76-77
<b>CHAPTER 7</b>		<b>78-79</b>
<b>Conclusions and Scope of Future Work</b>		<b>78-79</b>
7.1	Conclusions	77-78
7.2	Scope of Future Work	79
<b>References</b>		<b>80-87</b>
<b>List of Publication</b>		<b>88</b>
<b>List of Conference</b>		<b>89</b>

## List of Figures

<b>1.1</b>	Physical change during laser sample interaction	4
<b>1.2</b>	Laser beam drilling system	5
<b>1.3</b>	Mechanism of laser material processing	6
<b>1.4</b>	Performance characteristics in laser beam drilling	7
<b>1.5</b>	Classification of composite materials	8
<b>1.6</b>	Molecular structure of Kevlar	9
<b>1.7</b>	Chemical composition of basalt fiber	10
<b>2.1</b>	LBD of FRP composite materials	13
<b>3.1</b>	Steps in composite fabrication process	21
<b>3.2</b>	Composite fabrication	21
<b>3.3</b>	Composite fabrication process	22
<b>3.4</b>	Arrangement of set up for experiment	24
<b>3.5</b>	Hole circularity measurement	27
<b>3.6</b>	Measurement of HAZ	28
<b>3.7</b>	Block diagram of the PSO technique	31
<b>4.1</b>	Flow process of Chapter-4	33
<b>4.2</b>	Top side image of KFRP composite after laser drilling	34
<b>4.3</b>	Image of holes (9 nos.) obtained from optical microscope for KFRP composite (Top side)	34-35
<b>4.4</b>	Image of bottom side of KFRP composite after laser drilling	35
<b>4.5</b>	Image of holes (9 nos.) obtained from optical microscope for KFRP composite (Bottom side)	35-36
<b>4.6(a)</b>	Schematic representation	36
<b>4.6(b)</b>	Actual measurement	36
<b>4.7</b>	Variation of THC and BHC for all experiments	37
<b>4.8</b>	Variation of HT for all experiments	38
<b>4.9</b>	Main Effect Graph for S/N ratios	40
<b>4.10</b>	Main Effect Graph for Means	41

<b>4.11</b>	Full matrix of mean interaction plots for THC	42
<b>4.12</b>	Full matrix of Mean interaction plots for BHC	42
<b>4.13</b>	Main effect graph for S/N ratio	44
<b>4.14</b>	Main effect graph for Means for HT	45
<b>5.1</b>	Flow chart of methodology	48
<b>5.2</b>	Image of top side of hybrid KBFRP composite after laser drilling	49
<b>5.3</b>	Image of holes (9 nos.) obtained from optical microscope for KFRP composite (Top side)	49-50
<b>5.4</b>	Image of bottom side of hybrid KBFRP composite after laser drilling	50
<b>5.5</b>	Image of holes (9 nos.) obtained from optical microscope for KFRP composite (Bottom side)	50-51
<b>5.6(a)</b>	Schematic representation	51
<b>5.6(b)</b>	Actual measurement	51
<b>5.7</b>	Variation of THC and BHC for all experiments	53
<b>5.8</b>	Main effect graph for S/N ratios	54
<b>5.9</b>	Main effect graph for Means	55
<b>5.10</b>	Full matrix of Mean interaction plots for HC	56
<b>6.1</b>	The flowchart of the methodology	58
<b>6.2</b>	Procedure of laser drilling experimentation and hole circularity and HAZ analysis	59
<b>6.3</b>	Top side Image of BFRP composite after laser drilling	59
<b>6.4</b>	Top side Image of holes (27 Nos) obtained from optical microscope for BFRP composite	60-61
<b>6.5</b>	Bottom side Image of BFRP composite after laser drilling	62
<b>6.6</b>	Bottom side Image of holes (27 Nos) obtained from optical microscope for BFRP composite	62-64
<b>6.7(a, b)</b>	The schematic and actual representation of the measurement	65
<b>6.8</b>	Variation of THC and BHC for all experiments	67
<b>6.9</b>	Measurement of HAZ	67

<b>6.10</b>	Representation of HAZ at (HAZ at $(I) = 200$ amp, pulse $(f) = 25$ Hz, and $(p) = 8$ bar	68
<b>6.11</b>	Variation in Z versus number of particles	74
<b>6.12</b>	Comparison of optimum value of Z for PSO versus RSM	76

## List of Tables

<b>3.1</b>	Constituents of Kevlar-29 fabric	19-20
<b>3.2</b>	Constituents of Basalt fabric	20
<b>3.3</b>	Constituents of epoxy resin and hardener	20
<b>3.4</b>	Composition of fabricated laminates sheet	23
<b>3.5</b>	Set of (a) fabric and (b) fabricated composite sheet	23
<b>3.6</b>	Specification details of Nd: YAG laser machining set-up.	25
<b>3.7</b>	Number of experiments by different DOE techniques	25
<b>3.8</b>	Number of experiments performed by pilot experiment	26
<b>3.9</b>	Process parameters and their levels	27
<b>4.1</b>	Values of THC	36-37
<b>4.2</b>	Values of BHC and HT	37
<b>4.3</b>	Values of estimated model coefficients for SN ratios	38
<b>4.4</b>	Values of estimated model coefficients for Means	39
<b>4.5</b>	The result of S/N ratio under different process parameter	39-40
<b>4.6</b>	Result for S/N ratios	40
<b>4.7</b>	Result for Means	41
<b>4.8</b>	ANOVA for Means	43
<b>4.9</b>	ANOVA for S/N ratio	43
<b>4.10</b>	The result of S/N ratio under different parameter setting	44
<b>4.11</b>	Result for S/N ratios	45
<b>4.12</b>	Result for S/N ratio	46
<b>5.1</b>	Values of THC	52
<b>5.2</b>	Values of BHC	52
<b>5.3</b>	The result of S/N ratio under different parameter setting	53-54
<b>5.4</b>	Result for S/N ratios	55-56
<b>5.5</b>	Result for Means	54
<b>5.6</b>	ANOVA for Means	56
<b>6.1</b>	Values of THC	64-65

<b>6.2</b>	Values of BHC	65-66
<b>6.3</b>	The measured values of HAZ	68-69
<b>6.4</b>	Measured values of all hole quality characteristics	69-70
<b>6.5</b>	ANOVA for hole circularity	71
<b>6.6</b>	ANOVA for Hole Taper	71-72
<b>6.7</b>	ANOVA for HAZ	72
<b>6.8</b>	Optimum values obtained by PSO Method	74
<b>6.9</b>	Different optimum values obtained of Z for PSO and RSM	74-75

## List of Acronyms and Abbreviations

AFRP	Aramid fiber reinforced polymer
ANN	Artificial neural network
ANOVA	Analysis of variances
AWJ	Abrasive Water Jet
BBD	Box-Behnken Design
BFRP	Basalt Fiber Reinforced Polymer
BHC	Bottom Hole Circularity
CFRP	Carbon Fiber Reinforced Polymer
DOE	Design of Experiments
DOF	Degree of Freedom
ECM	Electro-Chemical Machining
EDM	Electro-Discharge Machining
FDM	Fused Deposition Modeling
FA	Firefly Algorithm
FEA	Finite Element Analysis
FEM	Finite Element Method
FL	Fuzzy Logic
FRP	Fiber Reinforced Polymer
GA	Genetic Algorithm
GFRP	Glass Fiber Reinforced Polymer
HAZ	Heat Affected Zone
HT	Hole Taper
KBFRP	Kevlar Basalt Fiber Reinforced Polymer



KFRP	Kevlar Fiber Reinforced Polymer
LASER	Light Amplification by Stimulated Emission Of Radiation
LBC	Laser Beam Cutting
LBD	Laser Beam Drilling
MASER	Microwave Amplification By Stimulated Emission Of Radiation
MCC	Metal Ceramic Composite
MMC	Metal Matrix Composite
MRA	Multiple Regression Analysis
MSS	Mean Sum of Square
Nd:YAG	Neodymium-Doped Yttrium Aluminium Garnet
OA	Orthogonal Array
OPAT	One Parameter at a Time
PCA	Principal Component Analysis
PCB	Printed Circuit Board
PMMA	Poly Methyl Methacrylate
PSO	Particle Swarm Optimization
PVC	Poly Vinyl Carbonate
QLF	Quality Loss Function
RA	Regression Analysis
RM	Re-Solidified Material
RRCAT	Raja Ramanna Centre of Advanced Technology
RSM	Response Surface Methodology
SA	Simulated Annealing
SEM	Scanning Electron Microscope
SS	Sum of Square

TLBO	Teaching Learning Algorithm Based Optimization
TM	Taguchi Methodology
THC	Top Hole Circularity
XRD	X-Ray Diffraction

# Chapter 1

## Introduction

### 1.1 Background

Nowadays, Fiber reinforced polymer (FRP) or plastic composites material used in industrial sectors like Glass Fiber reinforced polymer (GFRP), Carbon Fiber reinforced polymer (CFRP), Kevlar Fiber reinforced polymer (KFRP) and Basalt Fiber reinforced polymer (BFRP). FRP composite are made with same structure by using different types of machining operation for specific industrial application. These composite are difficult to machining as compared to metal due to their Heterogeneous and anisotropic properties. The selection of suitable machining techniques becomes significant for FRP machining. There are lots of machining problems arises during machining of KFRP and BFRP composites [1, 2]. The major machining defects like delamination, fiber pull out, are found [3]. Moreover, it is necessary to meet dimensional tolerances and rework of machining become essential. Sometimes, it reached up to 50% cost of the production. Therefore, the various researchers are found the other machining processes. There is no direct contact between tool and the work piece in laser machining in FRP due to which less Mechanical and thermal forces will be involved. Therefore Abrasive Water Jet Machining (AWJM) will used for best quality at low controllable process [4,5]. These factors are more responsible for health of operators as well as environment. Laser Beam Machining (LBM) has advantage of Non-contact and localized nature for composite's processing. LBM has major advantages of vibration, drilling forces and tool wear. High production rate will be provided by at high drilling speed in automation [6,7,8]. Generally two laser (CO<sub>2</sub> and Fiber) are mostly used in processing of FRP composite materials .Due to its higher peak power, laser has been used during machining of the material which maintained the undefined beam quality. Machining can be done by using higher drilling speed laser system in different interval mode. All the different types of hole characteristics can be evaluated by using Neodymium-Doped Yttrium Aluminium Garnet (Nd:YAG) laser system. Hole circularity (HC) will be considered as the main quality characteristics while Heat Affected Zone (HAZ) will be considered metallurgical characteristics [9]. In recent years, the conventional materials are replaced by FRP composites which are applied in the application of manufacturing, automobile, aircraft and power plants, Basically FRP materials are the combination of matrix and reinforcement.

In matrix phase, Fibers are classified in two ways; one types of fiber can be used in manufacturing such as natural fibers and synthetic fibers. Jute, coir and rice husk has been considered as natural fibers whereas glass, carbon, aramid and nylon has been considered as synthetic fibers. There are various types of methods can be used for fabrication of FRP composites such as hand lay-up, spray-up, pultrusion etc. Mostly hand lay-up approach is used widely in industries. In the present work, the fabricated laminate has constructed by using hand lay-up techniques due to their low cost and minimal setup requirement. As the industrial sector, there are lots of quality parameters are required for manufacturing by using the FRP composite material. Therefore, in present work laser drilling has been done on KFRP, BFRP and their hybrid (KBFRP) composite material. A very big challenge to maintain the precise and accurate geometry of hole for industrial applications, LBM are mostly using for drilling of FRP composites Thus, for the evaluation of hole quality characteristics, the dimensional accuracy can be maintained to overcome the variation in hole circularity (HC), HAZ and hole taper (HT) during the machining of the composite material. In the next stage, all the experimentally data are collected for different holes and it has been converted in to their empirical mathematical models for the prediction of their trends. Latest research presented that proper suitable way to adopt of drilling factors has been used for improvement in hole surface geometry. Therefore, various researches are used different optimization techniques for taking the suitable value of laser drilling factors. Therefore, in present work, different multi-response optimization techniques such as Taguchi optimization technique, RSM and PSO have been used to generate the optimum value of laser drilling factors.

## **1.2 Laser**

### **1.2.1 Background**

Light is in the form Electromagnetic radiation which generated from an energy resource. Depending upon the wave length, It may be divided as gamma, X-rays and radio etc. [10,11], it has a single wavelength for engineering applications. Thus, due to these properties of monochromatic light wave moves out. Therefore, the concept of LASER has been introduced [12]. Electromagnetic radiation has been stimulated with action of the molecules. In the advancement period, Laser has become more useable in industrial application as well as in communication system. In the present applications, laser can be used in engineering and

hospital etc. sectors [13, 14]. In recent years, a composite material which is based on polymer has been used in industrial application. The advanced machining techniques can be overcome processing defects [15]. Schawlow and Townes [16, 17, 18] was used the concept of higher resolution microwave spectroscopy in the field of the optics and radiation. Thereafter, three types of laser such as solid, liquid and gas were introduced. There are two types of lasers has been introduced for engineering applications. Due to characteristics of laser light, it has not been looked like normal light. Due to focusing in nature, it enables to be concentrated at a small space. It consists of higher power density [19]. The generation of Laser beam process begin from small power level to top power level by using high energy. There are three main steps, pumping, spontaneous emission and stimulated emission has been used in laser beam generation. Laser beam has been developed outside of the system with the help of amplification. Meanwhile, Stimulated emission has been developed by the population inversion [20,21,22].

## **1.2.2 Working Principle**

In Fig.1.1, The material has been heated firstly up to melting point then after up to boiling point. The photon energy has been participated during laser material processing mechanism. Photo-thermal mechanism has been developed due to lower energy level and it arises vibrating effects. The phase of the material will be changed due to higher the photon energy then vibrational effects. Three types of Phase conversion method has been employed such as melting, vaporization and plasma formation called the photochemical mechanism. Molecular bond of work piece material has been break down due to high photon energy laser beams. Photo-electric process has been used for another metal removal process by using high photon energies directly through burning [23,24,25].

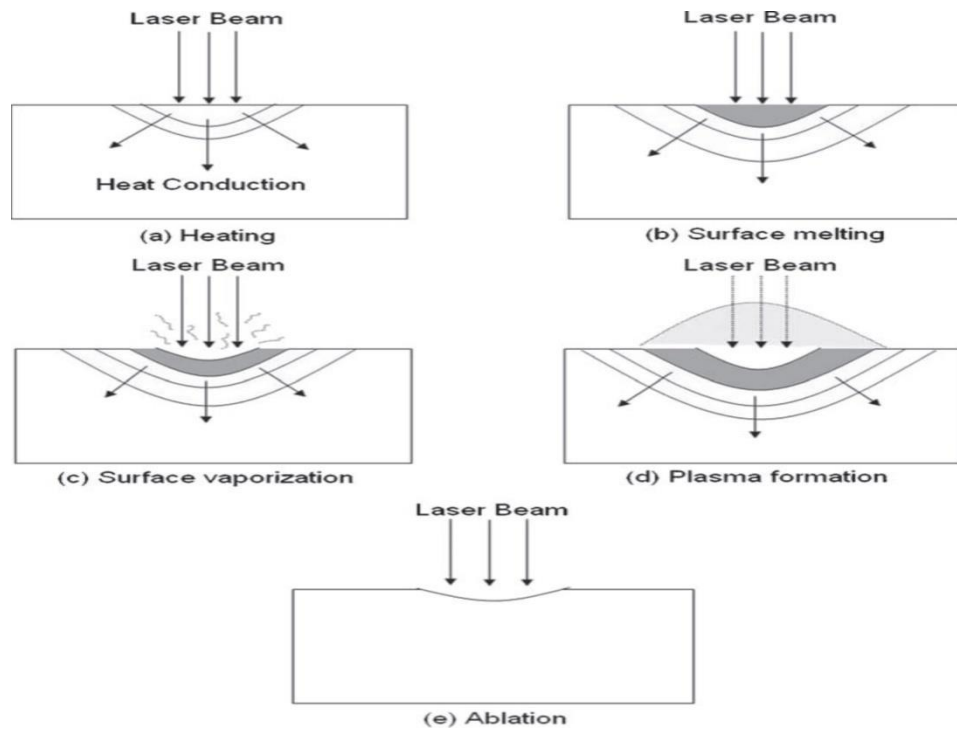


Fig. 1.1: Physical changes during laser sample interaction [25]

### 1.2.3 Nd:YAG Laser System

Nd:YAG laser uses solid-state gaining medium for beam generation. 1 to 2% neodymium ( $\text{Nd}^{3+}$  ion) doped with Yttrium Aluminium Garnet (YAG) ( $\text{Y}_3\text{Al}_5\text{O}_{12}$ ) crystal is used as gaining medium. An Nd:YAG laser has a near-infrared wavelength of  $1.06 \mu\text{m}$ . Power of laser beam may be developed from MW to over a KW with the help of these lasers. Moreover, the average power has been considered up to kW ranges in pulse mode. The response of Neodymium-Doped Yttrium Aluminium Garnet (Nd:YAG) laser may be converted by varying pumping discharge waveform. Higher pulse energy has been generated by long flash light. So the power is high that why energy is absorbed by the composite material/sample and converted in to thermal energy, causing a rough damage from instantaneous evaporation to form cracking and melting of the material which resulted in formation of crater like damage (degradation of machining chamfer of the composition). Power has been employed of 10-1000 W during laser processing. In Fig. 1.2, there are two types of optical resonators has been used, one resonator will be completely reflective and other partially for moving the photons in the beam generation unit. The response will be recorded by the partially transmissible mirror. Transmission of laser beam has been employed

by Optical fibers. The fumes and scatter has been removed with the help of assist gas [19, 26].

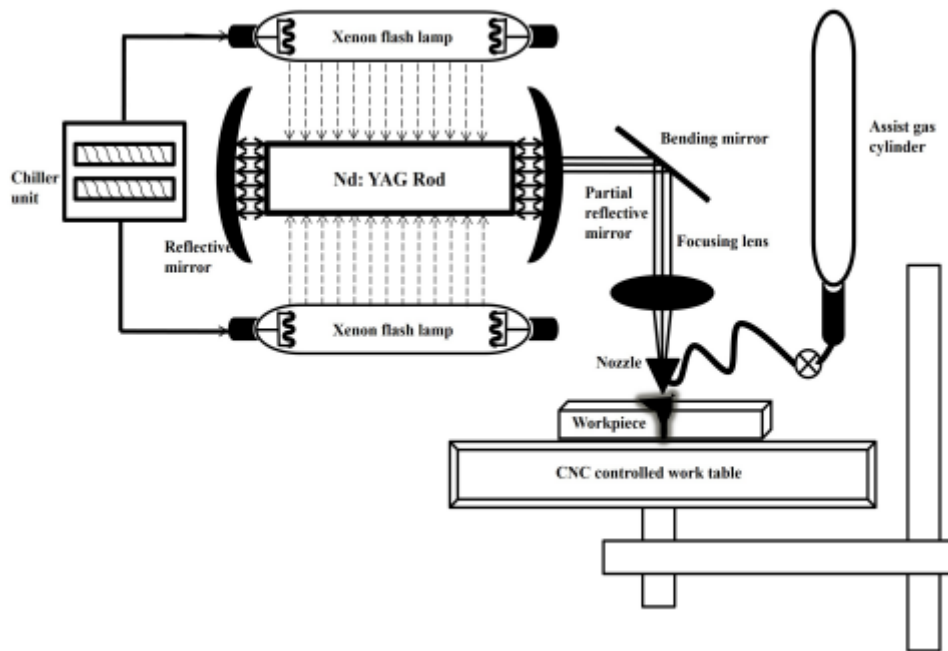


Fig. 1.2: Laser beam drilling system [25]

## 1.3 Laser Beam Machining (LBM)

LBM can be divided on the basis heat source movement [12, 27]. One dimensional machining has introduced as Laser Beam Drilling (LBD). Laser Beam Drilling can also be further divided in two ways such as hand trepanning and helical drilling [28]. Moreover, two dimensional laser machining has been considered as the laser cutting process and the three dimensional laser beam machining has been considered as laser milling and turning processes.

## 1.4 Laser Beam Drilling (LBD)

### 1.4.1 Mechanism

Nowadays, for developing hole in complex and intrinsic shape, laser drilling process is mostly used in industrial sector with high production rate. The different types of complex and intrinsic shapes have been generated with high production rate by using laser drilling process. It is far better in comparison of conventional machining method. It has higher accuracy and

flexibility without tool wear and frictional forces for various engineering materials and it is also economical process. It is depend on temperature of the erosion of the material, called steady-state thermal process. However, it is independent of time .in this process erosion will be developed just in front of the laser beam .After vaporization, molten materials are removed from the hole surface with the help of assist gases. These gases also responsible for the cooling of the work piece surface as shown in Fig. 1.3 [29].

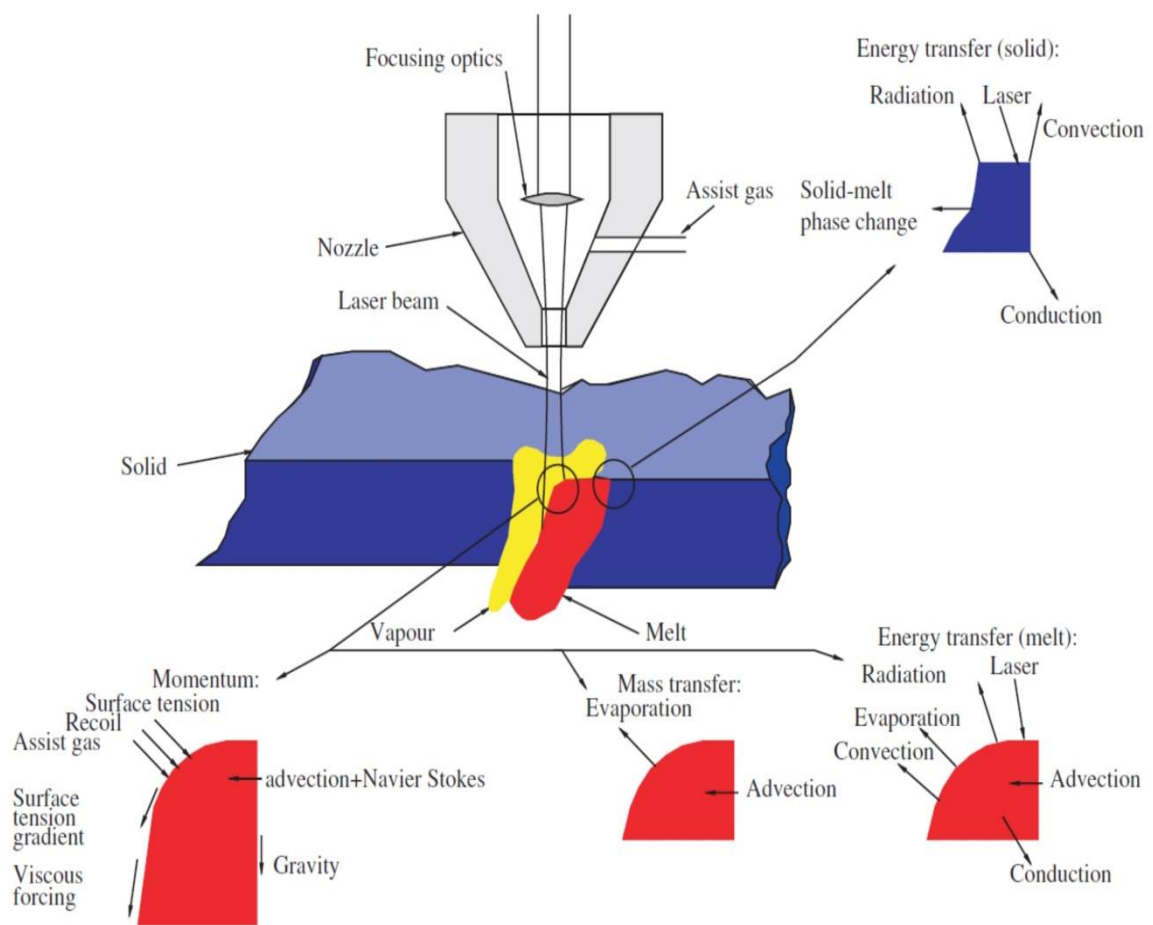


Fig. 1.3: Mechanism of laser materials processing [29]



## 1.4.2 Performance Characteristics

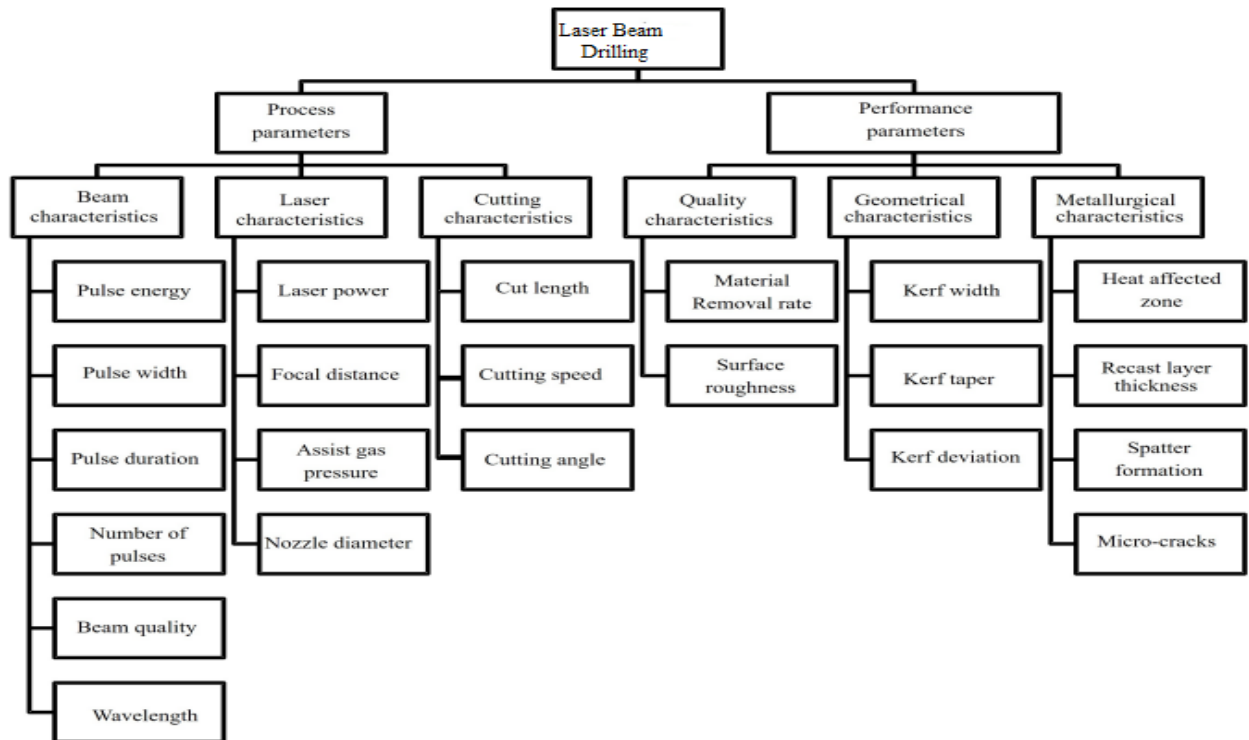


Fig. 1.4: Performance characteristics in laser beam drilling [18]

Fig. 1.4 shows the classification of Process parameters can be divided into three types as the beam, laser and drilling characteristics whereas performance can be measured by quality, geometrical and metallurgical characteristics. Performance factors in Laser Beam Drilling (LBD) process. Performance may be further divided in different quality, [18]. The important quality characteristics viz Hole Circularity (HC) and Hole Taper (HT) have been considered in geometrical characteristics while heat affected zone has been considered in metallurgical characteristics.

## 1.5 FRP Composites

### 1.5.1 Definition

Composite has been fabricated by mixing of two or more constituent materials in a fixed or variable proportion. Due to mixing of these constituents, properties of the composite have been improved. There are basically two types of phases have been used to develop the Composites such as matrix phase and reinforcement phase. Metallic, polymeric or ceramic

has considered Matrix phase while fibers or particles are considered as reinforcement phase. In composites, matrix and fibers are enclosed by the boundary called interface. The phase separation has been employed by the interface between the continuous and discontinuous phase of the composite. Shear resistant is provided by Matrix phases whereas tension resistance by reinforcement phase to the composite as shown in Fig. 1.5. There are two types of fiber are considered as Unidirectional and bidirectional fibers. These materials have highly effective as compared to their ingredients.

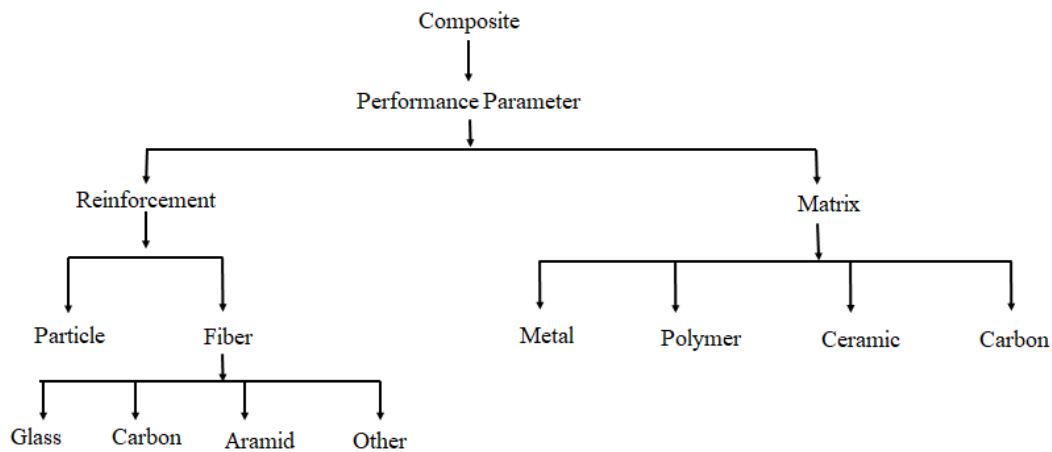


Fig.1.5: Classification of composite material

## 1.5.2 Characteristics

A higher degree of flexibility has been provided by FRP composite material to the vendor as per order. This flexibility has been given in terms of strength etc. Composite material has given the flexibility to the manufacturer for fabrication of the desired product. Many FRP composites having the potential to absorb vibrational energy. Due to which noise and vibrations generation has been reduced. FRP composite has given flexibility to reduced assembly requirement for complex shape manufacturing. This type of characterises has been used in different industrial sectors. In recent years, by considering these properties of FRP composite, most of the researchers have transferred from traditional materials to FRP composites for industrial purposes. FRP composites consists of different properties that make them suitable for industries, defence, medical, and transmission industries etc. [6, 30, 31].

### 1.5.3 Hybrid FRP Composites

Delamination is the main reason for strength degradation of FRP composites which suffer their service life [32]. Due to distinct properties of fiber hybridization, various researchers have focused to increase novel properties of composites. Some common type of hybrid [33-37].

### 1.6 KFRP Composite

Kevlar, most common type of aramid fibers such as Twaron, Nomex has been used. Besides, Nomex and Technora, Kevlar had been introduced in 1965 at Dupont. Kevlar have different properties such as high heat resistant, lighter in weight and much stronger than steel. Tensile strength of Kevlar has of about 3,620 MPa with a density of 1.44 kg/m<sup>3</sup>. There are three types chemical structure has been employed such as primary, secondary and tertiary. The monoclinic type is considered as primary structure and the pleated sheet configuration is considered as secondary. Kevlar has high chemical stability and high degree of resistivity [38]. Kevlar has most promising anti-ballistic material due to high heat and vibration absorbent properties. It has various applications such as body armor panels, bullet-proof jackets, fire-proof bodysuits, combustion protection material etc.

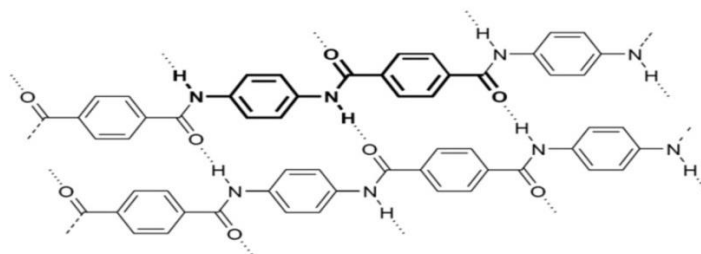


Fig. 1.6: Molecular structure of Kevlar [38]

### 1.7 BFRP Composites

Many researchers have suggested that Basalt fibers and their composites have very superior thermal, mechanical and structural properties. Due to which they have been concerned on BFRP composites. Glass fiber reinforced has been replaced by BFRP composite due to their high quality and environment friendly [39]. Basalt fiber has consists of SiO<sub>2</sub> and Al<sub>2</sub>O<sub>3</sub> in their chemical proportion as shown in Fig.1.7. It is less expensive than glass and carbon fiber due less energy consumption [40]. It is more suitable for automobile industries due high

loading capacity [5]. Basalt fiber has various properties such as higher heat resistant, higher oxidation, radiation resistive and shear strength, high strength and good modulus [41]. Basalt fiber has easily sustainable, non-toxic and eco-friendly in nature [42, 43, 44, 45]. Pipes are made by BFRP are powerful as comparison to pipes made by GFRP and it can be best for liquids and transportation [46, 47]. Besides of that, it is type of natural fiber so it can be reduced environmental issues. As the use of BFRP composites are many more such as such as defence, manufacturing, and transmission etc. but the production point of view, it is more important that which process is suitable.

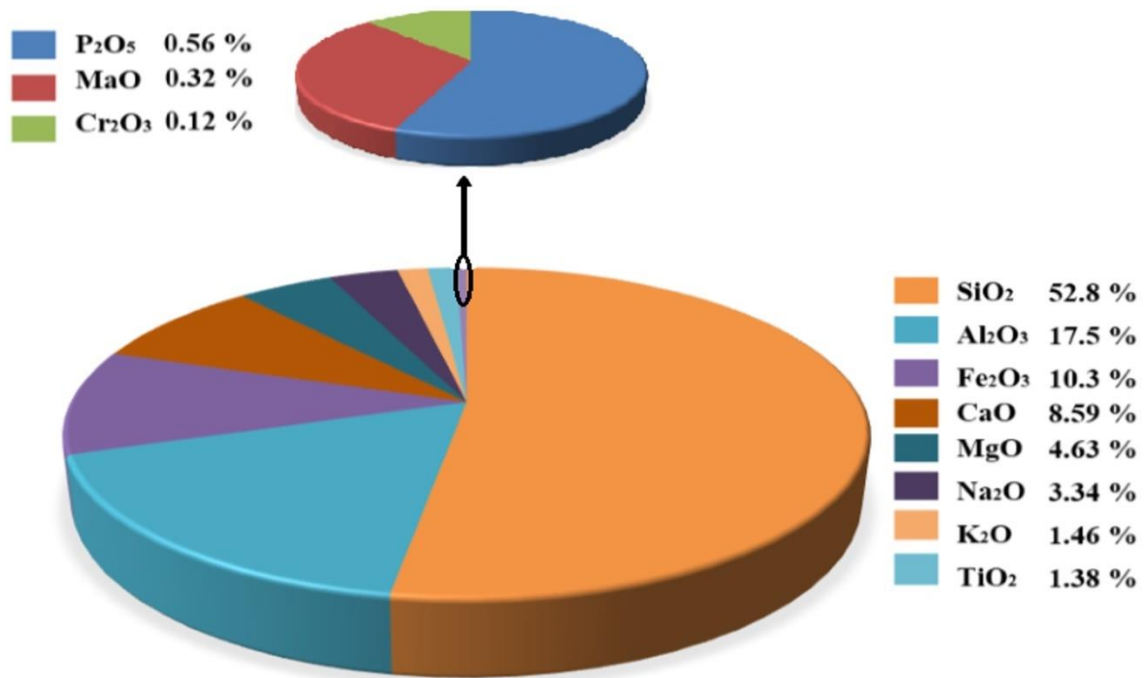


Fig. 1.7: Chemical composition of basalt fiber

## 1.8 Objectives

The main targets of the research work are considered as:

1. To fabricate different laminates of Aramid and Basalt fibers having suitable thickness for industrial applications.
2. To identify and apply the design of experiments for conduction of experiments for different process parameters in laser drilling.

3. To develop mathematical models and multi response optimization of evaluated hole quality characteristics.
4. To compare the results of all multi-objective optimization and identify the favourable range of laser drilling parameters

## 1.9 Thesis structure

The seven chapters have been discussed in detail.

**Chapter 1:** In this chapter, an introduction of the current work has been presented. This chapter also includes the main current work.

**Chapter 2:** This chapter consists of comprehensive research. It also includes concepts, merits and demerits of laser drilling have been considered.

**Chapter 3:** It provides a detailed description of experimental set up and experimentation has been discussed. It's also includes the various optimization methods has been considered in this chapter are also considered.

**Chapter 4:** In this chapter, the most advancement used in KFRP composites. The Taguchi method has been adopted for better Hole Circularity (HC) and Hole Taper (HT).

**Chapter 5:** In this chapter, the most advancement research in KBFRP hybrid composite sheet by using Nd: YAG Laser Beam Drilling (LBD). The Taguchi optimization methods have been employed for better Hole Circularity (HC).

**Chapter 6:** In this chapter, the most advancement research in laser drilling of BFRP composites. A Response Surface Method (RSM) based on Box Behnken Design (BBD) to develop the Mathematical model for hole quality characteristics. The Particle Swarm Optimization (PSO) based multi-response has been employed to optimize the Hole Circularity (HC), Hole Taper (HT) and Heat Affected Zone (HAZ) .In this chapter, PSO has adopted to determine the optimum value of factors to maximize hole quality and minimize Hole Taper and Heat Affected Zone, simultaneously. Also compare the results of PSO and RMS for optimum favourable condition and identify the favourable range of laser drilling parameters.

**Chapter 7:** Summarizes the present work and provide conclusions. This chapter also includes suggestions regarding coming work.

# Chapter 2

## Literature Review

### 2.1 Introduction

In the last chapter, the recent work is discussed. Main requirement of recent work and the structure of the thesis are also presented. In the present chapter, a short discussion of lasers Machining FRP composite materials as well as their applications has been presented. Moreover, optimization in laser drilling of FRP Composite has been also discussed. The laser machining on fiber composites has been adopted as the recent work targets.

### 2.2 Machining of FRP Composites

There are various types of typical manufacturing operation needed in different types of industries such as manufacturing and air force. Always composite are fabricated with proper size and shape but their machining has special requirement. These requirements have been fulfilled as per accurate intrinsic shapes; desired type of machining is required. It is totally dependent of end-product [48, 49]. In the ideal condition, FRP composite has inherent heterogeneity and anisotropy properties due to which the machining of FRP composites is tough through traditional drilling tools. Many types of machining defects have been found due to traditional machining. [6, 50]. These machining damages has played an important role for the structural strength of FRP composites [51]. There will be a lot of frictional force has been generated on drilling tool due to thermal expansion during traditional drilling processes. Due to which, hole quality will be changed. Traditional machining methods are not suitable for intricate types of shapes. High cut quality can be developed with the help advanced manufacturing techniques [7, 8]. Fig. 1.8 show the general outline of Laser beam drilling (LBD) of FRP materials.

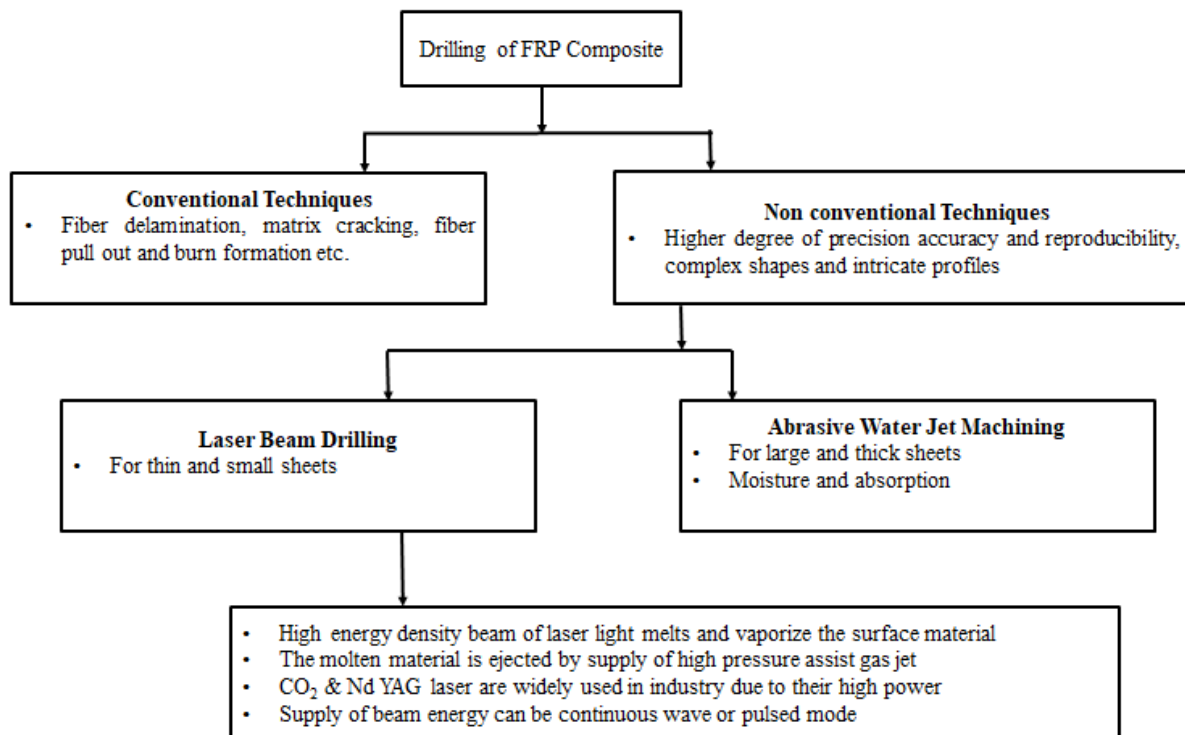


Fig. 2.1: LBD of FRP Composite Materials [28]

## 2.3 LBD of FRP Composites

Next section presents remarkable experimental and theoretical studies that have been conducted in the field of laser beam drilling on CFRP, GFRP and AFRP

LBM has been considered as best option of Non-traditional machining method with a high precision grades that determines them fit for in application. Laser drilling has different types of merits over the traditional drilling method such as good quality products, easy to operate with economical cost. Chan et al [52] has been developed Finite Difference Method (FDM) model and observed Material removal rate by vaporization and liquid expulsion. Cheng et al [53] have been developed a Numerical Finite Difference Heat Flow Model (NFDHFM) for Carbon Fiber Reinforced Polymer (CFRP) to determine the fine hole and HAZ in thin sheet of metal. Young et al [54] have observed the effect of laser drilled holes on the strength and stiffness of Carbon Fiber Epoxy Composite (CFRP) panel. Rodden et al [55] have been investigated the single pulse drilling characteristics for multilayer CFRP composite. M. Dellerba et al [56] has been investigated the interaction between Excimer lasers and CO<sub>2</sub> sources for Aramid fiber (Kevlar), Carbon fiber and Glass fiber with an epoxy resin matrix and found the better results for Kevlar than CO<sub>2</sub> sources whenever drilling with CO<sub>2</sub> sources,

it is generating an under size hole at given output power and critical cutting speed whereas the ablation rate is undoubtedly rather low compared with the CO<sub>2</sub> technology. E. Aoyama et.al [57] have been investigated the effect of surface roughness during drilling of multiple hole in multilayer boards using Aramid Fiber Reinforced Polymer (AFRP) and Glass Fiber Reinforced Polymer (GFRP). T. Hirogaki et al [58] have been observed the effect of surface roughness by using Aramid /Epoxy and Glass/epoxy composite for multilayer Printed Wiring Board (PWB) in relation to blind via laser drilling. M. M. Noor et al [59] have been investigated the four layer of GFRP having thickness of 2 mm with orientation (0, 90, 0, 90) through the CO<sub>2</sub> laser was employed to drill and resulted that the laser power had predominantly affected the quality of the hole. K. Ogawa et al [60] observed that the blind via holes (BVHs) by using Microvia formation technology has become the dominant method in PWBs resulted an overhang defect on drilled hole. K. Ogawa et al [61] have been observed that AFRP replaced by GFRP for the build-up layer through the microvia formation technology. S. Nagesh et al [62] have been observed the effect of nano fillers through the multiple responses such as Damage Width, Surface Damage Width and Taper Angle were optimized by using the Grey–Taguchi method. A. Solati et al [63] have been investigated the effect of drilling parameters on the HAZ and bearing strength by using Genetic Algorithm–Artificial Neural Network (GA-ANN) approach. It was found that the GA-ANN method could predict the HAZ and bearing strength more accurately than trial-and-error ANN. T. Hirogaki et al [64] have been generating blind via holes by using laser drilling of PWBs along with oxygen plasma treatment and resulted found the smooth roughness of the hole wall without any damage. E. Aoyama et al [65] described the features of Cu-direct laser drilled hole quality and overhang on multi-layer Printed Wiring Boards (PWBs) by employing thermo-graphic and mixing of fillers in to the build-up layer in order to reduce the amount of overhang. K. Ogawa et al [66] have been investigated the circuit connection reliability of printed wiring boards (PWBs) by Finite Element Method (FEM) and resulted that the build-up layer is effective by decreasing the thickness of the sheet. Abrate et al [67] have studied five types of different unconventional machining processes for composite material. But also they found more delamination during the water jet machining. Mathew et al [68] have examined the HAZ and observed the HAZ and cut quality characteristics are directly proportional to each other. Hocheng et al [69] studied the delamination of the composite during conventional drilling. Tsao et al [70] have been also investigated the delamination associated with the drilling of composite material. Davim et al [71] have examined the delamination in the composite during the conventional machining using digital



image analysis technique. Gaugel et al [72] have examined the various types of damages such as wear and laminate damage in the traditional operation of CFRP. From this research it has been confirmed that the traditional machining is not suitable for these types of materials. However, advance machining techniques has been suitable for FRP types of materials.

### **2.3.1 Optimization in Laser Drilling of FRP Composites**

It has been found that composite materials can be drilled with the help of laser by lasers efficiently due to incident beam burns the arising whiskers from the drill edges. The hole quality characteristics during LBD are highly depending on the proper selection of drilling parameters. If the laser drilling parameter are not suitable then so many thermal defects will arises and the product quality get worse. For getting good hole quality, the suitable drilling parameter is required. There are various types of optimization techniques have been employed to get optimum levels of machining parameters. G.D. Gautam et.al [73] has been investigated the minimum kerf deviation, viz lamp current, pulse frequency, pulse width and compressed air for 1.2mm Kevlar by using Box Benkhen design with two centre point and optimum result obtained . G.D.Gautam et al [74] has investigated kerf quality characteristics such as kerf width, kerf deviation, and kerf taper with consideration of five different process parameters lamp current, pulse frequency, pulse width, air pressure and cutting speed for 1.6 mm thick BFRP composite laminate by using A Firefly Algorithm (FA) based multi objective optimization approach and found the optimum levels for geometrically accurate cutting. G.D.Gautam et al [75] has been investigated the effect of lamp current, pulse width, pulse frequency, compressed air pressure and cutting speed on kerf width, kerf deviation and kerf taper for 1.35 mm thick Kevlar-29 and basalt fiber based hybrid composite sheet and found optimal condition by using Grey Relational Analysis and Genetic Algorithm (GRGA) for different kerf quality. G.D.Gautam et al [76] has been investigated different kerf quality characteristics such as top and bottom kerf width, top and bottom kerf deviation and kerf taper for 1.35 mm thick Kevlar-29 and Basalt Fiber-Reinforced Polymer (KBFRP) hybrid composite laminates considered five cutting parameter lamp current, pulse width, pulse frequency, compressed air pressure and cutting speed developed mathematical model by using RSM-based Box–Behnken design. G.D.Gautam et al [77] has been investigated the optimum levels for 2.34 mm thickness of basalt glass Kevlar 29 hybrid FRP composite laminates by considering the five cutting parameter as Lamp current, pulse width, standoff distance, compressed air pressure, and cutting speed thereafter, grey relational analysis

approach has been adopted and found that standoff distance has as the most influencing parameter for both top and bottom kerf deviation. G.D.Gautam et al [78] has been investigated the kerf width, kerf deviation, and kerf taper for 1.35 mm thick hybrid Kevlar/Basalt fiber reinforced polymer composite laminate by using cutting parameters as lamp current, pulse width, pulse frequency, compressed air pressure and cutting speed and Firefly algorithm technique has been adopted to attain optimal levels of the control parameters for better geometry of the cut. K. K. Sharma et al [79] has been investigated the flexural strength of the hybrid FRPs material made from three distinct laminates. It has been observed that the specimen having Kevlar at the topmost has the highest value of flexural strength. A.Jain et al [80] has been discussed the machinability of these FRPCs. The main problems in fiber-reinforced composite plastic machining were discussed in this review concerning the most recent research in this field. A. Jain et al [81] has been done laser beam drilling of basalt-glass hybrid composite , to predict a safe machining zone pertaining to high drill quality with minimum heat-affected zone and maximum hole-circularity. The prediction of the zone has been done by mathematical modeling and optimization using RSM and multi-objective Genetic Algorithm (GA), respectively. A. Jain et al [82] have been discussed about damages such as delamination and fiber pull-out. Therefore, the present work reviews the drilling of FRPCs and most of its related concerns. A. Jain et al [83] have been done laser beam drilling of a fabricated basalt–glass hybrid composite and observed a safe machining zone pertaining to high drill quality with minimum heat affected zone and maximum hole-circularity has been predicted by using Artificial Neural Network (ANN) merged with multi-objective Genetic Algorithm (GA). A. Jain et al [84] have been investigated the mechanical, thermal, and chemical properties of Basalt/Woven Glass Fiber Reinforced Polymer (BGRP) hybrid polyester composites. The Fourier Transform Infrared Spectroscopy (FTIR) was used to explore the chemical aspect, whereas the Dynamic Mechanical Analysis (DMA) and Thermo-Mechanical Analysis (TMA) were performed to determine the mechanical and thermal properties. The FTIR results showed that incorporating single and hybrid fibers in the matrix did not change the chemical properties. The DMA findings revealed that the B7.5/G22.5 composite with 7.5 wt% of Basalt Fiber (BF) and 22.5 wt% of Glass Fiber (GF) exhibited the highest elastic and viscous properties. R. Tewari et al [85] has been observed hole quality characteristics such as Kerf taper angle, heat-affected zone (HAZ), and surface roughness for laser-drilled kenaf/high-density polyethylene (HDPE) composites and resulted that predicted model exhibited good agreement with each other as they provide error less than 5.35%. H. Jiang et al [86] has been observed ultrafast laser drilling has been proven to

effectively reduce the heat-affected zone (HAZ) of carbon fiber-reinforced polymer (CFRP) composites. It also analyzed the forming process of the drilling depth in the spiral drilling mode and studied the influence of laser energy and drilling feed depth on the holes' diameters and the taper. A.T. Erturk et al [87] has been adopted CFRP by hybrid laminate composite containing carbon and glass fiber materials. Because using glass fiber prepreg instead of carbon fiber prepreg will lead the material to become cheaper. K. Giasin et al [88] has been investigated thrust force and surface roughness by the influence of spindle speed and feed rate for the ultrasonic-assisted drilling (UAD) of GLARE laminates. UAD resulted that the significant reduction in thrust force by up to 65% while surface roughness metrics Ra and Rz were unaffected by the type of drilling process. P. Madhu et al [89] has been introduced bio-fibers as reinforcement for the manufacturing of polymer composites due its availability, low cost, and environmental characteristics and bio-fiber hybridization gives superior mechanical and thermal properties. Rampal et al [90] has been reviewed the drilling of FRPCs and most of its related concerns. Moreover, non-traditional drilling techniques for FRPCs are also reviewed. Non-traditional drilling methods alleviated the hole damage to a larger possible extent. Microwave drilling of FRPCs can also be explored to produce good quality holes.

## **2.4 Conclusions Drawn from Literature Survey**

Key findings from a detailed literature survey are listed below:

1. A very few recent work is performed in the application of LBD of FRP sheet.
2. So many research works has already been conducted on the metal through LBD individually. But a very few research works has been reported yet on AFRP and BFRP composites through LBD process area.
3. The accurate machining of FRP composite is still a matter of concern, a very few research work has already been done on the Aramid and basalt fiber composite through Nd: YAG LBD individually. But a less research work has been considered in the application of hybrid fiber sheet through laser beam drilling process area.
4. A limited research work has been found by using multi-objective optimization approaches in laser drilling of FRP composites.

Based on these conclusions from the literature survey, the present work has been carried out.

## **2.5 Summary**

In this chapter, a detailed research has been concluded by the previous researchers by using Nd:YAG laser drilling of FRP composite materials. Moreover, a detail discussion about laser mechanism as well as different laser machining processes. The output performance parameters in the laser drilling of FRP composite have been increased by using different optimization techniques. The different objectives have been taken on the basis of literature survey. In the next Chapter 3, fabrication of FRP composite materials, methodologies related to perform experiments as well measurements of output are discussed.

# Chapter 3

## Materials, Methodology and Optimization Techniques

### 3.1 Introduction

In the previous chapter, works related to the laser drilling of FRP composite materials are presented. From the detailed literature review of the works carried out by the previous researchers, it has been inferred that the laser beam system is the necessary preferred advanced machining process for drilling of FRP composite materials for industrial applications. Moreover, it has been also observed that geometrically accurate and precise drilling is the utmost priority.

### 3.2 Materials

There are two types of different fiber fabrics have been used for fabrication of composite sample such as Kevlar-29 and Basalt fibers. Both fibers are purchased from Aerotech Technical Textile, Mumbai. The properties are listed in Table 3.1, 3.2 and 3.3, respectively. Den (Denier) is defined as gram per 9000 metres of yarn. Three various composite laminate are prepared by using these two types of fibers for conduction of laser drilling experiments.

Table 3.1: Constituents of KFRP fiber

<b>Kevlar-29</b>		
Reinforcement (yarn)	Wrap	1100 (Denier)
	Weft	1100(Denier)
Fiber count	Wrap ends	9
	Weft picks	9
Weave		Plain

Width (mm)	1650
Density(g/cm <sup>2</sup> )	0.28
Thickness (mm)	1.40
Strength (MPa)	2765
Weight (g/m <sup>2</sup> )	200

Table 3.2: Constituents of Basalt fabric

Properties	Unit	Basalt
Density	g/cc	2.8
Tensile Strength	MPa	4840
Modulus of elasticity	GPa	89
Break elongation	%	3.15
Relative humidity	60% RH	<0.1
Thermal properties		
Max. Application temp.	0 <sup>0</sup> C	982
Max. Operating temp.		700
Min. operating temperature	0 <sup>0</sup> C	-200
Thermal conductivity	W/Mk	0.031-0.038
Melting temperature	0 <sup>0</sup> C	1450

Table 3.3: Constituents of epoxy resin and hardener

Constituents	Standard	Unit	Epoxy resin	Hardener
Emergence		Visual	Clear liquid	Yellow
Color	ASTM D 1544	GS	Max 1	
Viscosity at 27°C	ASTM D 2196	MPa.S	7000-14000	60-80
Density at 27°C	ISO 1183	g/cc	1.05-1.150	-
Epoxy equivalent	ASTM D 1652	g/equivalent	180-210	-

### 3.2.1 Composite Fabrication

There are so many techniques considered for making of composite laminate. Most practiced Hand layup technique is used for fabrication due to easy to fabricate and economical. Automotive and aircraft industries have been used this technique for the fabrication of various components [48]. There are three steps used in this technique for the fabrication methodology as in Fig. 3.1. It provides the visual presentation of the fabrication.

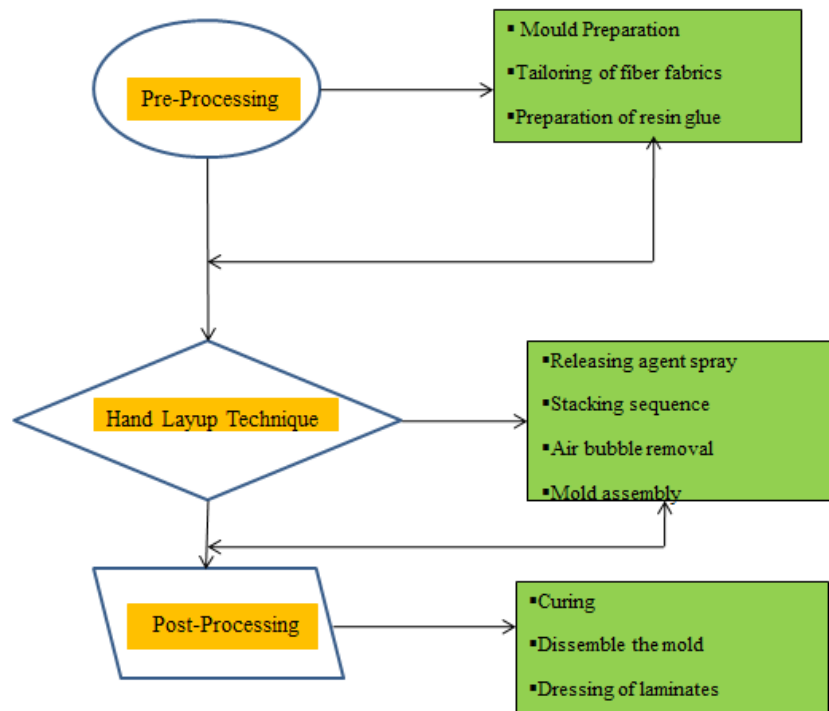


Fig. 3.1: Steps in composite fabrication process



Fig.3.2: Composite (a) top (b) bottom fabrication

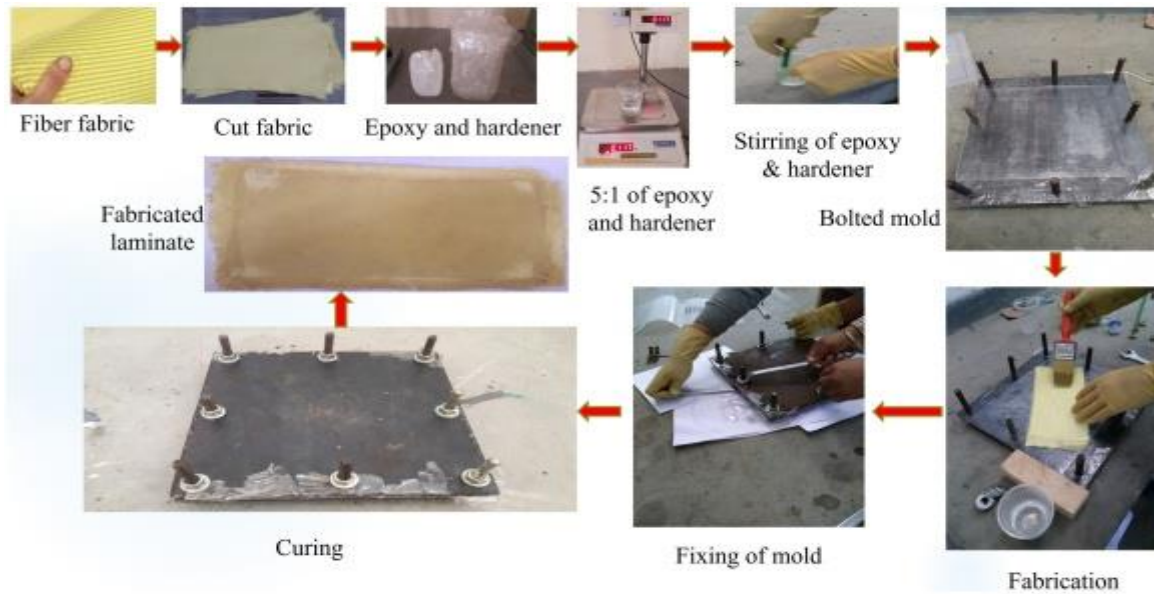


Fig. 3.3: Composite fabrication process

The methodology has been divided into four phases. The first phase focuses on the fabrication of fiber composite laminates with the help of hand layup method. Composite sheet has been fabricated in the laboratory environment using epoxy resin-520 with hardner-509 purchased from Electro coating and Insulation Technical Pvt. Ltd., Pune, India. The orientations of Basalt-Kevlar-29 hybrid fiber mats in fabricated laminates have been kept [B-0°/K-0°/B-45°/K-45°/B-0°] for the five layers. The orientation of fibers affects the physical properties of fabricated composite. Therefore, to ensure the smooth flow of epoxy resin, the orientation angle of (0°/45°) has been taken. A mild steel mould having dimension 150 mm × 150 mm × 20 mm used to fabricate the composite laminate. Silicon spray has been used as releasing agent. A homogeneous mixture of epoxy and hardener (5:1 ratio proportion) with resin glue has been prepared with the help a magnetic stirrer . At last, mould has been tighten by the bolts and rest for curing at room temperature. After 24 h, mould opened and fabricated laminate has been released and cut into the required size. The thickness of the laminate is 1.2 mm in Fig. 3.3.



Table 3.4: Composition of fabricated laminates sheet

Used Fiber	Matrix	Fiber Volume Fraction	Matrix Volume Fraction	Stacking Sequence	Laminate Thickness (mm)
<b>Kevlar-29</b>	E-520	89.50	10.50	[0°/45°]5	1.20
<b>Basalt</b>	E-520	87.41	12.59	[0°/45°]5	1.20
<b>Kevlar-29&amp; Basalt</b>	E-520	87.50	12.50	[0°/45°]5	1.20

The fibers orientation (0°/45°), has been combined in the matrix as shown in Table 3.5

Table 3.5: Set of fabric and fabricated sample sheet

Composite	Raw fabric	Fabricated composite laminate
<b>KFRP</b>		
<b>BFRP</b>		
<b>KBFRP</b>		

## 3.3 Experiment Method

### 3.3.1 Laser System

All the experiment has been conducted at Raja Ramanna Centre of Advanced Technology (RRCAT), Indore by using Nd:YAG laser system . Compressed natural air has been used as an assist gas during the experimentation. The natural compressed air flows through a 1 mm diameter nozzle. The flow rate of the compressed air is maintained constant throughout the experiment. The distance between the workpiece and the nozzle is called standoff distance. The standoff distance has been varied in steps of 0.5, 1 and 1.5 mm. The lens of 50 mm focal length has been selected for focusing the laser beam. It is required for protecting the focusing lens from emitted fume due to vaporization and burning of the workpiece material. It consists of three axes CNC-Controlled table with 250W average output power laser beam is employed for the fabricated FRP composite sheet as shown in Fig. 3.4 .The specification of laser system as following: Laser wave length =1069 nm, beam diameter =10mm, Beam Divergence (Full Angle) = 6 m-rad Average Pump Power =5 KW, Average Output Power (Max)=250kw, Peak Power (Max) = 5 KW, Pulse Energy (Max) = 100 J, Pulse Width =1-20 ms, Pulse Repetition Rate=1-20 Hz, Beam Delivery Fiber (Core Diameter) = 600  $\mu$  m, Transmission Efficiency (Through Fiber) = 90%, Focused Spot Size On Job = 600  $\mu$  m. Compressed air is used as an assist gas to expel molten material from the hole surface.. Moreover, standoff distance 1mm is fixed between the nozzle and specimen for entire range of experiments.

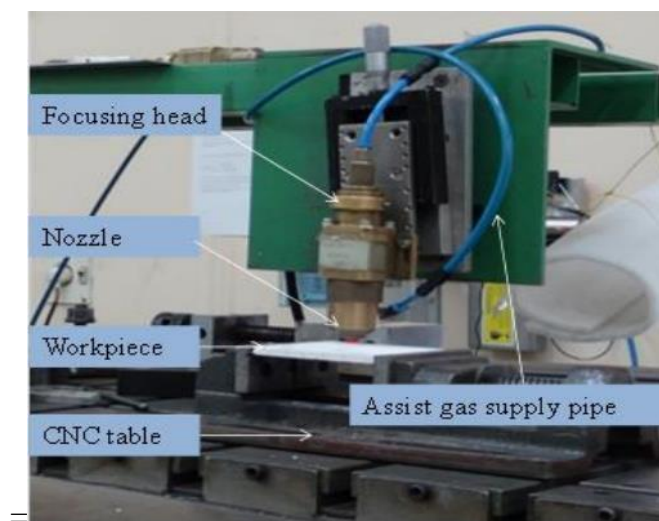


Fig. 3.4: Arrangement of setup for experiment

### 3.3.2 Design of Experiments (DOE)

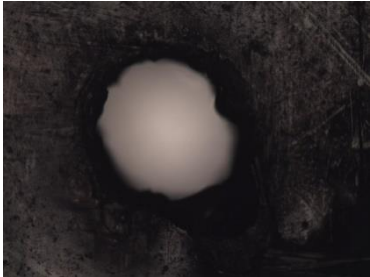
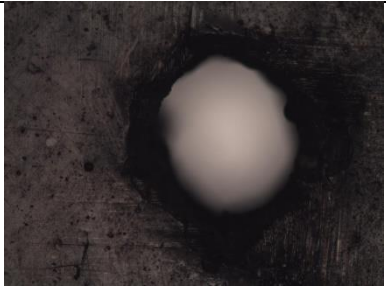

A Proper plan is to be design for conduction of experiments. However, it has not depend on the number of experiment performed [10]. In the present report, Taguchi optimization and Response Surface Method (RSM) based Box-Behnken Design (BBD) is employed to perform experiments. It is represented by Table 3.7, which consists of three factors and their levels by different DOE techniques. From this table, it has been observed that RSM based BBD technique neither has fewer experiments like Taguchi based L<sub>9</sub> & L<sub>27</sub> approaches nor as high as like full factorial design and RSM based CCD approach.

Table 3.7: Number of experiments by different DOE techniques

S.No.	Number of Input Parameters	Levels	Techniques	Number of Experiments	
1	3	3	Full Factorial Design	27	
2	3	3	Taguchi design	L <sub>9</sub>	9
3	3	3		L <sub>27</sub>	27
4	3	3	RSM	CCD Full	52
				Half	32
5	3	3	BBD	42	

We can be performed thousand numbers of experiments but on the basis on the basis of literature survey, range of experiment has been already decided for getting optimum result that why we have done only 20 numbers of pilot experiments and identify the suitable parameters and their levels. The range of each control factors and their levels have been decided by the help of pilot experiments. One Parameter at A Time (OPAT) approach has been used to perform pilot experiments and decide range of laser drilling parameters as in Table 3.8.

Table 3.8: Number of experiments performed by Pilot experiment

Exp.no	Lamp current ( $I$ ) Amp	Pulse frequency ( $f$ ) Hz	Air pressure ( $p$ ) Kg/cm <sup>2</sup>	Hole circularity (HC)	Images holes from optical microscope
1	160	20	8	0.84	
2	160	30	10	0.85	
3	170	20	10	0.58	
4	170	25	12	0.65	
5	180	18	7	0.68	
6	180	20	8	0.82	
7	180	25	9	0.87	
8	180	27	10	0.72	
9	180	30	11	0.78	
10	190	20	10	0.76	
11	190	30	8	0.75	
12	200	20	8	0.92	
13	200	20	9	0.88	
14	200	25	10	0.86	
15	200	30	8	0.88	
16	220	20	9	0.64	
17	220	25	9	0.58	
18	240	20	12	0.63	
19	240	25	12	0.67	
20	250	20	12	0.71	

Three levels are selected due to limited number of experiments. However, in literature various studies show that three level studies are sufficient to explore the process performance. The three drilling parameters viz.  $I$ ,  $f$ , and  $p$  with three levels of each as in Table 3.9.

Table 3.9: Process Parameters and their levels

Symbol	Factor	Unit	Level 1	Level 2	Level 3
$I$	Lamp current	Amp	160	180	200
$f$	Pulse frequency	Hz	20	25	30
$p$	Air pressure	Kg/cm <sup>2</sup>	8	9	10

### 3.3.3 Hole Quality Measurement

Hole quality has been considered such as Hole Circularity (HC), Hole Taper (HT) and Heat Affected Zone (HAZ). The geometrical characteristics such as Top and bottom side hole circularity, HT and HAZ has been considered as metallurgical characteristics. Measurement of both sides have provided the loss of material due to over drilling. The hole circularity is defines as degree of roundness of a hole. It may be found by using relation used in eq.(3.1). The schematic representation of hole circularity measurement as shown in Fig.3.5.

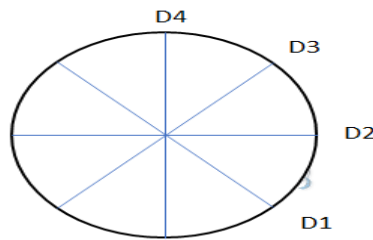


Fig.3.5: Hole Circularity Measurement

$$\text{Hole circularity} = \frac{D_{min}}{D_{max}} \quad (3.1)$$

Diameters  $D_1$ ,  $D_2$ ,  $D_3$  and  $D_4$  have been measured of all the drilled holes at an interval of 45° angles respectively as shown in Fig.3.5. Those areas which are not melted during laser machining called as HAZ but it gives effect on the microstructures.

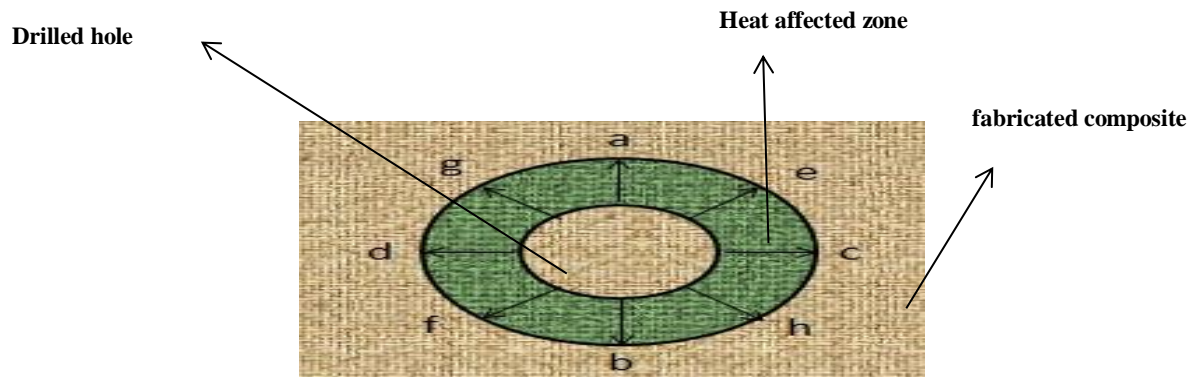


Fig.3.6: Measurement of HAZ

After performing experiment, there will be non-uniformity in the hole dimension due to different motion of laser beam. so for better hole circularity, hole taper should be lower [50]. It is found by relation given in eq. (3.2).

$$\tan\theta = \frac{D_1 - D_2}{2t} \quad (3.2)$$

Where  $\theta$  is taper angle and  $D_1$ ,  $D_2$  are the inlet and outlet hole diameter respectively.

### 3.4 Purpose of Optimization

Optimization is the process to identify the solution of a complex problem known as an objective function having the aim of either maximization or minimization within the acceptable range of function variables. This approach is able to provide more information and insight into the problem. In the present age, manufacturing industries are facing various issues like quality of products, safety, minimum processing cost and time etc. These demands provoke the application of optimization process in manufacturing sectors. Optimization plays a vital role to confirm the increased quality of products with reduced cost and time. However, it is a challenge to represent a manufacturing process in a highly constrained non-linear mathematical model due to their discontinuous and non-explicit nature. In many cases, conventional optimization approaches are not able to sufficient due to so many machining parameter and the difficulty in the machining processes like LBD [51]. Conventional optimization techniques are deterministic in nature and unable to provide a globally optimum solution. These approaches are usually very slow in convergence. Thereby the applications of various advanced modeling and optimization method have proposed by researchers for optimization purpose in manufacturing. For effective optimization of any manufacturing process, development of an empirical model of that process is the primary step. This model can be developed by various approaches like statistical regression, fuzzy Logic, and Artificial Neural Network (ANN). Basically, this model represents the functional correlation between

these two parameters. In this work, models of output responses are developed using statistical regression analysis. Thereafter, the selected optimization approach is employed to find the solution of the developed model into the defined range of process variables. In the present work, two advanced optimization techniques viz. Taguchi, Response Surface Method (RSM) based BBD and Particle Swarm Optimization (PSO) have been employed to identify optimal solutions in laser drilling of different composite materials. The detailed working procedure of these techniques is discussed in the next section.

## 3.5 Optimization Techniques

Three different optimization methods such as Taguchi Method, Response Surface Method based BBD Design and Particle Swarm Optimization (PSO) was used to find the suitable value of laser drilling parameters.

### 3.5.1 Taguchi Optimization Technique

A lot of industrial application has shown the power of Taguchi's overall approach. But there had been dispute that a lots of optimization techniques available in spite of Taguchi approach. However, most accepters were ready to adopt Taguchi's loss function concept.

The Signal to Noise (S/N) Ratio may be calculated [46] by relation given in eq. (3.3).It can be measured in decibels (dB)

$$\eta = -10 \log (M.S.D.) \quad (3.3)$$

Where, *M.S.D.* is the Mean-Square Deviation for the output characteristic.

Lower is the best concept of S/N ratio is used by the relation given in eq. (3.4)

$$M.S.D. = \frac{1}{n} \sum_{i=1}^n Y_i^2 \quad (3.4)$$

. The total mean value of S/N ratio (*m*) is calculated by the relation given in eq. (3.5)

$$m = \frac{1}{n} \sum_{i=1}^n \eta_i \quad (3.5)$$

### 3.5.2 Response Surface Methodology (RSM).

In this RSM, develop the mathematical model consists of the response and variables  
In general, the relation is developed

$$y = f(\xi_1, \xi_2, \dots, \xi_k) + \varepsilon; \quad (3.6)$$

Generally  $\varepsilon$  has been involved the effects of measurement error, background noise, other variables effect etc. it is also called a statistical error,. Then

$$E(y) = \eta = E[f(\xi_1, \xi_2, \dots, \xi_k)] + E(\varepsilon) = f(\xi_1, \xi_2, \dots, \xi_k) \quad (3.7)$$

The relation given in equation (3.3.9) are generally called the natural variables, Now RSM work , natural variables has been converted in to coded variables  $x_1, x_2, \dots, x_k$ , which are usually dimensionless, the response function eq. (3.3.8) may be explain

$$\eta = f(x_1, x_2, \dots, x_k) \quad (3.8)$$

$$\eta = \beta_0 + \beta_1 x_1 + \beta_2 x_2 \quad (3.9)$$

The Eq. (3.9) is also called a main effects model, when the interaction has been considered The  $\beta$ 's are a set of unknown parameters. Generally, polynomial models are linear functions of the unknown  $\beta$ 's, That are also consider in regression analysis .The values has been added easily as below:

$$\eta = \beta_0 + \beta_1 x_1 + \beta_2 x_2 + \beta_{12} x_1 x_2 \quad (3.10)$$

if two variables are used, it is developed given below

$$\eta = \beta_0 + \beta_1 x_1 + \beta_2 x_2 + \beta_{11} x_1^2 + \beta_{22} x_2^2 + \beta_{12} x_1 x_2 \quad (3.11)$$

In general, the first-order model is developed as follows:

$$\eta = \beta_0 + \beta_1 x_1 + \beta_2 x_2 + \dots + \beta_k x_k \quad (3.12)$$

$$\eta = \beta_0 + \sum_{j=1}^k \beta_j x_j + \sum_{j=1}^k \beta_{jj} x_j^2 + \sum_{i < j} \sum_{j=2}^k \beta_{ij} x_i x_j \quad (3.13)$$

In many critical situations, higher polynomial of second order has been used.

$$\eta = \beta_0 + \beta_1 x_1 + \beta_2 x_2 + \dots + \beta_k x_k + \varepsilon \quad (3.14)$$

### 3.5.3 Particle Swarm Optimization (PSO)

This method was proposed by Kennedy and Eberhart in 1995. , when a group of birds are flying for food searching, for this instant of time, all birds in the flock can spread their search and they help to each other for getting food in short period of time . The main terms are such as SWARM means population of the algorithm, PARTICLE means individual swarm, P-best individual best position, g-best global best position, Leader has been followed by other



particles and moving towards the best position. PSO is based on bio-inspired algorithms and found an optimal result in the given problem. It has differential algorithms in comparison to other optimization algorithms. It has considered the only the objective function is needed. There will be no requirement of the gradient or any differential form of the objective. Few hyper parameters have also be consider.it is shown by block diagram in Fig.3.7.

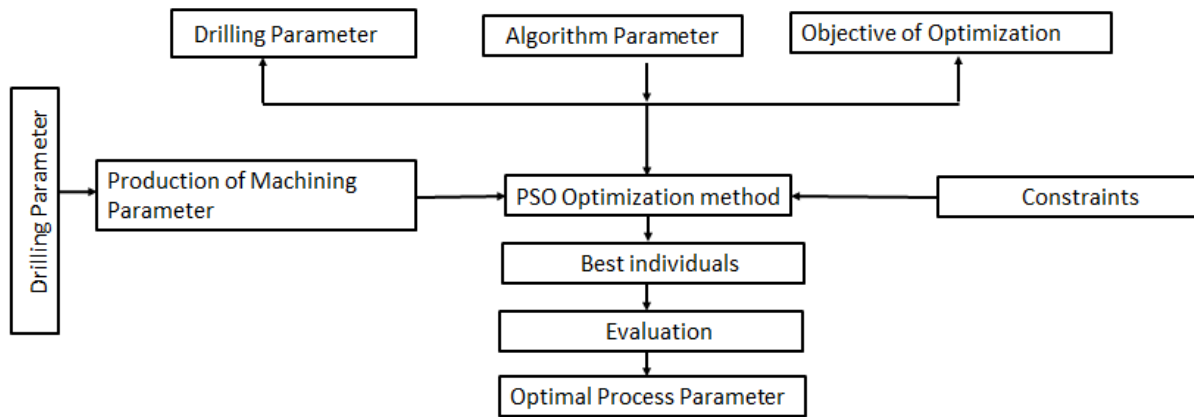


Fig.3.7: Block diagram of the PSO technique

It consists of three main phases 1. Particles Generation 2. Speed and its location 3. Speed confirmation and final destination location. Firstly fixed the initial position and mentioned that point to reach its final position from 1<sup>st</sup> movement which is depending on new speed. The varying location is denoted by  $P_{ik}$  and speed is denoted by  $V_{ik}$  of particle swarm and the time limit has been considered by  $D_t$  as shown in Eq. (3.15-3.17). The  $i$ th particle of position and velocity with time  $k$  represent the vector form. From Equation 3.3.17-3.3.19 random variables choice with uniform distribution represented by  $rand$  and the value varies from 0 to 1 through the design space. The time  $k + 1$  is the next step to update the new velocity of all particles and the time  $k$  represent the current position insight the design space. The  $V_{iK}$  provide information about the current motion and search direction,  $V_{iK+1}$  provides information about the next iteration. The current motion, self-memory of particle and influence of swarm with other three weight features  $w$  inertia factor,  $C_1$  self-confidence level, and  $C_2$  confidence level of the swarm are play an important role for new search direction respectively.

$$P_{o}^i = X_{min} + rand(X_{max} - X_{min}) \quad (3.15)$$

$$V_o^i = \frac{X_{min} + \text{rand}(X_{max} - X_{min})}{\Delta t} = \frac{\text{position}}{\text{time}} \quad (3.16)$$

$$V_{k+1}^i = W * V_{k+c_1}^i * \text{rand} \frac{(p^i - p_k^i)}{\Delta t} + C_2 * \text{rand} \frac{(p_k^G - p_k^i)}{\Delta t} \quad (3.17)$$

### 3.5.4 Summary

The Selected FRP composite materials and their fabrication process have been discussed in this chapter. The details of the experimental setup with selected input laser parameters and their levels have also been discussed in this chapter. Different types of hole quality characteristics along with their measurement process have also been discussed in this chapter. Moreover, the mechanism of three different optimization techniques Taguchi, RSM based on BBD and PSO have also been discussed in details. In the next Chapter 4, Parametric optimization of hole quality Characteristics in Laser drilling of Kevlar-29 Fiber composite sheet have been discussed.

# Chapter 4

## Parametric Optimization of Hole Quality

### Characteristics in Laser Drilling of Kevlar-29

#### Fiber Composite

##### 1.1 Introduction

As discussed in the last chapters that the geometrical quality of the laser drilling on FRP composite materials is governed by different factors. Therefore, it is quite required to ascertain the effects of these process parameters to achieve a higher hole quality. For this purpose, in this report, a KFRP sheet has been prepared and selected as the sample. Three factors such as  $I$ ,  $f$ , and  $p$  have been considered for conduction of experiments. Various quality response of laser drilling such as HC and HT for both the surfaces of the sheets has been considered as output response. Process flow of this chapter is shown in Fig. 4.1

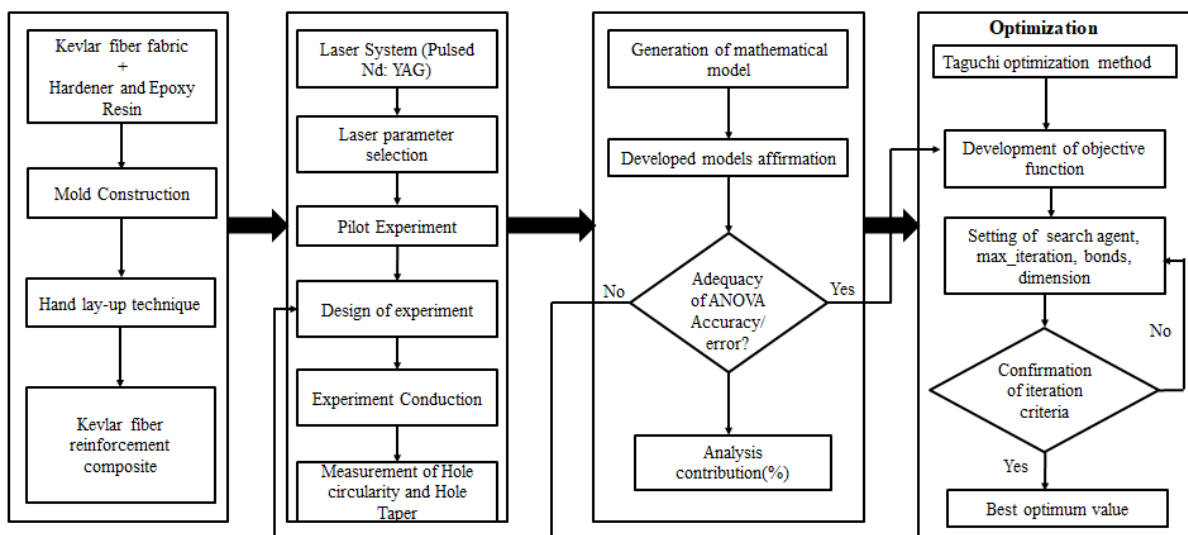


Fig. 4.1: Flow chart of Methodology

## 4.2 Material, Experimentation and Measurement

### 4.2.1 Material

KFRP composite laminate having thickness 1.20 mm is used as sample. Sample has been prepared by Hand layup method. The stacking sequence of sample has been considered like  $[K-0^\circ/K-45^\circ/K-0^\circ/K-45^\circ/K-0^\circ]_5$  for five layers of fibers.

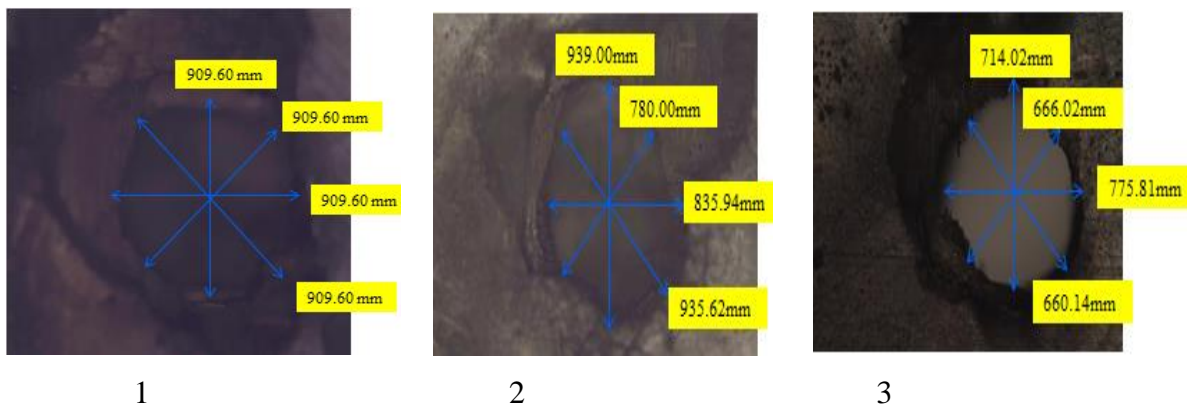
### 4.2.2 Experimentation and Analysis

The DOE has been performed by applying Taguchi method. Conduction of experiment has been performed on the basis of  $L_9$  Orthogonal array. After that, the response such as HC and HT has been measured and optimize the HC and HT. Further confirm and validate the response result.

A 1.0 mm drilled hole has been considered to find various hole quality characteristics. Fig. 4.2 & 4.3 show the both sides of images of KFRP composite.



Fig. 4.2: Top side image of KFRP composite after laser drilling



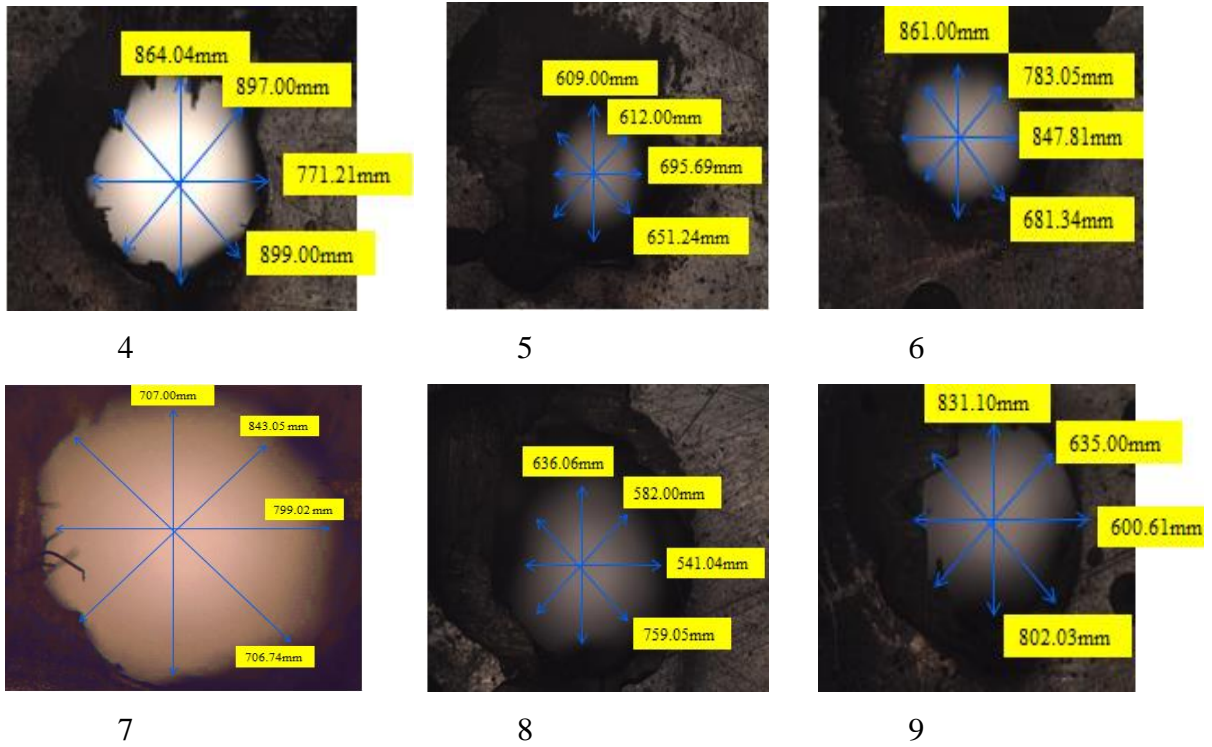
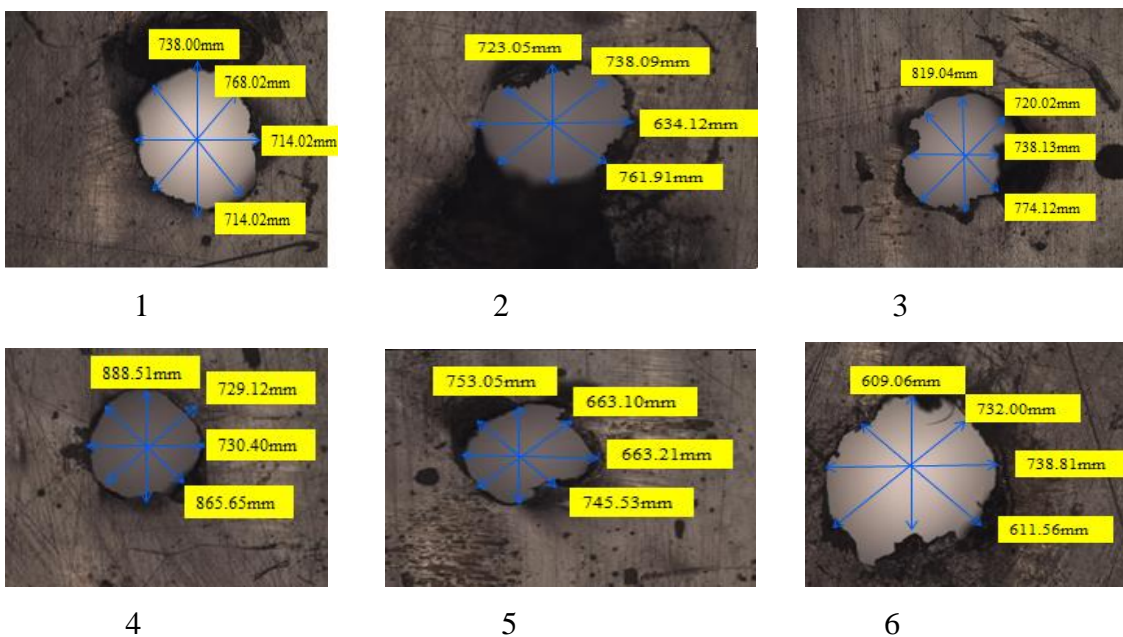


Fig. 4.3: Image of holes ( 9 nos.) obtained from optical microscope for KFRP composite (Top side)



Fig. 4.4: Image of bottom side of KFRP composite after laser drilling



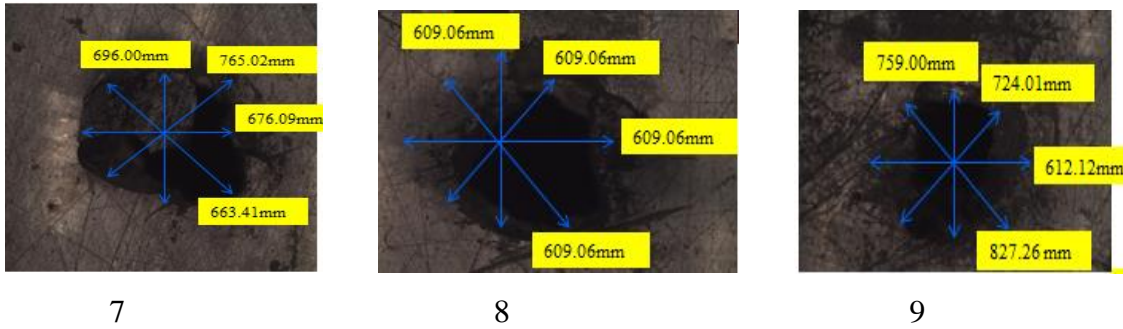


Fig. 4.5: Image of holes (9 nos.) obtained from optical microscope for KFRP composite (Bottom side)

The HC and HT are found with the help of relation given in eq. (3.1-3.2) respectively. For better hole circularity, it should be maximized always. The error has been considered as the deviation of the hole. The hole diameter has been measured by optical microscope and HC has been listed in Table 4.1.

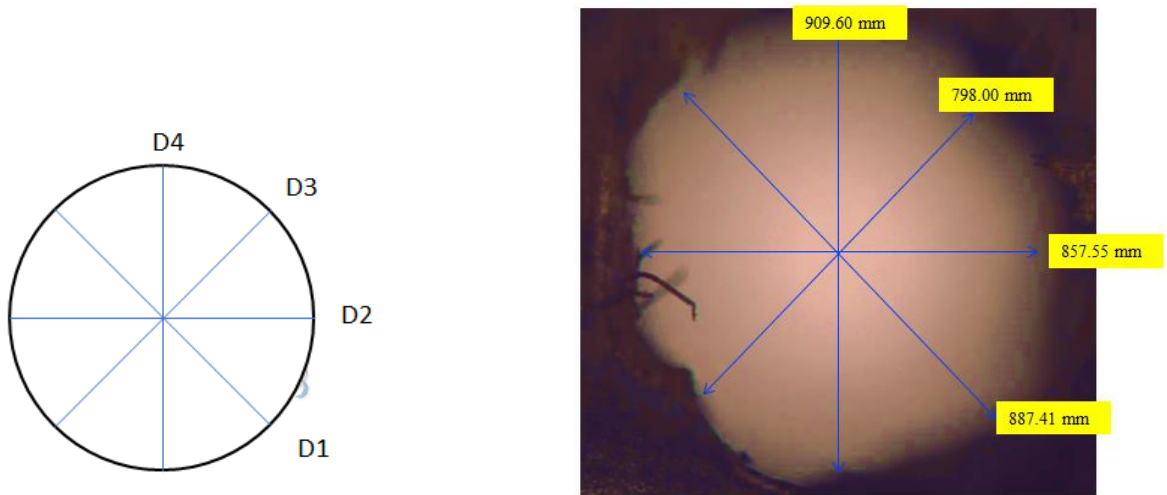


Fig.4.6: (a) Schematic measurement of hole diameter (b) Actual measurement of hole diameter

Table 4.1 and 4.2. has been listed the value of HC and HT. Fig.4.6 (a) and (b) presented the schematic and actual measurement of Hole diameter. Fig. 4.7 and Fig. 4.8 presented the variations between HC and HT respectively.

Table 4.1: Values of THC

Exp.No.	Parameters and their levels			D1	D2	D3	D4	Response
	$I(Amp)$	$f(Hz)$	$p(Kg/cm^2)$					THC
1	160	20	8	909.60	798.00	857.55	887.41	0.877
2	160	25	9	939.00	780.00	835.94	935.62	0.830
3	160	30	10	714.02	666.02	775.81	660.14	0.850



4	180	20	9	864.04	897.00	771.21	899.00	0.857
5	180	25	10	609.00	612.00	695.69	651.24	0.875
6	180	30	8	861.00	783.05	847.81	681.34	0.791
7	200	20	10	707.00	843.08	799.02	706.74	0.838
8	200	25	8	636.06	582.00	541.04	759.05	0.712
9	200	30	9	831.10	675.00	600.61	802.03	0.722

Table 4.2: Values of BHC and HT

Exp.No.	Parameters and their levels			D1	D2	D3	D4	Response	
	$I(\text{Amp})$	$f(\text{Hz})$	$p(\text{Kg/cm}^2)$					BHC	HT(degree)
1	160	20	8	738.00	768.02	714.76	777.89	0.918	2.29
2	160	25	9	723.05	738.09	634.12	761.91	0.832	2.30
3	160	30	10	819.04	720.02	738.13	774.12	0.879	1.14
4	180	20	9	888.51	729.12	730.40	865.65	0.820	1.14
5	180	25	10	753.05	663.10	663.21	745.53	0.880	1.14
6	180	30	8	609.06	732.00	738.81	611.56	0.824	2.20
7	200	20	10	696.00	765.02	676.09	663.41	0.867	1.14
8	200	25	8	738.00	756.14	706.68	732.68	0.934	2.29
9	200	30	9	759.00	724.01	612.12	827.26	0.739	2.10

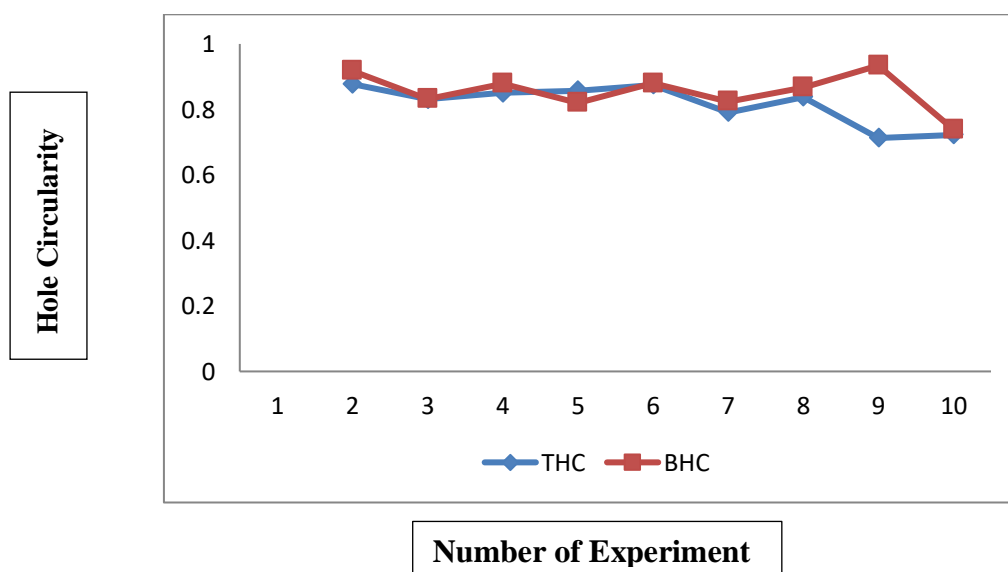


Fig. 4.7: Variation of THC and BHC for all experiments

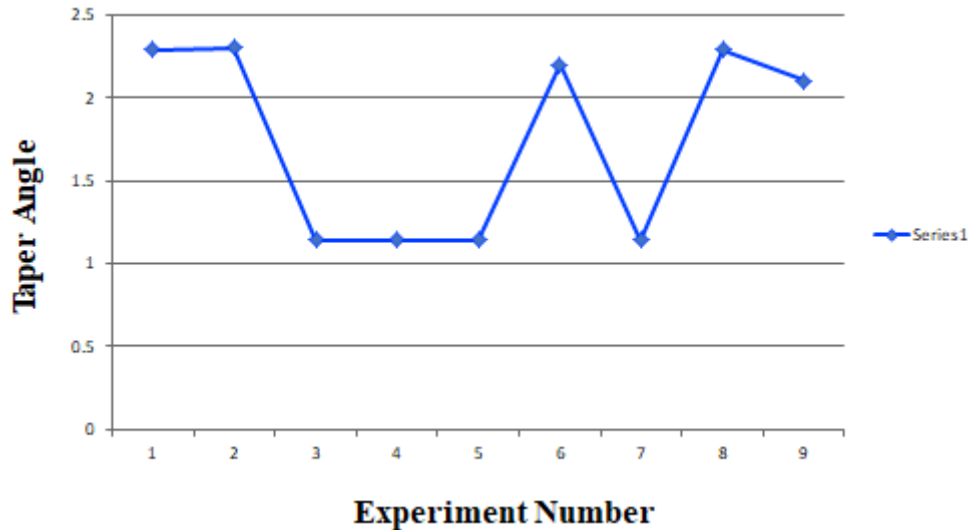


Fig. 4.8: Variation of HT Versus number of experiments

### 4.3 Linear Model Analysis and Validation

The Linear model has been analysed for THC, BHC and HT. The measured data has been considered to provide linear models of all calculated hole characteristics level. The estimated model coefficients have been calculated for S/N Ratios and Mean by MINITAB 17 expert software as listed in Table 4.3 and 4.4.

Table 4.3: Values of estimated model coefficients for SN ratios

<b>Term</b>	<b>Coef</b>	<b>SE Coef</b>	<b>T</b>	<b>P</b>
Constant	-1.7747	0.05924	-29.956	0.001
I 160	0.3904	0.08378	4.660	0.043
I 180	0.2672	0.08378	3.189	0.086
f 20	0.4405	0.08378	5.258	0.034
f 25	-0.1290	0.08378	-1.539	0.264
p 8	-0.2627	0.08378	-3.136	0.088
p 9	-0.1475	0.08378	-1.761	0.220
<b>S 0.1777</b>	<b>R-Sq98.31%</b>	<b>R-Sq(adj) 93.23%</b>		



Table 4.4: Values of estimated model coefficients for Means

<b>Term</b>	<b>Coef</b>	<b>SE Coef</b>	<b>T</b>	<b>P</b>
Constant	0.81740	0.005351	152.755	0.000
I 160	0.03550	0.007568	4.691	0.043
I 180	0.02407	0.007568	3.180	0.086
f 20	0.04037	0.007568	5.334	0.033
f 25	-0.01120	0.007568	-1.480	0.277
p 8	-0.02363	0.007568	-3.123	0.089
p 9	-0.01373	0.007568	-1.815	0.211

## 4.4 Optimization Technique

In this research, Optimize the response such as HC and HT by using Taguchi method such as .Further, identify the optimal value of drilling parameters.

### 4.4.1 Taguchi Optimization Technique

In this research, optimize the response such as HC and HT by using Taguchi method to obtain the S/N ratio for better HC suitable HT. Further, identify the optimal value of drilling parameters.

### 4.4.2 Result and Discussion for Hole Circularity

The response of S/N Ratio for hole circularity under various factors are listed in Table 4.5

Table 4.5: The response of S/N Ratio for different parameter settings

<b>Exp. No.</b>	<b>(I)Amp</b>	<b>(f)Hz</b>	<b>(p)Kg/cm<sup>2</sup></b>	<b>S/N Ratio</b>
1	160	20	8	-1.13704
2	160	25	9	-1.61216
3	160	30	10	-1.40345
4	180	20	9	-1.33228
5	180	25	10	-1.15686

6	180	30	8	-2.03318
7	200	20	10	-1.53305
8	200	25	8	-2.94186
9	200	30	9	-2.82204

The level values have been calculated by MINITAB 17 Program and represented in Table 4.5. Fig. 4.9 and Table 4.6 and Table 4.7 represented that the parameter (I) at first, parameter (f) at first and parameter (p) at third level. Therefore all the experiments have been done according to result obtained from MINITAB 17 Program. The result has been considered for obtain optimal drilling condition as 160 amp(I), 20 Hz (f) and 10 kg/cm<sup>2</sup>(p).

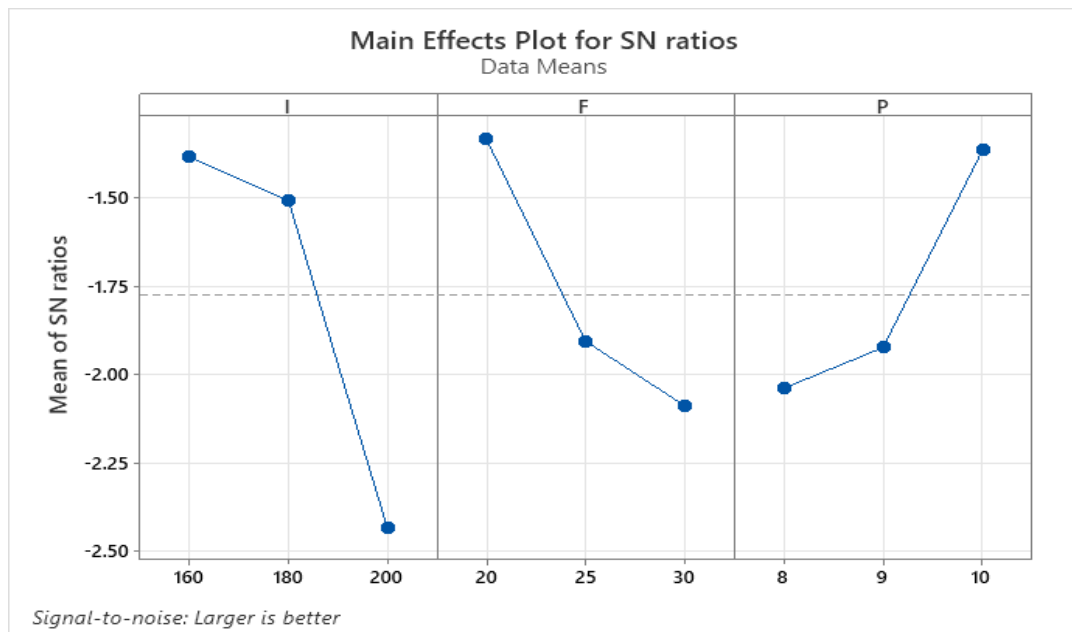


Fig.4.9 : Main effect graph for S/N ratios.

Table 4.6: Result for S/N Ratio

Level	(I)Amp	(f)Hz	(p)Kg/cm <sup>2</sup>
1	-1.384	-1.334	-2.037
2	-1.507	-1.904	-1.922
3	-2.432	-2.086	-1.364
<b>Delta</b>	0.286	0.752	0.673
<b>Rank</b>	1	2	3

Since we have found signal to noise ratio by considering “larger is better” in case of hole circularity, it should be maximized. So From Table 4.6 S/N ratio for lamp current (I) have values (-1.384) corresponding their level (160 amp),for frequency (f) has their value (-1.334) corresponding their level (20 Hz) and for air pressure (p) has value (-1.364) corresponding their level (10 kg/cm<sup>2</sup>) so we can say that the optimal condition for Hole circularity will be I=(160amp), f = 20Hz, and p = 10 kg/cm<sup>2</sup>

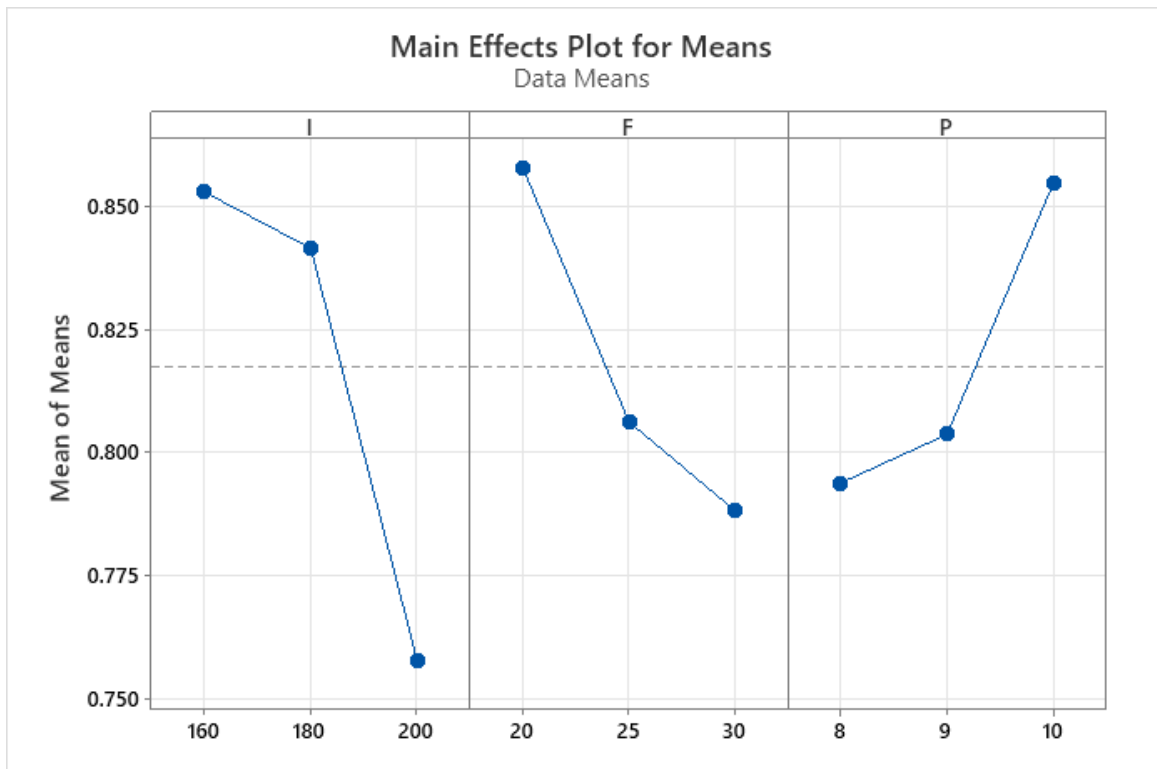


Fig.4.10: Main effect graph for Means

Table 4.7: Result for Means

Level	(I)Amp	(f)Hz	(p)Kg/cm <sup>2</sup>
1	0.8529	0.8578	0.7938
2	0.8415	0.8062	0.8037
3	0.7578	0.7882	0.8548
<b>Delta</b>	0.0951	0.0695	0.0610
<b>Rank</b>	1	2	3

Main effect plot has been considered the variation of response with respect to drilling parameters value. From analysis, the air pressure has been considered small effect as compare to (I) and (f). Previous researchers have been suggested that the pulse frequency has more

significant than air pressure on the HC. But from Table 4.6 and Table 4.7. It is represented that (I) has major significant than (f) and (p) has been obtained small impact on hole circularity.. The full matrix of mean interaction plots for HC and HT are shown in Fig. 4.11 and 4.12 respectively.

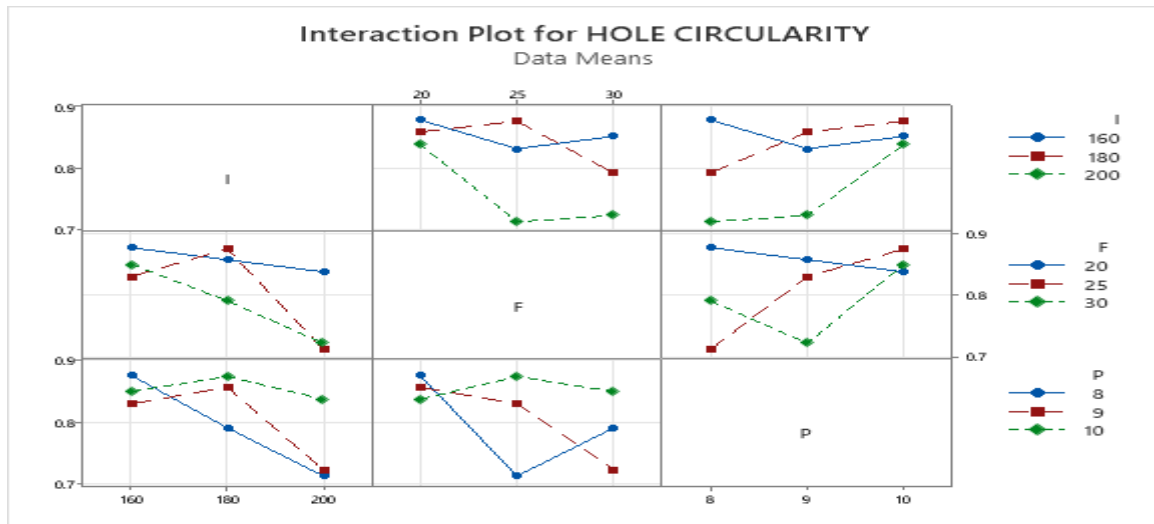


Fig. 4.11: Full matrix of mean interaction plots for THC

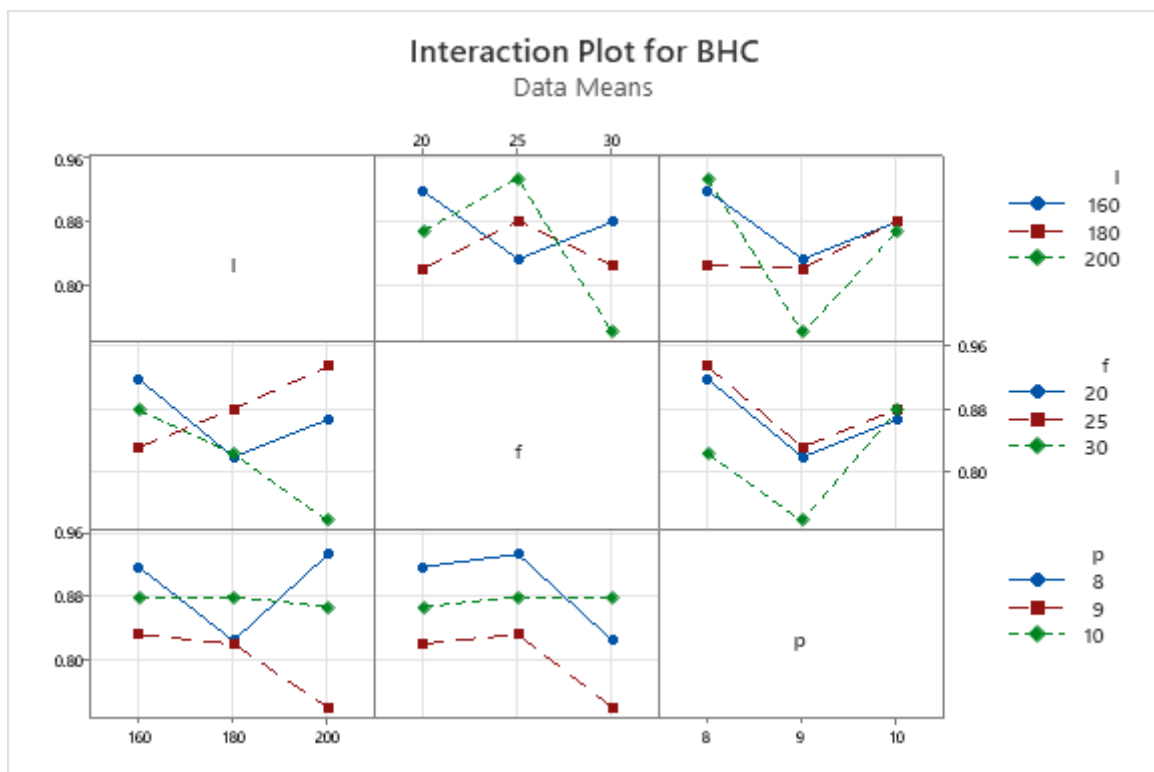


Fig. 4.12: Full matrix of mean interaction plots for BHC

The lowest value of THC was achieved at the higher level of I (200 Amp), moderate levels of f (25 Hz), and lower level of p (9 kg/cm<sup>2</sup>). While, lowest value of BHC was achieved at the

moderate levels of  $f$  (25 Hz) and  $I$  (200 Amp) and higher level of  $p$  (10 kg/cm<sup>2</sup>). Since Kevlar has high heat resisting material due to which heat affected zone may also be increases. The reason is behind that the value of  $I$  (200 Amp) increase the amount of absorbed thermal energy as shown in Fig.4.12 , therefore moderate ranges of lamp current ( $I$ ) are required for proper drilling.

### 4.4.3 ANOVA for Hole Circularity

The  $p$  values have been considered in Table 4.8 and Table 4.9. For drilling factor, It is found as 0.031, 0.062 and 0.074 and Percentage contribution are 0.522, 0.252 and 0.207 respectively. Previous researcher has suggested the same result [84].

Table 4.8: ANOVA for Means

S. No.	Factor	DF	SS	MS	F	P	Percentage Contribution
1	$I$	2	0.016163	0.008081	31.36	0.031	0.5227
2	$F$	2	0.007817	0.003908	15.17	0.062	0.2528
3	$P$	2	0.006430	0.003215	12.48	0.074	0.2079
4	Residual Error	2	0.000515	0.000258			0.0166
5	Total	8	0.030925				

Table 4.9: ANOVA for S/N Ratio

S. No.	Source	DF	SS	MS	F	P	Percentage contribution
1	$I$	2	1.96910	0.98455	31.17	0.031	0.5275
2	$F$	2	0.92334	0.46167	14.62	0.064	0.2474
3	$P$	2	0.77711	0.38856	12.30	0.075	0.2082
4	Residual Error	2	0.06317	0.03159			0.0169
5	Total	8	3.73272				

## 4.4.4 Result and Discussion for Hole Taper

In this study, Taguchi technique has considered to obtain the suitable result of drilling factor to minimize the response .S/N Ratio has been evaluated and observed the plot as listed in Table 4.10.

Table 4.10: S/N Ratio under different parameter settings

Exp. No.	$I(\text{Amp})$	$f(\text{Hz})$	$p(\text{Kg/cm}^2)$	S/N Ratio
1	160	20	8	-7.19671
2	160	25	9	-7.23456
3	160	30	10	-1.13810
4	180	20	9	-1.13810
5	180	25	10	-1.13810
6	180	30	8	-6.84845
7	200	20	10	-1.13810
8	200	25	8	-7.19671
9	200	30	9	-6.44439

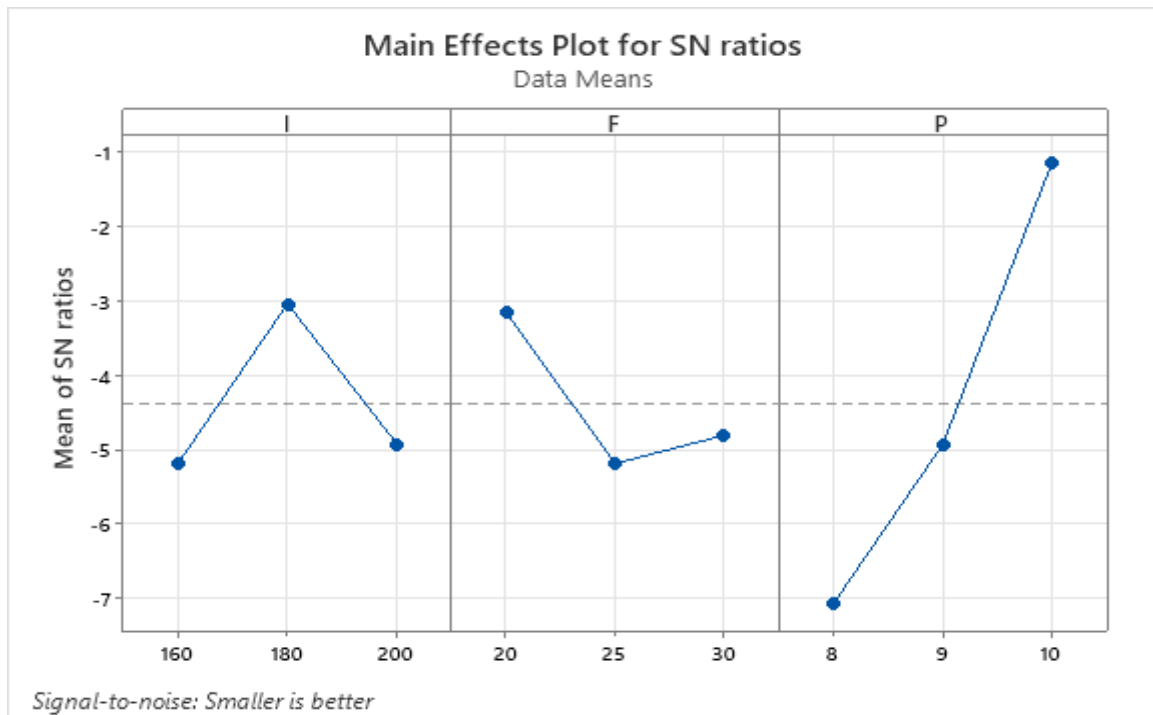


Fig.4.13: Main effect graph for S/N ratio

Table 4.11: Result for S/N ratio

Level	<i>I(Amp)</i>	<i>f(Hz)</i>	<i>p(Kg/cm<sup>2</sup>)</i>
1	-5.190	-3.158	-7.081
2	-3.042	-5.190	-4.939
3	-4.926	-4.810	-1.138
Delta	2.148	2.032	5.943
Rank	2	3	1

Fig.4.13 and Table 4.11 represented The factor I , f and p has been followed the sequence of level as per (121). Therefore all experiments it has been found that optimal solutions may be achieved at 160 amp for I, 25 Hz for f and 8 kg/cm<sup>2</sup> for p. Since we have found signal to noise ratio by considering “Smaller is better” in case of hole taper, it should be minimized. So From Table 4.11 S/N ratio for lamp current (I) has value(-5.190) corresponding their level (160 amp),for frequency (f) has their value (-5.190) corresponding their level (25 Hz) and for air pressure (p) has value (-7.081) corresponding their level (8 kg/cm<sup>2</sup>) so we can say that the optimal condition for Hole Taper will be I=(160amp), f = 25Hz, and p = 8 kg/cm<sup>2</sup>

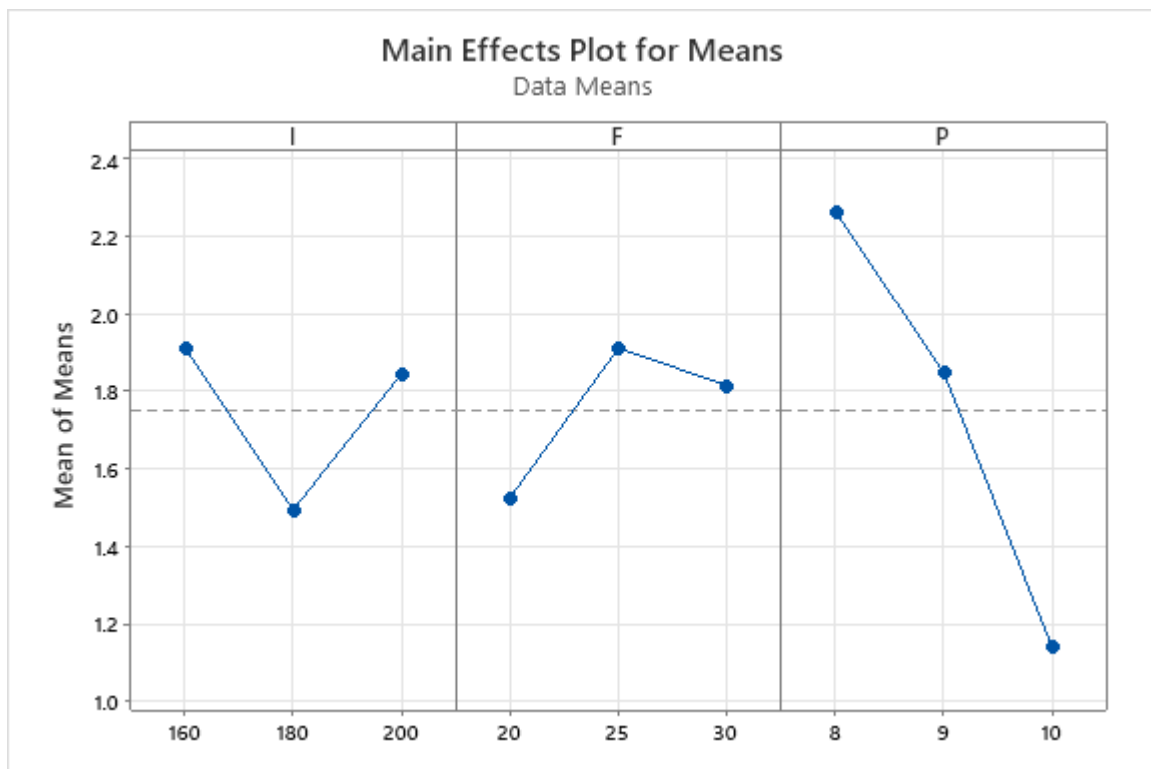


Fig.4.14: Main effect graph for Means

Table 4.12: Result for S/N ratio

Level	$I(\text{Amp})$	$f(\text{Hz})$	$p(\text{Kg/cm}^2)$
1	1.910	1.523	2.260
2	1.493	1.910	1.847
3	1.843	1.813	1.140
Delta	0.417	0.387	1.120
Rank	2	3	1

As the rank represented that the (p) has high significant factor for HT as in comparison to other two factors but it has been observed in Fig.4.14 and Table 4.12 that (p) has major role then (I) and after then (f) has been observed less impact.

#### 4.4.5 Optimal Values of Process Parameters

Table 4.6 and Table 4.11 presented suitable values of drilling factors to maximize the hole for HC and minimize the HT. By using response, it has been observed that suitable values of I for hole circularity are 160 Amp,  $f=20\text{Hz}$  and  $p= 10\text{kg/cm}^2$  respectively. Similarly it has been also observed that optimal values for Hole Taper I=160 Amp,  $f= 25\text{Hz}$  and  $p= 8 \text{ kg/cm}^2$  respectively. From Table 4.8 and Table 4.9, The p values have been, found as 0.031, 0.062 and 0.074 and F values have been found as 31.36, 15.17 and 12.48.

### 4.5 Conclusions

The main outcomes drawn by this research are concluded in below:

- The response of HC and HT have been recorded and analysed for KFRP Composite sheet.
- It is found that most significant factor as lamp current while (p) as less reliable factor for HC of KFRP sheet.
- The most reliable parameter is air pressure for the HT while (f) has less factor
- In this research, the proposed methodology will be provided the new approach to new researcher for developing the relation for drilling parameters and response during laser drilling of KFRP composite laminate



## **4.6 Summary**

In this chapter, Experimental Investigation and Parametric Optimization of the Hole Circularity and Hole Taper during Laser Drilling of 1.2 mm thickness of Kevlar-29 have been discussed. Experiments have been conducted on the basis of proper design of experiments technique. The optimum value of laser drilling parameters has been identified by using Taguchi techniques. In the next chapter, Parametric Optimization of Hole Quality in Laser Drilling of 1.2mm thickness of Kevlar/Basalt Hybrid FRP Composite has been discussed. The optimum value of laser drilling parameters has been identified by using Taguchi techniques.

# Chapter 5

## Parametric Optimization of Hole Quality In Laser Drilling Kevlar/Basalt Hybrid FRP Composite

### 5.1 Introduction

In the previous chapter, A mathematical model has been presented for various hole quality characteristics by using pulsed Nd:YAG laser drilling of KFRP composite laminate. Moreover, the optimal process parameter has been fixed in Taguchi method. In the present chapter, KBFRP hybrid composite laminate having thickness 1.20 mm has been prepared and used as a workpiece for laser drilling. Three different laser drilling parameter has been considered such as I, p & f to conduct experiments. Both sides of quality characteristics like Top side and bottom side hole circularity have been considered as output response. For better hole circularity, S/N ratio should be maximized. Further the confirmation of experiment has been considered and validated the result. Pictorial representation of phase methodology used in this chapter is shown in Fig. 5.1.

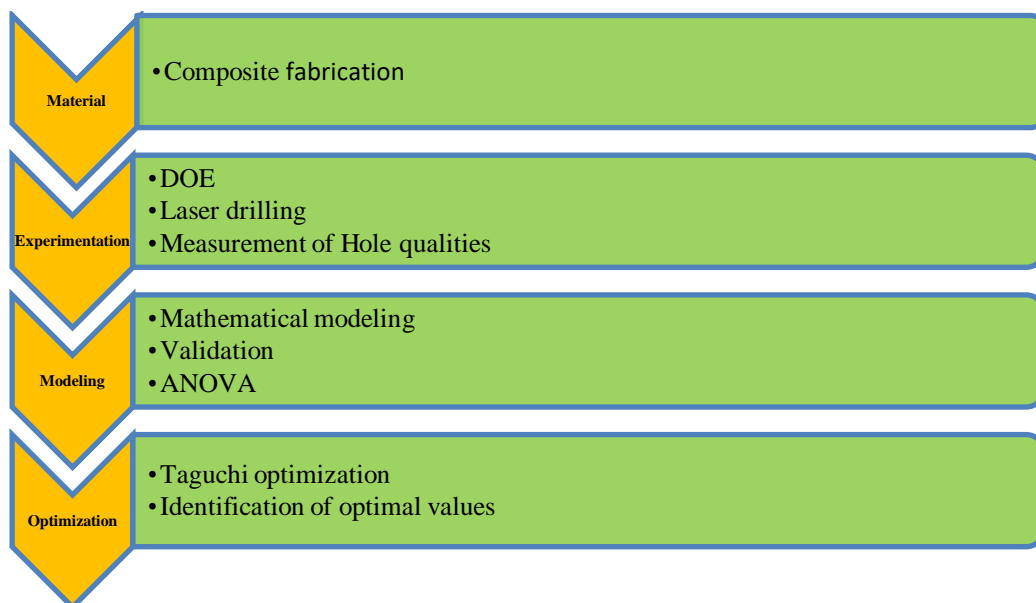


Fig. 5.1: Flow Chart of methodology

## 5.2 Material, Experimentation and Measurement

### 5.2.1 Material

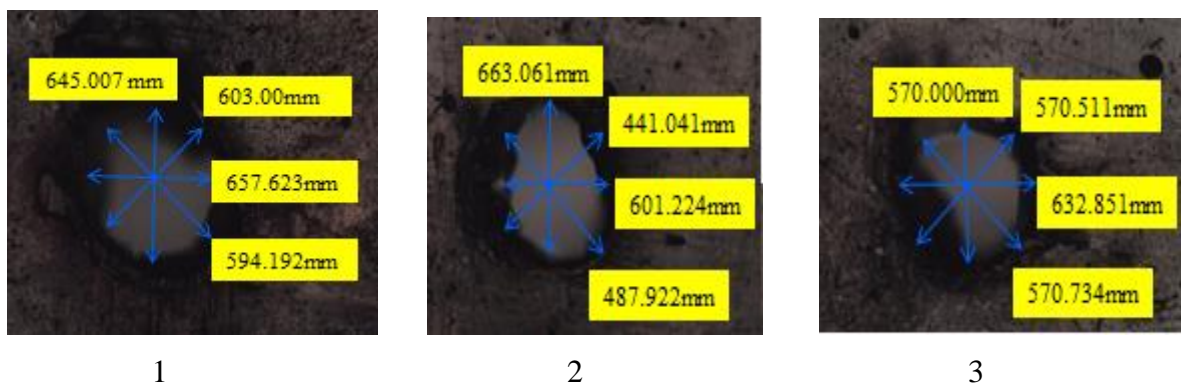
KBFRP composite laminate having thickness 1.20 mm is used as sample. Sample has been prepared by Hand layup method. The stacking sequence of sample has been considered like  $[B-0^\circ/K-0^\circ/B-45^\circ/K-45^\circ/B-0^\circ]_5$  for five layers of fibers.

### 5.2.2 Experimentation & Measurement

Conduction of experiment on KFRP Composite has been employed by 250W Nd:YAG Laser in RRCAT, Indore. Conduction of experiment has been performed on the basis of  $L_9$  Orthogonal array. After that, the response such as hole circularity has been measured as shown in Fig.5.6 (a) & (b) for Experiment no.1 and optimize the hole circularity. Further confirm the experiment and validate the response result. A 1.0 mm drilled hole has been conducted to find different hole quality characteristics. Fig. 5.2 & 5.4 shows the both side images of KBFRP composite after conducting experiments.



Fig. 5.2: Image of top side of hybrid KBFRP composite after laser drilling



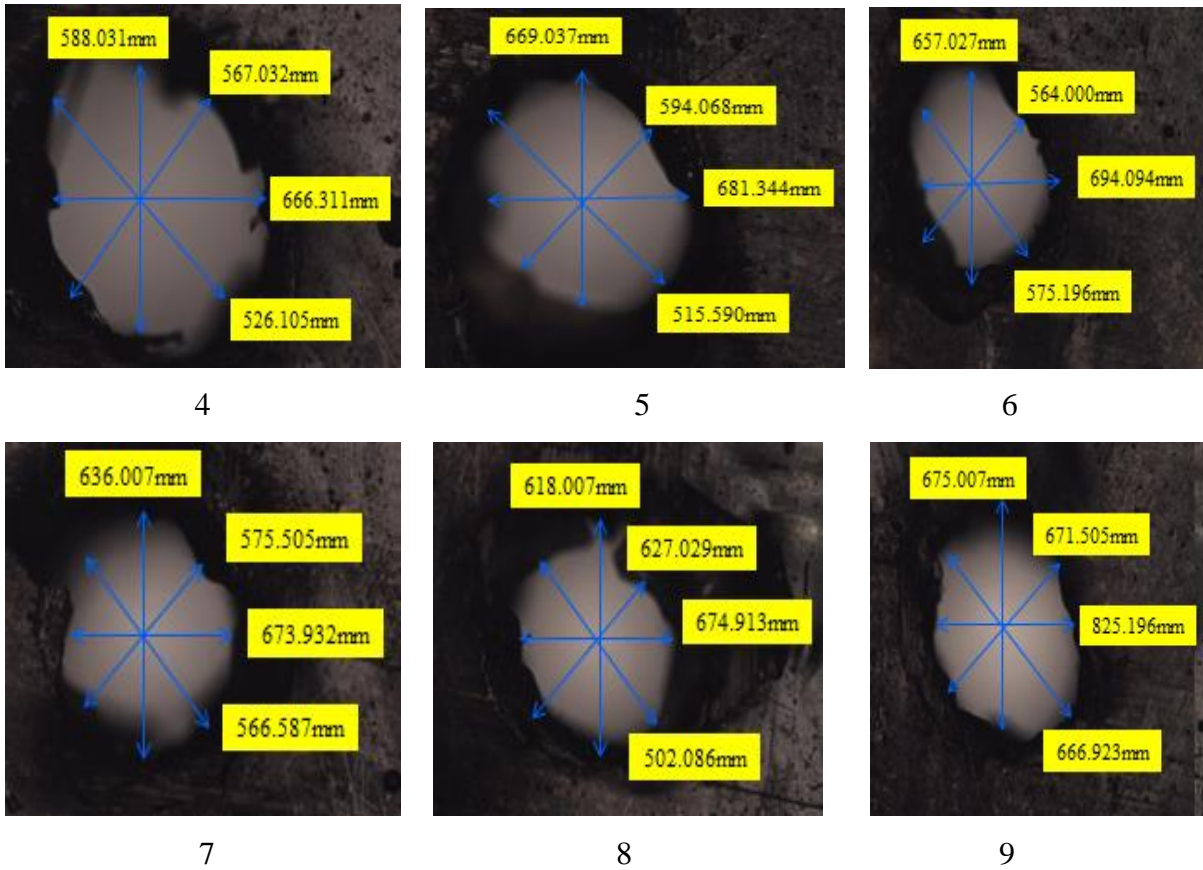


Fig. 5.3: Image of holes (9 nos.) obtained from optical microscope for KFRP composite (Top side)

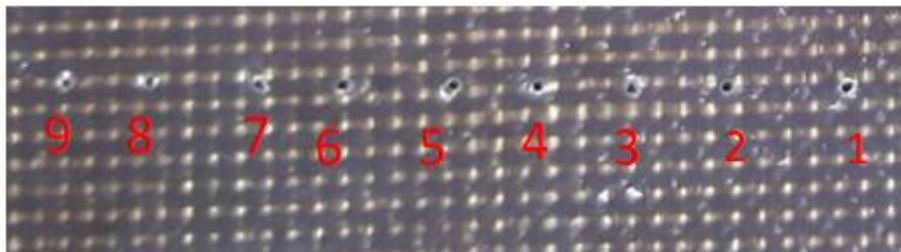
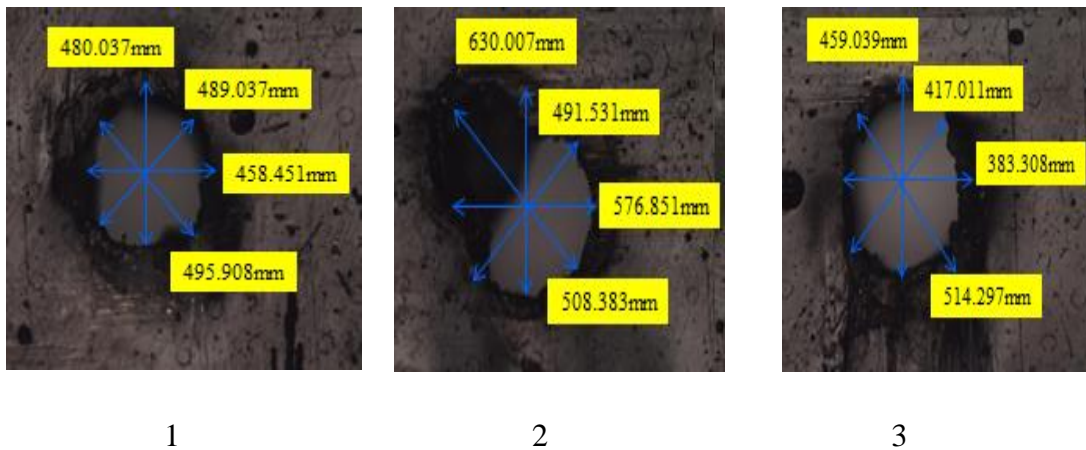


Fig. 5.4: Image of bottom side of hybrid KBFRP composite after laser drilling





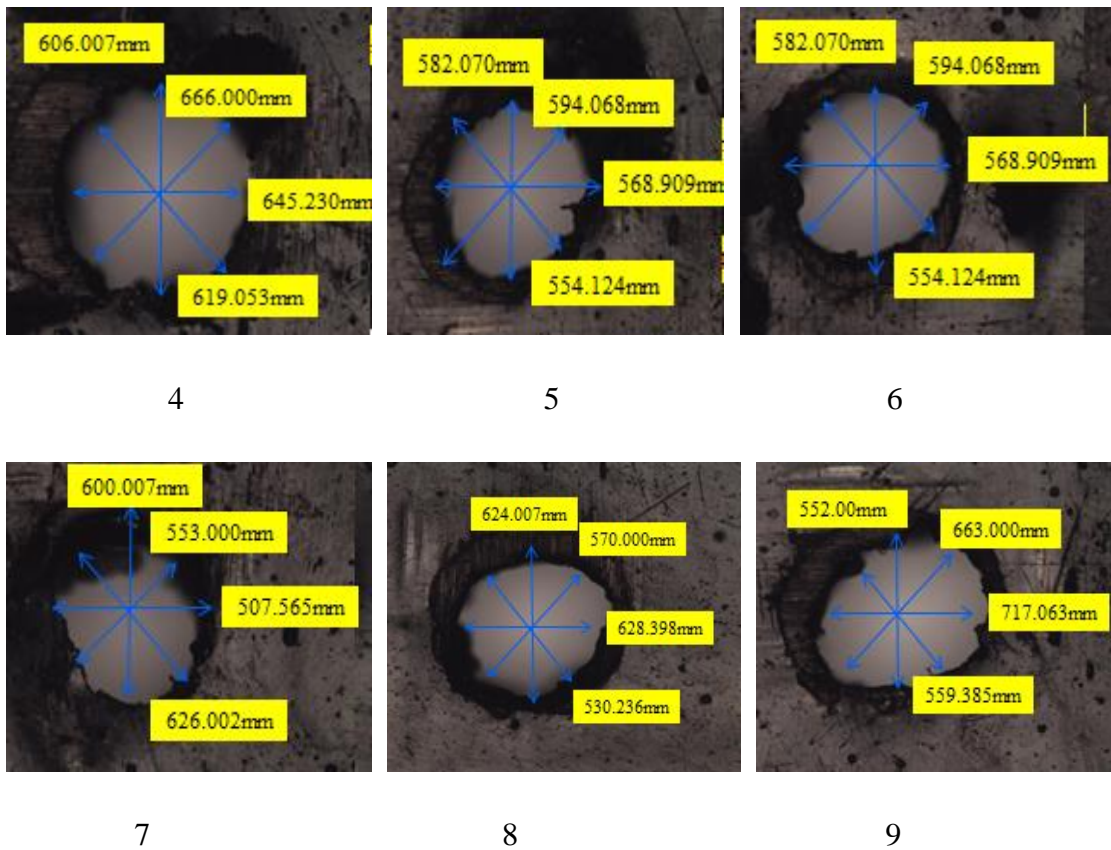


Fig. 5.5: Image of holes (9 nos.) obtained from optical microscope for KFRP composite (Bottom side)

The Hole Circularity is calculated by using Eq. (3.1) respectively. For better hole circularity, it should be maximized always. The error has been considered as the deviation of the hole. Hole diameter has been measured by stereo optical microscope as represented by Fig.5.6 (a) and (b). The Hole Circularity (HC) has been calculated as listed in Table 5.1.



Fig.5.6: (a) Schematic measurement of hole diameter (b) Actual measurement

The Hole Circularity is listed in Table 5.1 and 5.2. The variations in Hole Circularity of both sides are shown in Fig. 5.7 respectively.

Table 5.1: Values of THC with parameters setting

Exp.No.	Factors and their levels								Response
	<i>I</i>	<i>f</i>	<i>p</i>	D1					D2
	(Amp)	(Hz)	(Kg/cm <sup>2</sup> )						
1	160	20	8	645.007	603.000	657.623	594.192	0.9169	
2	160	25	9	663.061	441.041	601.224	487.922	0.6650	
3	160	30	10	570.000	570.511	632.851	570.734	0.9006	
4	180	20	9	588.031	567.032	666.311	526.105	0.7895	
5	180	25	10	669.037	594.068	681.344	515.59	0.7706	
6	180	30	8	657.027	564.000	694.094	575.196	0.8584	
7	200	20	10	636.007	575.505	673.932	566.587	0.8908	
8	200	25	8	618.007	627.029	674.913	502.086	0.8007	
9	200	30	9	675.007	671.505	825.196	666.923	0.8081	

Table 5.2: Values of BHC

Exp.No.	Parameters and their levels								Response
	<i>I</i>	<i>f</i>	<i>P</i>	D1					D2
	(Amp)	(Hz)	(Kg/cm <sup>2</sup> )						
1	160	20	8	480.037	489.037	458.451	495.908	0.9244	
2	160	25	9	630.007	491.531	576.851	508.383	0.7801	
3	160	30	10	459.039	417.011	383.308	514.297	0.7453	
4	180	20	9	606.007	666.000	645.23	619.053	0.9099	
5	180	25	10	582.070	594.068	568.909	554.124	0.9327	
6	180	30	8	611.505	573.031	594.212	587.245	0.937	
7	200	20	10	600.007	558.000	507.565	626.002	0.8108	
8	200	25	8	624.007	570.000	628.398	550.236	0.8756	
9	200	30	9	552.000	663.000	717.063	559.385	0.7698	

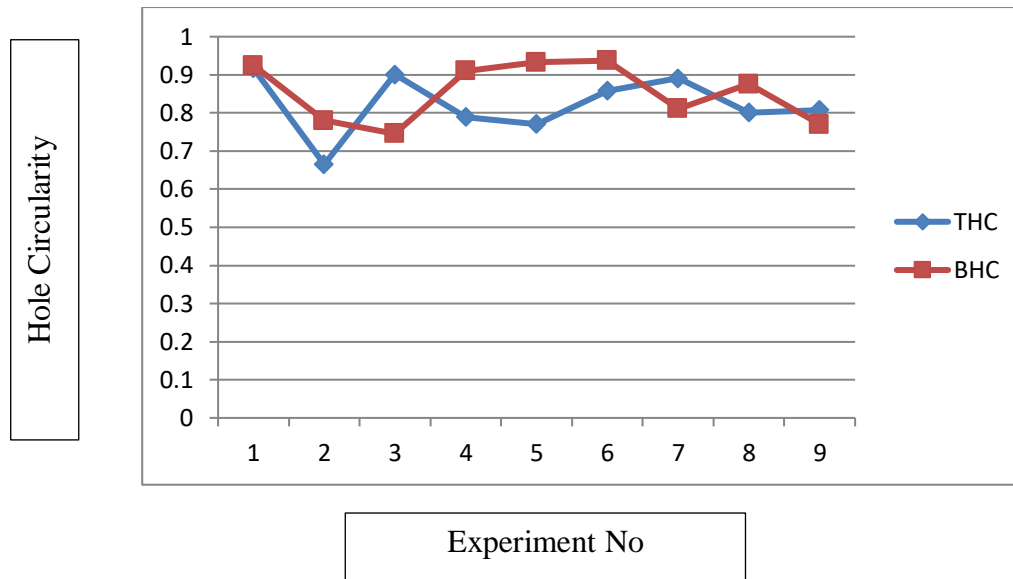


Fig. 5.7: Variation of THC and BHC for all experiments

### 5.3 Optimization Technique

In this research, optimize the response such as hole circularity by using Taguchi method. Further, identify the suitable value of drilling parameters for KBFRR composite laminate.

#### 5.3.1 Taguchi Optimization Technique

Result has been observed on the basis of (S/N) ratio. Two different graphs related to main effect graph for mean and S/N Ratio has been considered for HC for each experiments.

#### 5.3.2 Result and Discussion

The response of S/N Ratio for HC for different parameter setting are given in Table 5.3

Table 5.3: The response of S/N Ratio for different setting

Exp. No.	$I(\text{Amp})$	$f(\text{Hz})$	$p(\text{Kg/cm}^2)$	S/N Ratio
1	160	20	8	-4.09631
2	160	25	9	-5.22439
3	160	30	10	-4.64205
4	180	20	9	-4.64205
5	180	25	10	-4.22250

6	180	30	8	-4.12419
7	200	20	10	-4.25079
8	200	25	8	-4.36489
9	200	30	9	-2.98708

Table 5.3 represented the level values for different drilling factors which may be calculated with the help of MINITAB 17 Program. Fig. 5.8 and Table 5.4 and Table 4.7 represented the factors such as I, f and p has been followed the level sequence as (311) for conducting the experiment and Table 4.7. Therefore conduction of experiments has been performed according to 200 Amp (I), 20 Hz (f) and 8 Kg/cm<sup>2</sup> (p) to obtain optimum drilling condition.

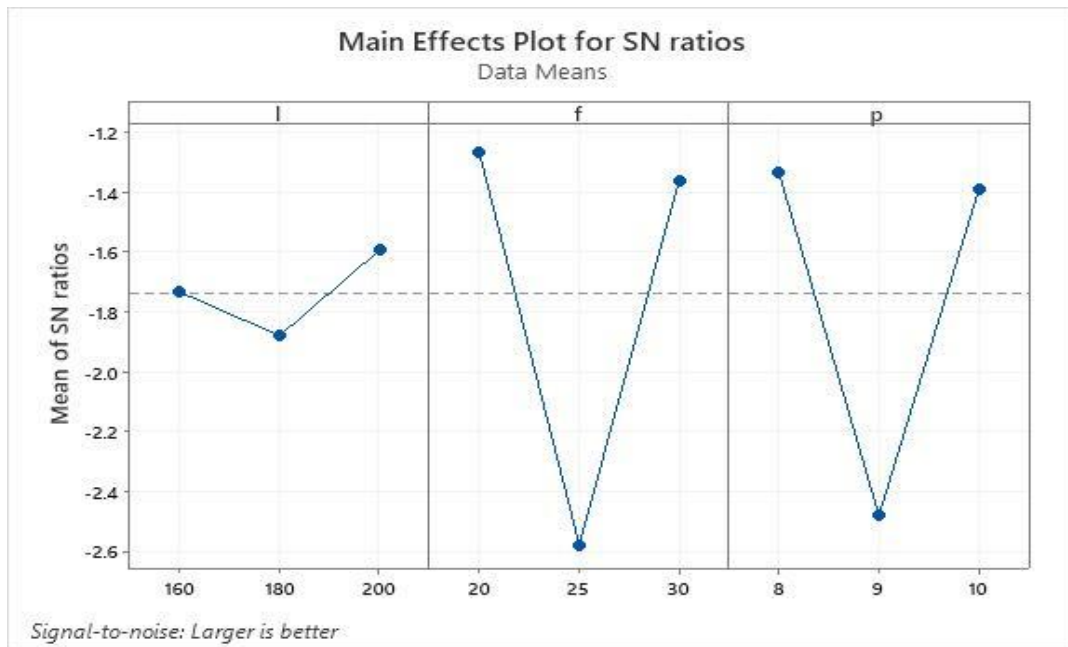


Fig.5.8: Main Effect graph for S/N ratios.

When lamp current will be changed from 160-180amp, the corresponding S/N Ratio values will be decreased, further increased the value of lamp current from 180-200amp, the corresponding S/N Ratio will be increased and this pattern will be same in case of pulse frequency as well as gas pressure.



Table 5.4: Result for S/N Ratios

Level	$I(\text{Amp})$	$f(\text{Hz})$	$p(\text{Kg/cm}^2)$
1	-1.735	-1.270	-1.332
2	-1.881	-2.579	-2.482
3	-1.595	-1.362	-1.392
Delta	0.286	1.309	1.146
Rank	3	1	2

Since we have found signal to noise ratio by considering “larger is better” in case of hole circularity, it should be maximized. So From Table 5.4 S/N ratio for lamp current (I) have values (-1.595) corresponding their level (200 amp), for frequency (f) has their value (-1.270) corresponding their level (20 Hz) and for air pressure (p) has value (-1.332) corresponding their level (8 kg/cm<sup>2</sup>) so we can say that the optimal condition for Hole circularity will be I=200amp), f = 20Hz, and p = 8 Kg/cm<sup>2</sup>

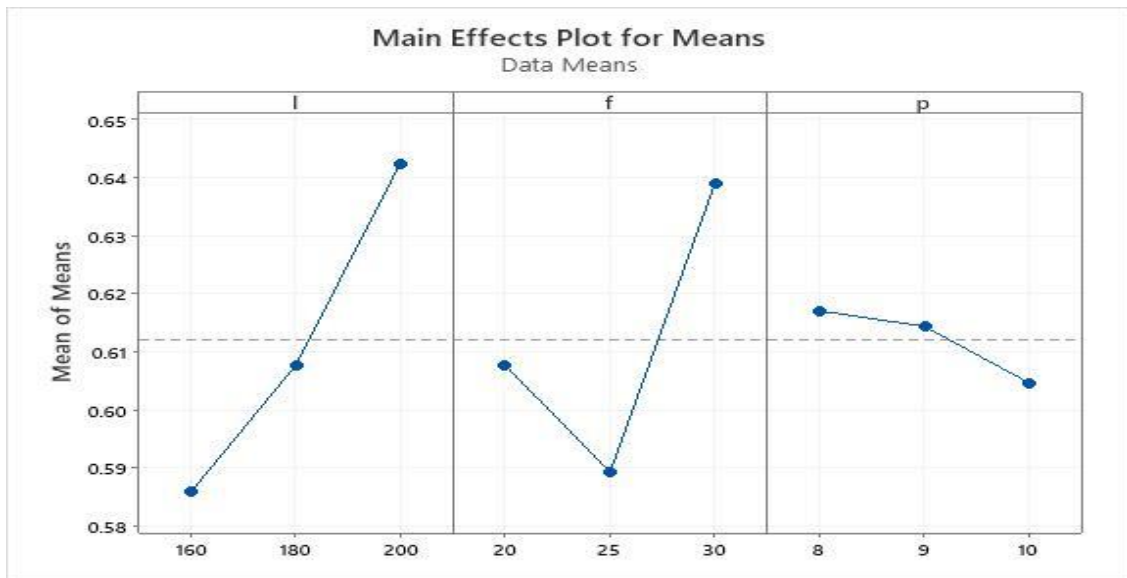


Fig.5.9: Main Effect graph for Means

Table 5.5: Result for Means

Level	$I(\text{Amp})$	$f(\text{Hz})$	$p(\text{Kg/cm}^2)$
1	0.8275	0.8657	0.8587
2	0.8062	0.7454	0.7542
3	0.8332	0.8557	0.8540

Delta	0.0270	0.1203	0.1045
Rank	3	1	2

Main effect plot has been considered the variation of response with respect to drilling parameters value. From analysis, the lamp current has been considered small effect as compare to pulse frequency and pulse air pressure.

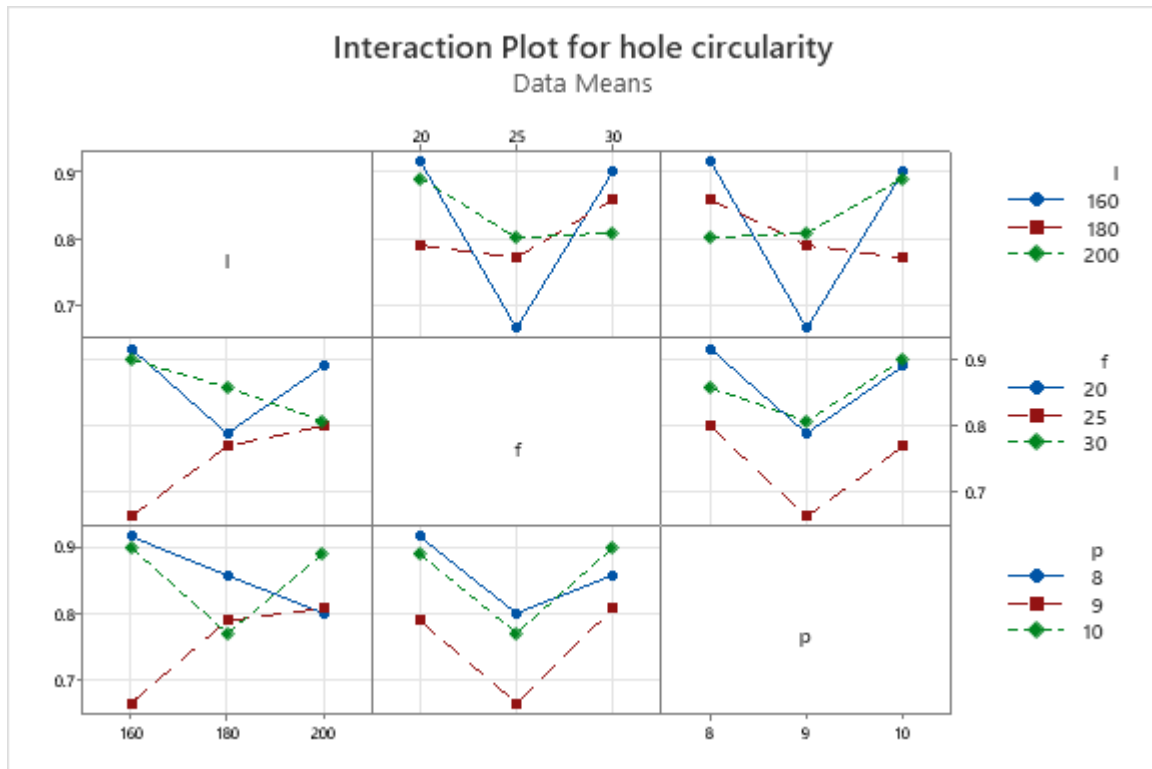


Fig.5.10: Full matrix of mean interaction plots for HC

From Fig.5.10, The lamp current (I) was achieved the lowest and highest value of HC that is (0.7) at lower level of I (160 Amp) as shown in the mean interaction plot. Similarly pulse frequency (f) was achieved lowest value of HC at the moderate levels of f (25 Hz) and highest value of HC that is (0.9) at the lowest levels of f (20 Hz) as shown in the mean interaction plot, Moreover Gas pressure (p) was achieved the lowest value of HC that is (0.7) at moderate level of p (9 kg/cm<sup>2</sup>). as shown in the mean interaction plot and highest value of HC that is (0.9) at lowest level of p (8 kg/cm<sup>2</sup>) as shown in the mean interaction plot

### 5.3.3 ANOVA

The p values have been listed in Table 4.8 and Table 4.9. For drilling factor, It is found as 0.642, 0.064 and 0.081 and Percentage contribution are 0.020, 0.529 and 0.413 respectively. Previous researcher has suggested the same result.

Table 5.6: ANOVA for Means

S. No.	Factor	DF	Sum of square	Mean square	F	P	Contribution
1	<i>I</i>	2	0.1224	0.06119	0.56	0.642	0.020
2	<i>F</i>	2	3.2030	1.60149	14.58	0.064	0.529
3	<i>P</i>	2	2.5037	1.25183	11.40	0.081	0.413
4	Error	2	0.2196	0.10981			0.036
5	Total	8	6.0486				

### 5.4 Conclusions

The optimum value of drilling parameter has been identified for KBFRP hybrid fiber composite during Nd:YAG laser. The analysis of the result has been done by ANOVA and proposed methodology has been accepted for improved response. Main conclusions of this work are:-

1. Optimum drilling conditions has been obtained by considering the suitable drilling parameter and their level as followed drilling sequence operation '311' were found to be 200 Amp for 'lamp current (I), 20 Hz for the 'pulse frequency (f) and 8 Kg/cm<sup>2</sup> for the 'air pressure (p).
2. Satisfactory result has been obtained by performing less conduction of experiment
3. Pulse frequency(f) is the most influencing factor for HC

### 5.5 Summary

In this chapter, Parametric Optimization of Hole Quality in Laser Drilling of 1.2mm thickness of Kevlar/Basalt Hybrid FRP Composite has been discussed. The optimum range of laser drilling parameters has been identified by using Taguchi techniques. In the next chapter; Evaluation of Hole Quality Characteristics in Laser Drilling of BFRP Composite Using Multi-Response Optimization Technique has been discussed.

# Chapter 6

## Particle Swarm based Optimization of Hole

### Characteristics during Laser Drilling of BFRP

#### 6.1 Introduction

In the last chapter, A mathematical model for various hole quality characteristics have been developed by using experimental results. Moreover, Taguchi optimization method has been used to fix their levels of process parameters. In the present report, a Basalt FRP composite laminate has been prepared and selected as the sample of work piece. Three laser drilling parameters have been considered like I, f and p to perform experiments. Different types of quality characteristics for both the sides have been considered like as Hole Circularity, Hole Taper and HAZ as response. Further, a mathematical model has been developed for both sides of HC, HT and HAZ by RSM. Two different techniques such as RSM based on Box-Behnken Design (BBD) and PSO are employed for multi-objective optimization. The optimal value of LBD parameters is signified as compared to the results of optimization method. Moreover, parametric effects on different hole quality characteristics also have been presented in detail. Process flow of this chapter is shown in Fig. 6.1

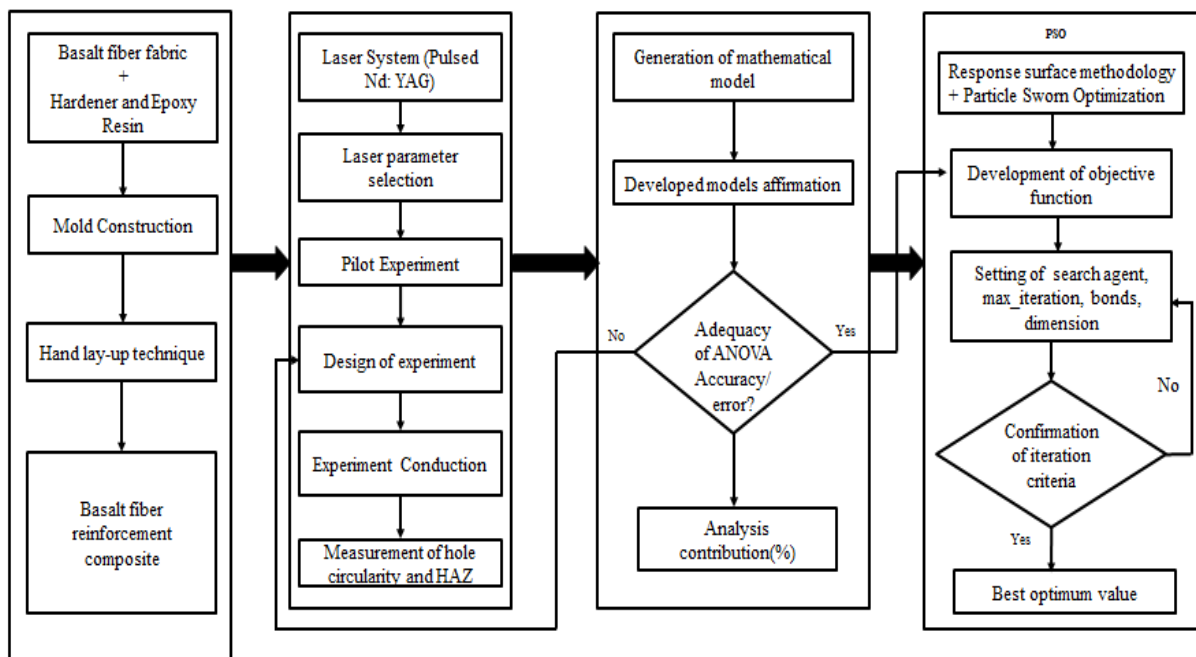


Fig.6.1: The flowchart of the methodology

## 6.2 Material, Experimentation and Measurement

### 6.2.1 Material

BFRP composite laminate having thickness 1.20 mm is used as sample. Sample has been prepared by Hand layup method. The stacking sequence of sample has been considered like of  $[B-0^\circ/B-45^\circ/B-0^\circ/B-45^\circ/B-0^\circ]_5$  for five layers of fibers.

### 6.2.2 Experimentation & Measurement

A 1.0 mm drilled hole has been performed to find different hole quality. Procedure of laser drilling experimentation and Hole Circularity, Taper Angel and HAZ analysis as shown in Fig. 6.2. The both sides of images of BFRP composite after conducting experiments as shown in Fig. 6.3 and 6.5.

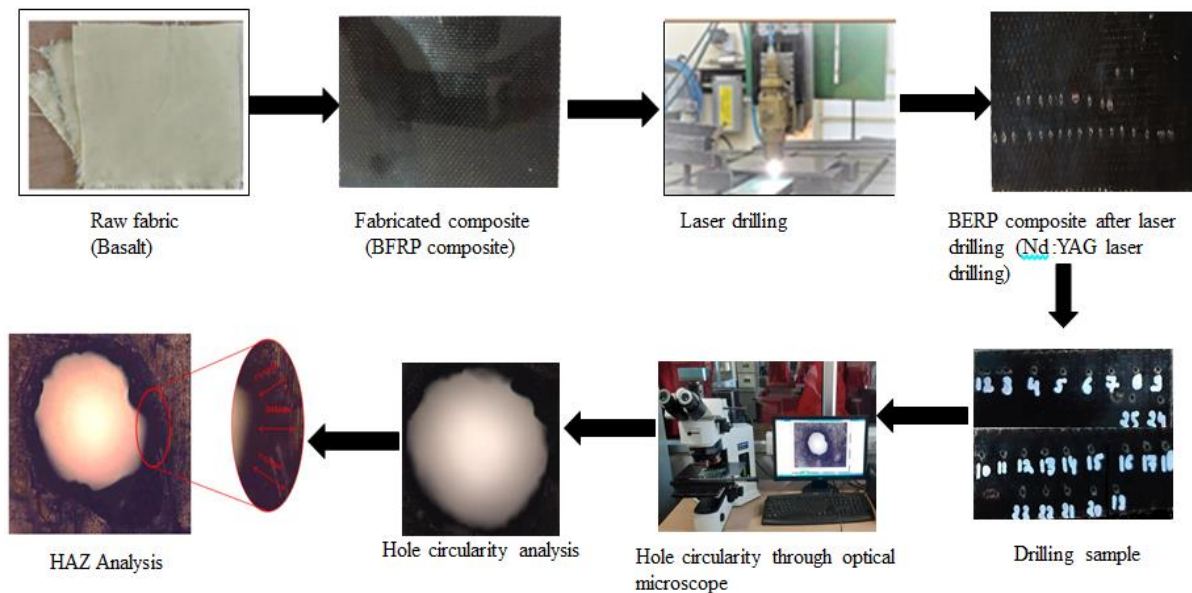


Fig.6.2: Procedure of laser drilling experimentation and Hole Circularity and HAZ analysis

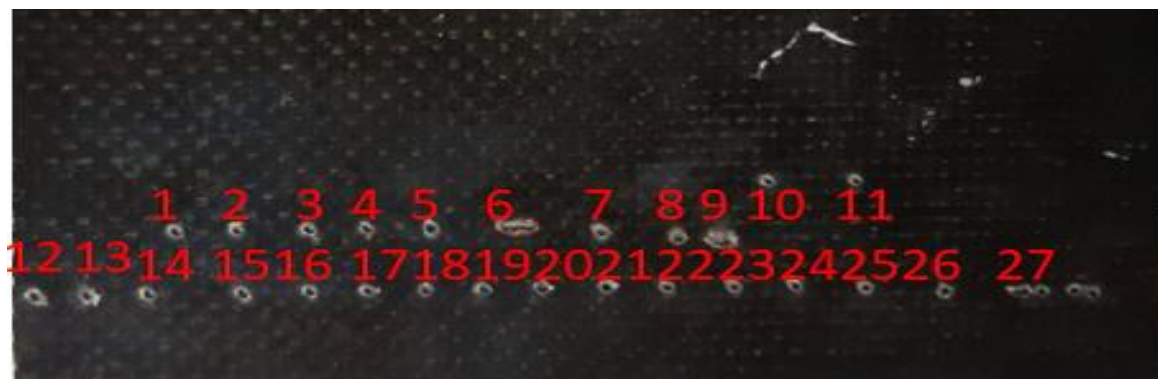
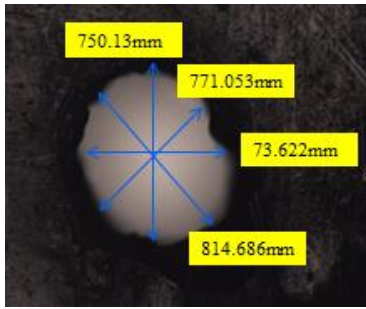
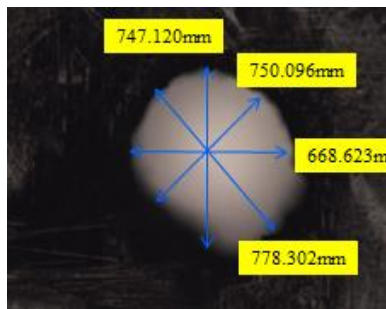


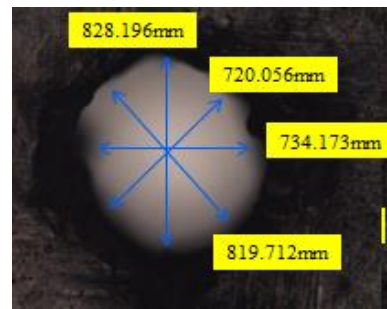
Fig.6.3: Top side Image of BFRP composite after laser drilling



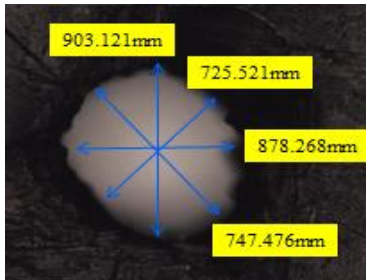
1



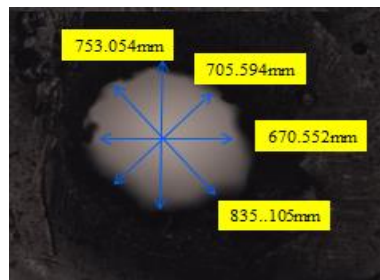
2



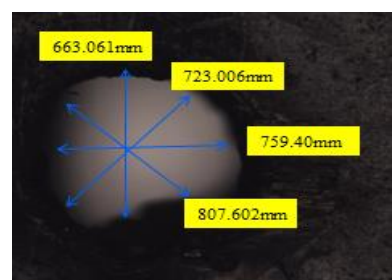
3



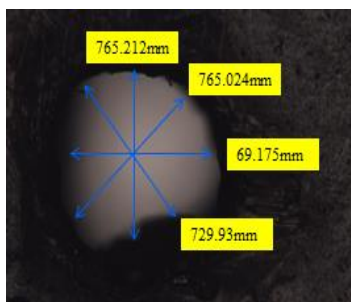
4



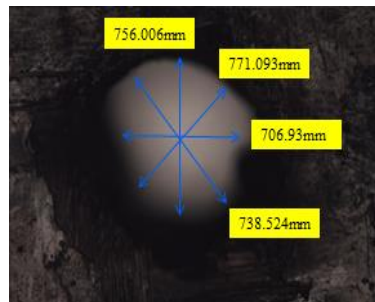
5



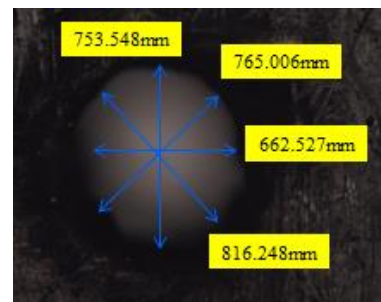
6



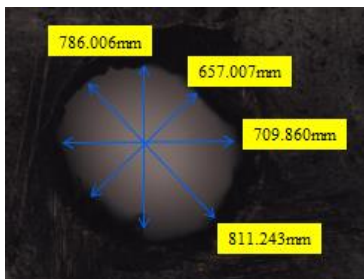
7



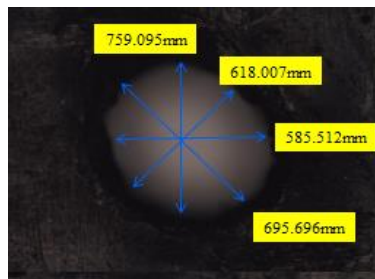
8



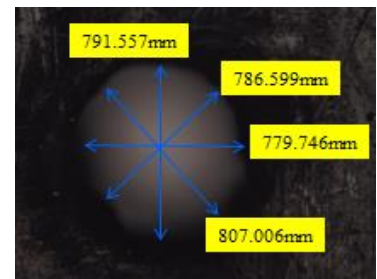
9



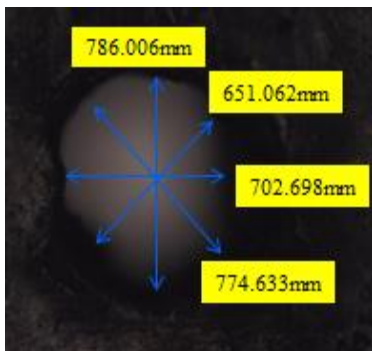
10



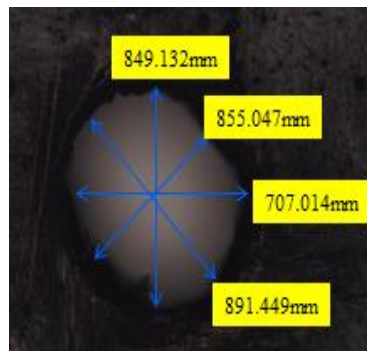
11



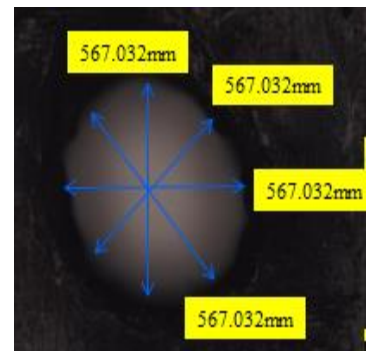
12



13



14



15



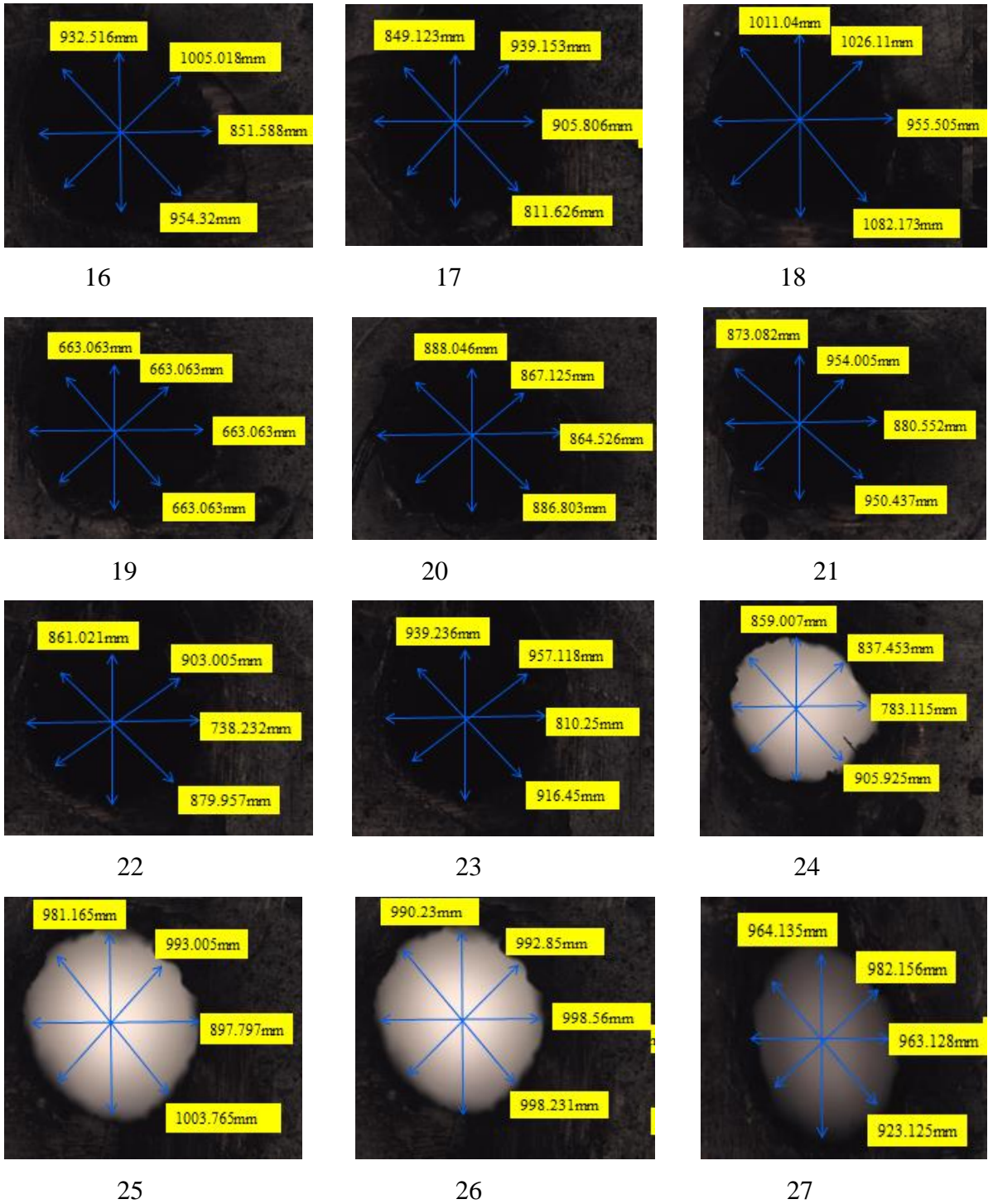
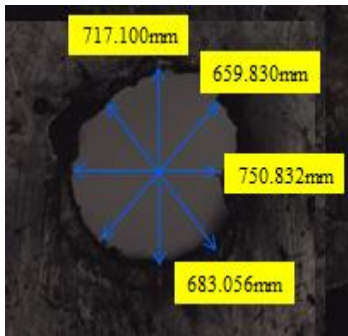


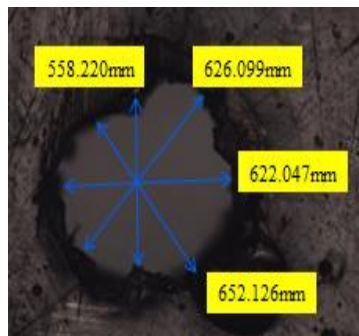
Fig. 6.4: Top side Image of holes (27 Nos.) obtained from optical microscope for BFRP composite



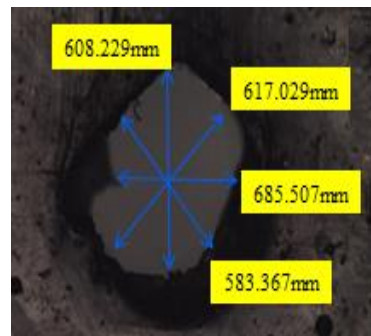
Fig. 6.5: Bottom side Image of BFRP composite after laser drilling



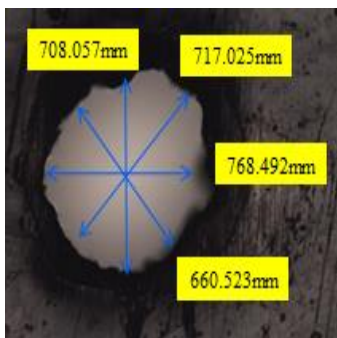
1



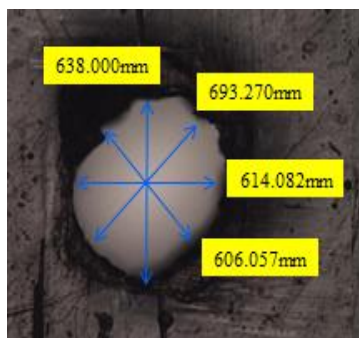
2



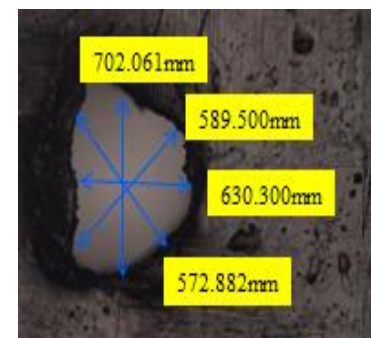
3



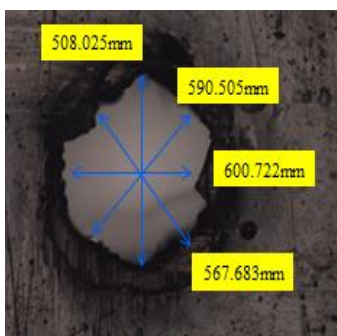
4



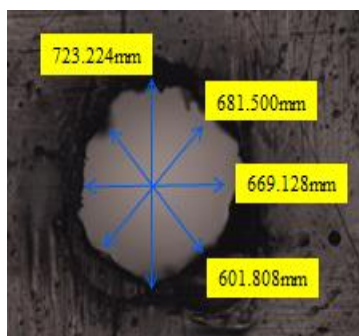
5



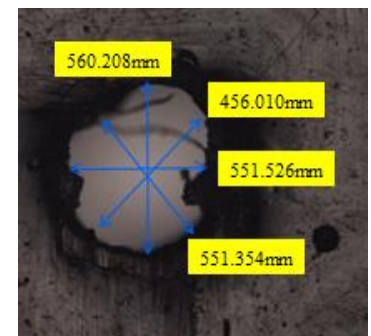
6



7

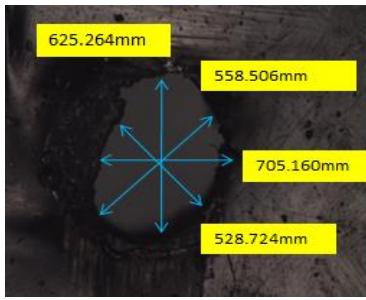


8

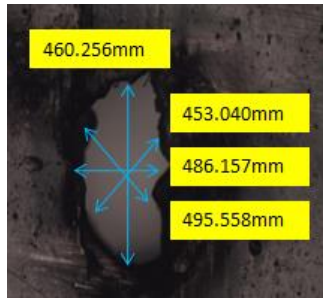


9

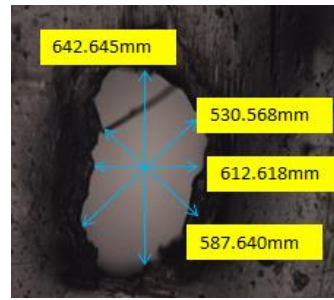




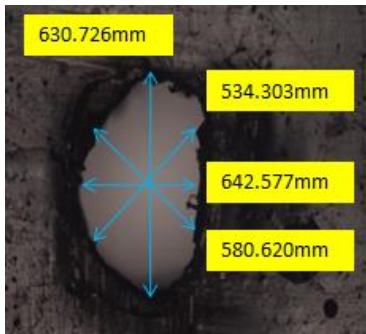
10



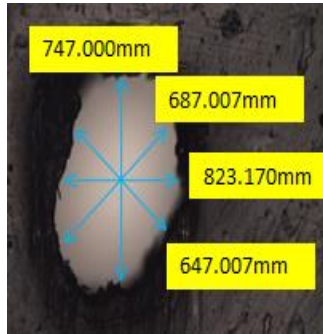
11



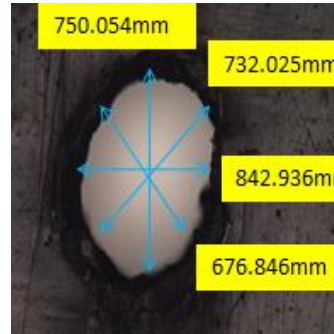
12



13



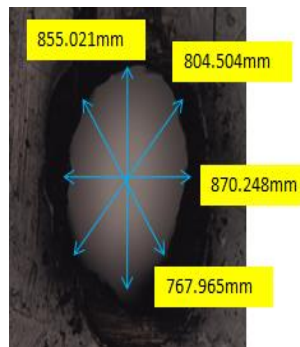
14



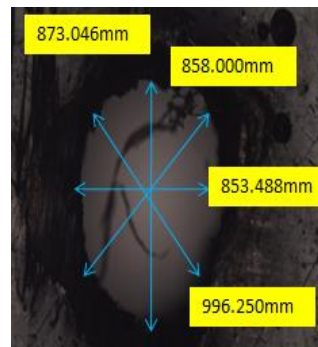
15



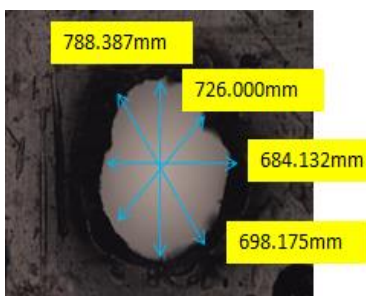
16



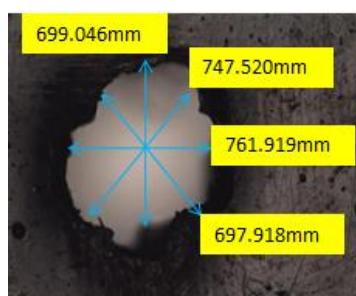
17



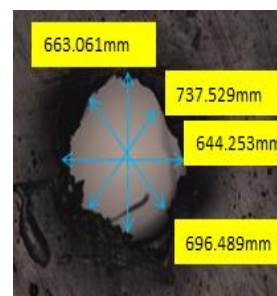
18



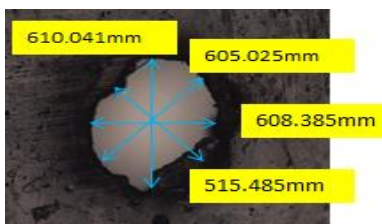
19



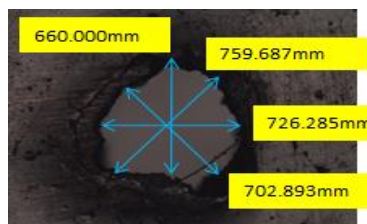
20



21



22



23



24

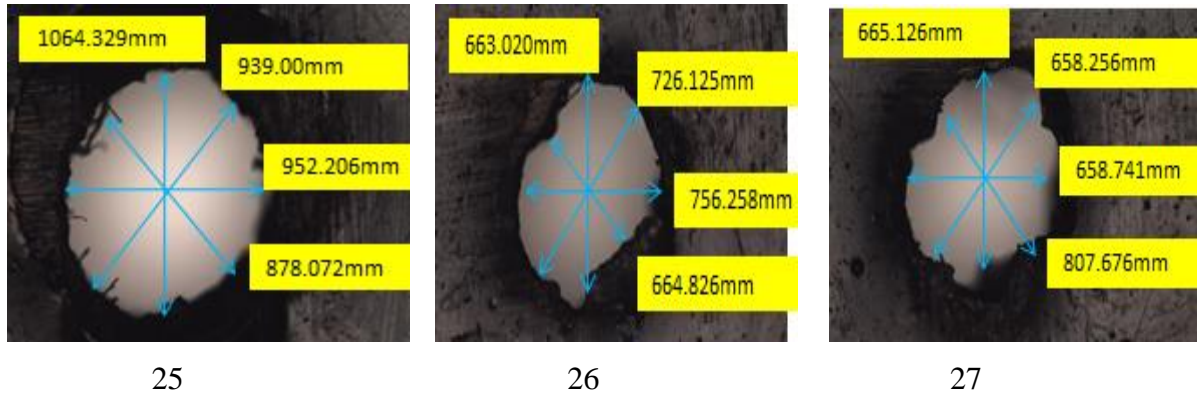


Fig. 6.6: Bottom side Image of holes (27 Nos.) obtained from optical microscope for BFRP composite

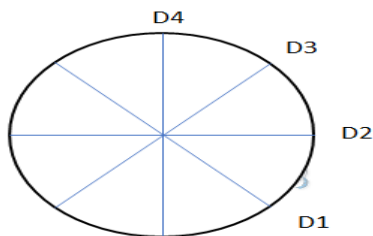
Three drilling parameter has been considered with their level as listed in Table 6.1. Further conduction of experiment has been performed on the basis of Box Behnken design. There are 27 no. of experiments have been performed as per design of experiment.

Table 6.1: Values of THC with parameters setting

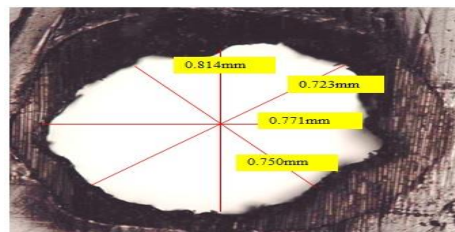
Exp. no.	(I) Amp	(f) Hz	(p) Kg/cm <sup>2</sup>	D1	D2	D3	D4	Top side hole Circularity (THC)
1	160	20	8	750.216	771.053	723.622	814.686	0.833028
2	160	20	9	747.120	750.096	668.623	778.302	0.857806
3	160	20	10	828.196	720.056	734.173	819.712	0.889250
4	160	25	8	903.121	725.521	878.268	747.476	0.829250
5	160	25	9	753.054	705.594	670.552	835.105	0.823444
6	160	25	10	663.061	723.006	759.480	807.602	0.824306
7	160	30	8	765.212	765.024	698.175	729.932	0.903139
8	160	30	9	786.006	771.093	706.938	738.524	0.866750
9	160	30	10	753.548	765.006	662.527	816.248	0.837028
10	180	20	8	786.006	657.007	709.86	811.243	0.843306
11	180	20	9	759.095	618.007	585.512	695.696	0.876333
12	180	20	10	791.557	786.599	779.746	807.006	0.916028
13	180	25	8	786.006	651.062	702.698	774.633	0.835778
14	180	25	9	849.132	855.047	707.014	891.449	0.838222

15	180	25	10	894.005	788.717	810.25	899.53	0.847333
16	180	30	8	932.516	1005.018	851.588	954.32	0.905917
17	180	30	9	849.123	939.153	905.806	811.626	0.877778
18	180	30	10	1011.04	1026.11	955.505	1082.173	0.856306
19	200	20	8	963.019	1020.11	1048.628	860.77	0.868250
20	200	20	9	888.046	867.125	864.526	886.803	0.909528
21	200	20	10	873.082	954.005	880.552	950.437	0.957472
22	200	25	8	861.021	903.005	738.232	879.957	0.856972
23	200	25	9	939.236	957.118	810.25	916.45	0.867667
24	200	25	10	859.007	837.453	783.115	905.925	0.885028
25	200	30	8	981.165	993.005	897.797	1003.765	0.894000
26	200	30	9	990.23	992.85	998.56	998.231	0.896000
27	200	30	10	964.125	982.156	963.128	923.125	0.882000

The Hole Circularity (HC) is calculated from equation (3.1). Top side hole and bottom side have been analysed by measuring four diameters and Hole Taper (HT) have been calculated by the equation (3.2) as shown in Table 6.1 and Table 6.2



(a) Schematic measurement of Hole diameter



(b) Actual measurement

Fig.6.7: (a) & (b): Presentation of the measurement

Table 6.2: Values of BHC with parameters setting

Exp. no.	(I) Amp	(f) Hz	(p) Kg/cm <sup>2</sup>	D1	D2	D3	D4	Bottom side hole Circularity (BHC)
1	160	20	8	717.100	659.830	750.832	683.065	0.8780
2	160	20	9	558.22	626.099	622.047	652.126	0.8560
3	160	20	10	608.229	617.029	685.507	583.367	0.8510

4	160	25	8	708.057	717.025	768.492	660.523	0.8590
5	160	25	9	638.000	693.270	614.082	606.057	0.8742
6	160	25	10	702.061	589.500	630.300	572.882	0.8160
7	160	30	8	508.025	590.505	600.722	567.683	0.9450
8	160	30	9	723.224	681.500	669.128	601.808	0.8321
9	160	30	10	560.208	456.010	551.526	551.354	0.8140
10	180	20	8	625.264	558.506	705.16	528.724	0.8456
11	180	20	9	460.256	453.040	486.157	495.558	0.9142
12	180	20	10	642.645	530.568	612.618	587.640	0.8256
13	180	25	8	630.726	534.303	642.577	580.620	0.8315
14	180	25	9	747.000	687.007	823.170	647.007	0.7859
15	180	25	10	750.054	732.025	842.936	676.846	0.8034
16	180	30	8	666.734	653.054	821.94	630.064	0.945
17	180	30	9	855.021	804.504	870.248	767.965	0.8824
18	180	30	10	873.046	858.000	853.488	996.250	0.8567
19	200	20	8	788.387	726.000	684.132	698.175	0.868
20	200	20	9	699.046	747.52	761.919	697.918	0.916
21	200	20	10	663.061	737.529	644.253	696.489	0.925
22	200	25	8	610.041	605.025	608.385	515.485	0.845
23	200	25	9	660.000	759.687	726.285	702.893	0.8687
24	200	25	10	885.020	807.006	886.727	766.035	0.8655
25	200	30	8	1064.329	939	952.206	878.072	0.825
26	200	30	9	663.020	726.125	756.258	664.826	0.8767
27	200	30	10	665.126	658.256	658.741	807.676	0.815

---

The variations of measured values of both top side hole circularity (THC), bottom side hole circularity (BHC) are shown in Fig. 6.8 respectively

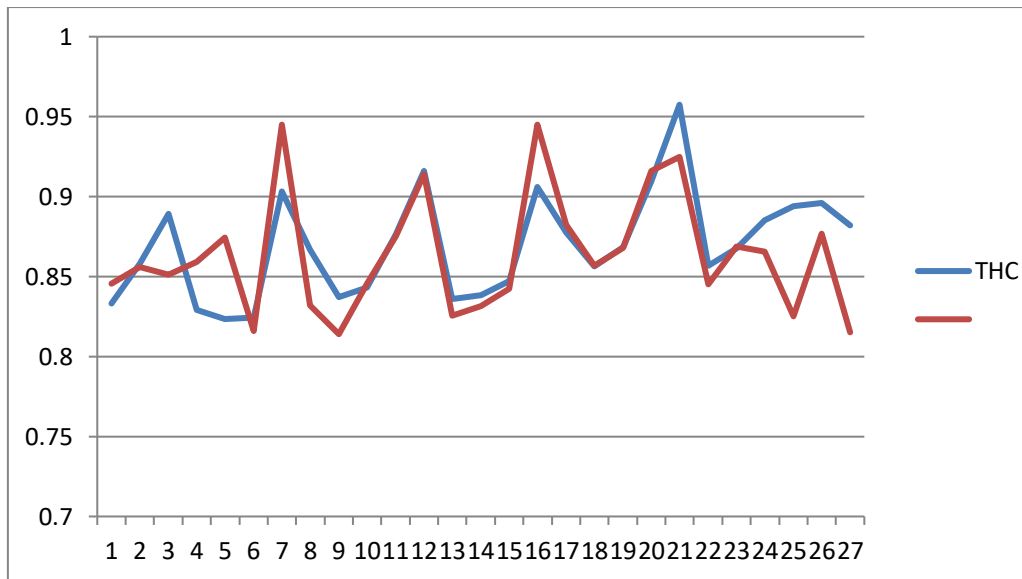


Fig.6.8: Variation of THC and BHC for all experiments

In the present work, those areas which are not melted during laser machining called as HAZ but it gives effect on the microstructures. Moreover, the measurement of HAZ has been listed in Table 6.3.

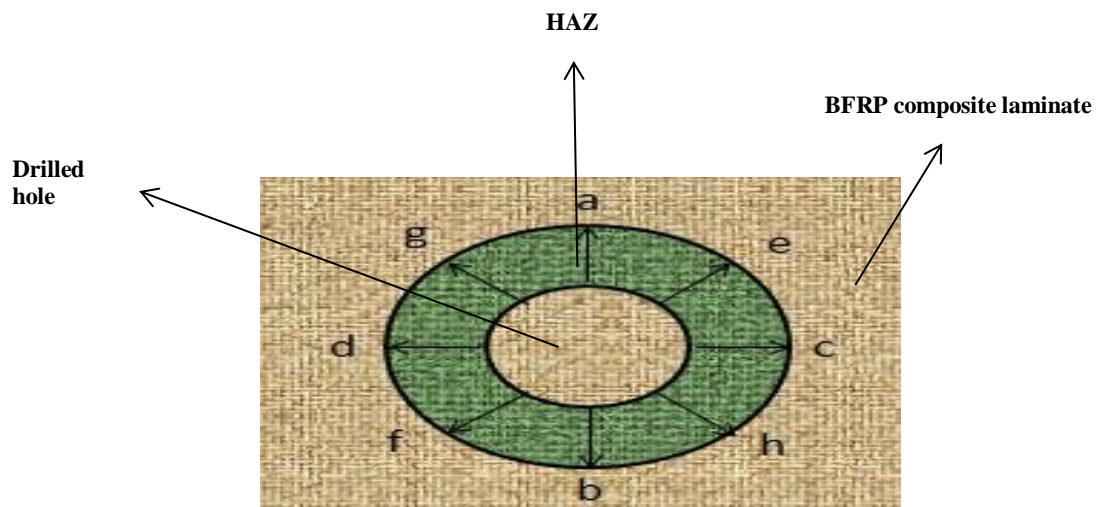


Fig.6.9: Measurement of HAZ



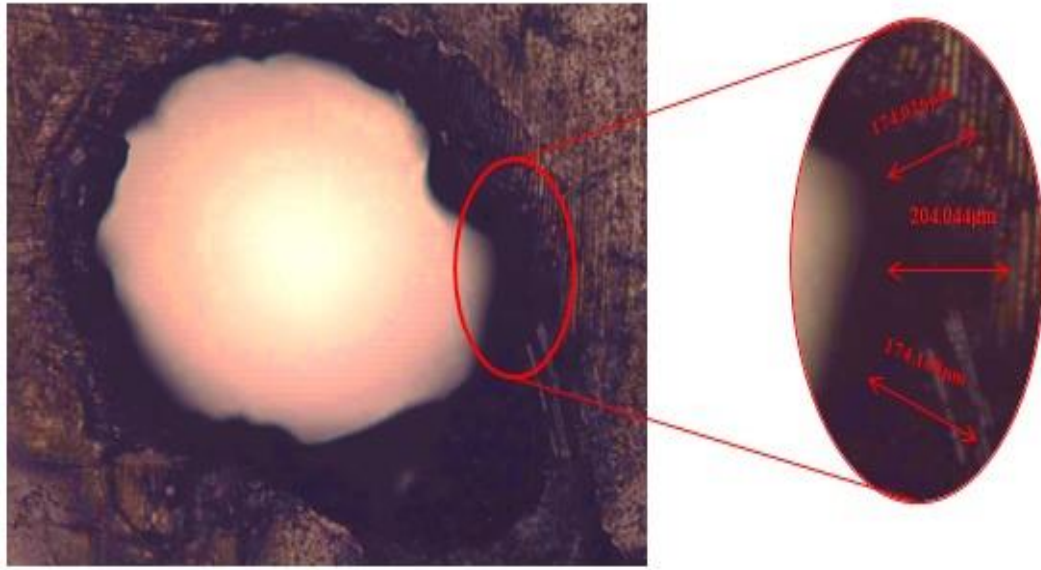


Fig.6.10: Representation of HAZ at  $(I) = 200$  amp,  $(f) = 25$  Hz, and  $(p) = 8$  bar

Table.6.3: The measured values of HAZ

Exp. no.	$(I)$ Amp	$(f)$ Hz	$(p)$ Kg/cm <sup>2</sup>	a	b	c	d	e	f	G	h
1	160	20	8	126.036	153.029	123.000	90.06	205.801	95.718	96.047	285.804
2	160	20	9	102.044	156.12	210.021	510.009	144.499	318.459	169.307	106.066
3	160	20	10	132.034	279.26	276.016	237.21	129.035	161.471	133.220	105.000
4	160	25	8	75.060	51.088	198.231	204.42	292.865	103.966	51.614	73.239
5	160	25	9	240.075	183.025	255.123	1440.31	162.111	204.749	148.219	320.003
6	160	25	10	45.100	219.021	90.123	159.028	112.61	110.635	120.934	258.94
7	160	30	8	300.00	159.000	129.035	120.000	195.000	106.532	434.337	106.066
8	160	30	9	195.023	126.000	126.000	108.706	138.683	111.606	228.079	223.185
9	160	30	10	285.000	141.032	369.11	111.606	636.255	82.377	287.640	280.750
10	180	20	8	474.038	219.021	387.012	171.604	183.221	84.906	190.541	198.120
11	180	20	9	120.000	210.086	141.000	284.542	169.759	133.963	162.25	168.520
12	180	20	10	123.037	216.021	246.018	206.303	180.624	104.957	124.02	125.120
13	180	25	8	66.068	174.774	136.029	137.379	133.963	218.403	165.952	162.230
14	180	25	9	159.000	84.054	265.377	99.905	74.518	87.207	159.000	162.120
15	180	25	10	135.030	147.000	148.219	116.499	237.171	85.802	135.03	132.12
16	180	30	8	261.017	99.045	144.000	141.000	156.461	109.859	267.825	267.31
17	180	30	9	252.018	246.079	141.000	573.07	334.56	145.245	76.026	78.198

18	180	30	10	192.023	309.000	111.041	274.201	213.654	175.571	179.72	182.45
19	200	20	8	132.034	183.098	141.000	156.605	184.203	174.026	204.044	174.168
20	200	20	9	171.026	183.000	147.000	139.201	96.607	170.816	141.51	142.16
21	200	20	10	87.000	249.018	186.097	164.454	136.029	147.275	232.166	236.12
22	200	25	8	132.034	189.095	150.120	106.405	129.835	121.491	171.421	178.152
23	200	25	9	192.054	234.077	174.103	228.650	115.256	183.663	346.263	128.16
24	200	25	10	114.039	208.969	215.520	240.468	405.278	214.348	276.065	270.132
25	200	30	8	327.000	246.018	210.021	238.948	220.229	97.350	498.443	240.121
26	200	30	9	132.034	183.098	141.000	156.605	184.203	174.026	204.044	132.15
27	200	30	10	171.026	183.000	147.000	139.201	96.607	170.816	141.51	141.123

**Table 6.4:** Measured values of all Hole Quality Characteristics.

Exp. no.	( <i>I</i> ) <i>Amp</i>	( <i>f</i> ) <i>Hz</i>	( <i>p</i> ) <i>kg/cm<sup>2</sup></i>	Hole circularity	Hole Taper(degree)	HAZ (micron)
1	160	20	8	0.833028	1.52917	141.379
2	160	20	9	0.857806	1.53278	154.954
3	160	20	10	0.889250	1.52972	179.804
4	160	25	8	0.829250	1.53667	128.783
5	160	25	9	0.823444	1.54111	140.373
6	160	25	10	0.824306	1.53889	163.239
7	160	30	8	0.903139	1.54083	146.472
8	160	30	9	0.866750	1.54611	156.079
9	160	30	10	0.837028	1.54472	176.960
10	180	20	8	0.843306	1.52750	147.198
11	180	20	9	0.876333	1.53111	151.545
12	180	20	10	0.916028	1.52806	167.167
13	180	25	8	0.835778	1.53000	132.177
14	180	25	9	0.838222	1.53444	134.539
15	180	25	10	0.847333	1.53222	148.177
16	180	30	8	0.905917	1.52917	147.442
17	180	30	9	0.877778	1.53444	147.820

18	180	30	10	0.856306	1.53306	159.473
19	200	20	8	0.868250	1.52250	152.825
20	200	20	9	0.909528	1.52611	147.943
21	200	20	10	0.957472	1.53000	145.231
22	200	25	8	0.856972	1.51000	131.231
23	200	25	9	0.867667	1.51000	121.456
24	200	25	10	0.885028	1.51000	134.231
25	200	30	8	0.894000	1.52000	156.231
26	200	30	9	0.896000	1.53000	123.561
27	200	30	10	0.882000	1.52000	141.561

## 6.3 Optimization Technique

In this study PSO method has been employed to identify the suitable values of input factors to maximize hole circularity and minimize the HT and HAZ during LBD of BFRP sheet.

### 6.3.1 PSO Approach

All the measured data has been evaluated on the basis of three important phases, first for generation of particles second for velocity and its position and the last one is velocity information and its final updated position.

### 6.3.2 Result and Discussion

In the recent research, a model has been created with the help of RSM of Hole Circularity, Hole Taper and Heat-Affected Zone. Further it will be converted in to coded terminology. The coded equation has been given as eq. (6.1-6.3).

$$I_{\text{Coded}} = \frac{I-180}{20} \quad (6.1)$$

$$F_{\text{Coded}} = \frac{f-25}{5} \quad (6.2)$$

$$P_{\text{Coded}} = \frac{p-9}{1} \quad (6.3)$$



Table 6.5: ANOVA for HC

Source	DF	SS	MS	F	P
Model	9	0.027779	0.003087	158.21	0.000
Linear	3	0.007846	0.002615	134.06	0.000
I	1	0.006919	0.006919	354.68	0.000
F	1	0.000057	0.000057	2.93	0.105
P	1	0.000870	0.000870	44.57	0.000
Square	3	0.008084	0.002695	138.13	0.000
I <sup>2</sup>	1	0.000140	0.000140	7.17	0.016
f <sup>2</sup>	1	0.007919	0.007919	405.90	0.000
p <sup>2</sup>	1	0.000026	0.000026	1.32	0.266
2-Way	3	0.011848	0.003949	202.44	0.000
Interaction					
I*f	1	0.000676	0.000676	34.66	0.000
I*p	1	0.001202	0.001202	61.62	0.000
f*p	1	0.009970	0.009970	511.04	0.000
Error	17	0.000332	0.000020		
Total	26	0.028111			
R-Square	98.82%				

$$\begin{aligned} \text{Hole circularity} = & 1.254 - 0.00599 \times I - 0.00762 \times f + 0.0237 \times p + 0.000012 \times I \times I + 0.001453 \times f \times f \\ & + 0.00207 \times p \times p - 0.000075 \times I \times f + 0.000500 \times I \times p - 0.005765 \times f \times p \end{aligned} \quad (6.4)$$

Table 6.6: ANOVA for HT

Source	DF	SS	MS	F	P
Model	9	0.001948	0.000216	8.50	0.000
Linear	3	0.001566	0.000522	20.49	0.000
I	1	0.001447	0.001447	56.80	0.000
f	1	0.000095	0.000095	3.74	0.070
p	1	0.000024	0.000024	0.95	0.344
square	3	0.000185	0.000062	2.42	0.102
I <sup>2</sup>	1	0.000032	0.000032	1.25	0.280

$f^2$	1	0.000087	0.000087	3.42	0.082
$p^2$	1	0.000066	0.000066	2.59	0.126
2-Way	3	0.000197	0.000066	2.58	0.088
Interaction					
I*f	1	0.000197	0.000197	7.73	0.013
I*p	1	0.000000	0.000000	0.00	0.963
f*p	1	0.000000	0.000000	0.00	0.963
Error	17	0.000433	0.000025		
Total	26	0.002381			
R-Square	81.81%				

$$\begin{aligned} \text{Taper angle} = & 1.050 + 0.00260 \times I + 0.00025 \times f + 0.0606 \times p - 0.000006 \times I \times I + 0.000152 \times f \times f \\ & - 0.00332 \times p \times p - 0.000041 \times I \times f + 0.000003 \times I \times p - 0.000014 \times f \times p \end{aligned} \quad (6.5)$$

Table 6.7: ANOVA for HAZ

Source	DF	SS	MS	F	P
Model	9	5181.83	575.76	29.43	0.000
Linear	3	2022.19	674.06	34.45	0.000
I	1	994.18	994.18	50.82	0.000
f	1	58.48	58.48	2.99	0.102
P	1	969.53	969.53	49.56	0.000
square	3	1797.05	599.02	30.62	0.000
$I^2$	1	15.32	15.32	0.78	0.389
$f^2$	1	1402.82	1402.82	71.71	0.000
$p^2$	1	378.91	378.91	19.37	0.000
2-Way	3	1362.58	454.19	23.22	0.000
Interaction					
I*f	1	65.43	65.43	3.34	0.085
I*p	1	1253.26	1253.26	64.06	0.000
f*p	1	43.90	43.90	2.24	0.152
Error	17	332.58	19.56		
Total	26	5514.41			
R-Square	93.97%				

$$HAZ = 20 + 6.25 \times I - 23.30 \times f - 34.2 \times p - 0.00399 \times I \times I + 0.6116 \times f \times f + 7.95 \times p \times p - 0.0233 \times I \times f - 0.5110 \times I \times p - 0.383 \times f \times p \quad (6.6)$$

- **PSO based Multi-Objective Optimization**

This report has been presented the PSO-based multi-objective optimization method to determine suitable values for drilling parameters. For better result, maximize hole circularity and minimize HAZ and hole taper during drilling of BFRP composite laminate. PSO based multi-objective optimization technique are given below:

First prepare the main objective function (Z) given in equation 6.7 by considering the mathematical model equation for HC, HAZ and HT as calculated by Equation. 6.4, 6.5 and 6.6.

$$Z = \left[ \frac{W_1 \times HC}{HC_{(max)}} \right] + \left[ \frac{W_2 \times HAZ}{HAZ_{(min)}} \right] + \left[ \frac{W_3 \times HT}{HT_{(min)}} \right] \quad (6.7)$$

Where,  $W_1(0.3)$ ,  $W_2(0.3)$  and  $W_3(0.4)$  has been considered as weights for RSM models of HC, HAZ and HT respectively. Whereas  $HC_{(max)}$ ,  $HAZ_{(min)}$  and  $HT_{(min)}$  are denoted by the maximum, minimum values of HC, HAZ and minimum value of HT models.

$$Z = 0.825783 + 0.013494 \times I - 0.06073 \times f - 0.06036 \times p - 0.0000034 \times I \times I + 0.002163 \times f \times f + 0.019747 \times p \times p - 0.000099 \times I \times f - 0.00105 \times I \times p - 0.0034 \times f \times p \quad (6.8)$$

PSO based multi-objective optimization method has been considered to solve unconstrained problem by developing MATLAB codes. In this report, 30 number of population of particles has been taken for as 30 for laser drilling factors. The operating range of 3drilling parameters was  $160 \leq A \leq 200$ ,  $20 \leq B \leq 30$  and  $8 \leq D \leq 10$ . The given weight for HC, HAZ and HT model was 0.3, 0.3 and 0.4, respectively. Table 6.8 represented the optimum value for the HC, HAZ and HT. Fig.6.11 represented values of combined Z function for all 25 populations of particles.

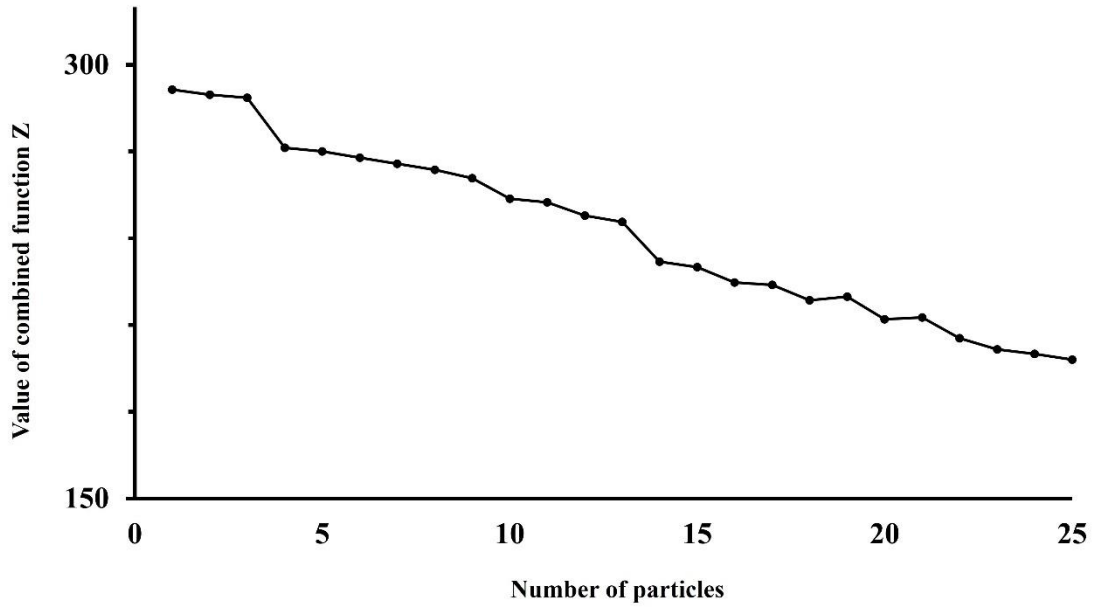


Fig. 6.11: Variation in Z versus number of particles

Table 6.8: Optimum values obtained by PSO Method

Combined function	Optimal parametric combination			Responses		
	I (A)	f (C)	p (D)	HC	HAZ	HT
Z	192.80 Amp	29.35 Hz	8.24 kg/cm <sup>2</sup>	0.94	118.02 micron	1.28°

Moreover, the model calculated values of all hole quality characteristics by using optimum levels of drilling parameters achieved by PSO, and RMS are Tabulated in Table 6.9. The Comparison of optimum value of Z for PSO versus RSM is represented by Fig.6.12, Which has been represented that the optimum result obtained by PSO is more reliable in comparison to RSM.

Table 6.9: Different optimum values obtained of Z for PSO and RSM

Exp.No.	PSO	RSM
1	291.4	405.6
2	289.65	401.23
3	288.65	387.65
4	271.34	384.2
5	270.1	381.65

6	267.9	376.2
7	265.8	365.23
8	263.65	364.2
9	260.75	350.87
10	253.64	350.2
11	252.46	345.7
12	247.88	342.8
13	245.68	339.65
14	231.87	336.56
15	229.98	331.5
16	224.68	329.8
17	223.87	326.98
18	218.6	322.4
19	219.8	321.8
20	211.98	317.5
21	212.67	312.88
22	205.45	301.89
23	201.6	299.86
24	199.99	288.46
25	198.08	275.56
26	197.02	265.8
27	196.24	251.24

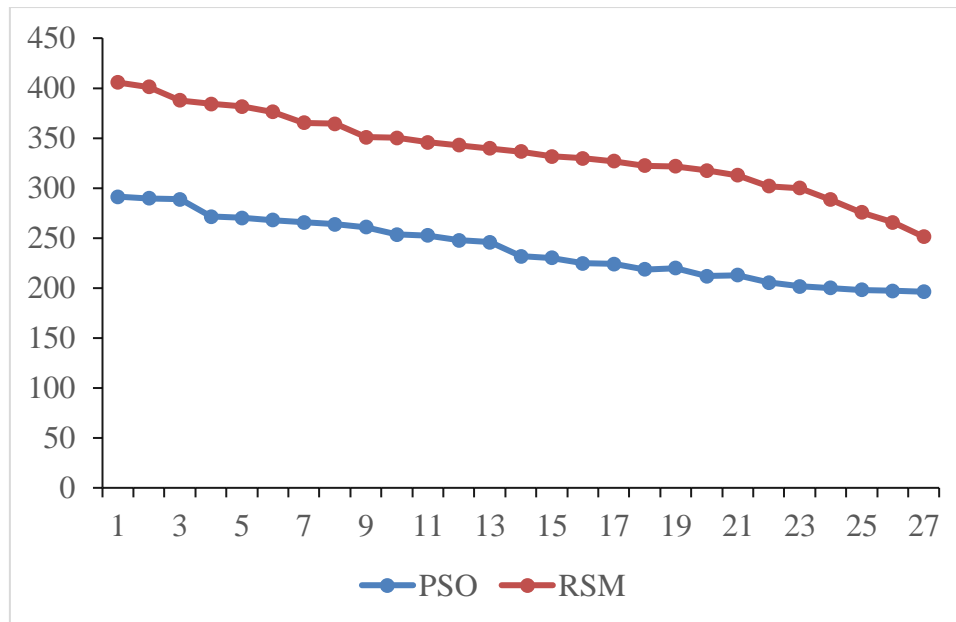


Fig.6.12: Comparison of optimum value of Z for PSO versus RSM

### 6.3.3 Conclusion

The Following observations have been discussed in this chapter.

1. RSM Based Box- Behnken Design (BBD) and PSO two different multi-response optimization techniques have been successfully employed to identify the optimal drilling values of input parameters.
2. The optimum operating value has been identified for BFRP composite as lamp current at 192.80 Amp, pulse frequency at 29.35 Hz, air pressure at 8.24 Kg/cm<sup>2</sup>.
3. The output response on optimum drilling condition will be as Hole Circularity 0.94; Heat Affected Zone (HAZ) 118.02 mm and Hole Taper are found 1.28 degree.
4. The optimum result obtained by PSO is more reliable in comparison to RSM.
5. The contribution of this research will provide the benefits of better quality products of high precision with geometrical accuracy to the modern industries.

## 6.4 Summary

In this chapter, Evaluation of Hole Quality Characteristics in Laser Drilling of BFRP Composite Using Multi-Response Optimization Technique has been discussed. The suggested optimum operating value for BFRP composite are found as (I) at 192.80 Amp, (f) at 29.35 Hz, (p) at 8.24 kg/cm<sup>2</sup>. The output response on optimum drilling condition will be as HC = 0.94, HAZ =118.02 micron and HT are found 1.28 degree. Finally, in the next chapter

general conclusions drawn from the analysis carried out in the present thesis and scope of future works are summarized.

# Chapter 7

## Conclusions and Scope of Future Work

### 7.1 Conclusions

A systematic experimental study on novel KFRP, BFRP and their hybrid KBFRP composite have been conducted in this work. Multiple optimization techniques have been used to identify the optimal range of laser drilling parameters to minimize different hole quality characteristics simultaneously.

Following conclusions have been drawn in this thesis.

1. Pulsed Nd:YAG laser drilling 1.20 mm thick KFRP composite, 1.20 mm thick hybrid KBFRP composite and 1.20 mm thick BFRP composite has been successfully performed.
2. The accuracy of hole quality is quantified in the terms of Top Hole Circularity (THC), Bottom Hole Circularity (BHC), Hole Taper (HT) and Heat Affected Zone (HAZ).
3. Three different multi-response optimization techniques such as Taguchi, Response Surface Method (RSM) Based on Box-Behnken Design (BBD) and Particle Swarm Optimization (PSO) have been well employed to identify the optimal drilling condition.
4. The suggested suitable operating values for KFRP composite are found as; lamp current (I) at 160 Amp, pulse frequency (f) at 20 Hz and air pressure (p) at 10 Kg/cm<sup>2</sup>.
5. The suggested optimum operating value for hybrid KBFRP composite are found as; lamp current (I) at 200 Amp, pulse frequency (f) at 20Hz and air pressure (p) at 8 Kg/cm<sup>2</sup>.
6. The suggested optimum operating value for BFRP composite are found as lamp current (I) at 192.80 Amp, pulse frequency (f) at 29.35 Hz, air pressure (p) at 8.24 Kg/cm<sup>2</sup>.
7. The output response on optimum drilling condition will be as Hole Circularity (HC) = 0.94, Heat Affected Zone (HAZ) =118.02 mm and Hole Taper (HT) are found 1.28 degree.
8. In the laser drilling of KFRP sheet, lamp current has been found as the highly influencing factor for Top Hole Circularity (THC) and Bottom Hole Circularity (BHC). Whereas, Air pressure (p) has less influencing factor in Laser Beam Drilling of KFRP sheet.



9. Air pressure ( $p$ ) has been found the high influencing factor for the Hole Taper (HT) while pulse frequency ( $f$ ) less influencing factor in Laser Beam Drilling of KFRP sheet.
10. It has been examined that lower values of pulse frequency ( $f$ ), air pressure ( $p$ ) and higher value of lamp current ( $I$ ) are able to improve the quality of hybrid KBFRP sheet.
11. Pulse frequency and air pressure ( $p$ ) have been found the high influencing factor for the hole circularity (HC) while lamp current less influencing factor in Laser Beam Drilling of KBFRP sheet.
12. The result of this research will be directly associated with modern industries for manufacturing the better quality product with high geometrical accuracy.

## **7.2 Scope of Future Work**

1. More Laser parameters such as spot diameter, laser power, standoff distance, assist gas type etc can be selected as variable process parameters in further research.
2. The analysis can be done further such as surface irregularities, Material Removal Rate etc.
3. Curved profile drilling of FRP composites with varying thickness may be considered for future investigation.
4. Laser drilling of FRP hybrid composite materials fabricated by using different stacking sequence will also be an area of research in future.
5. Employed multi-response optimization techniques in present research work can also be implemented in other Laser Beam Machining (LBM) such as laser percussion drilling, laser trepanning and laser milling etc. to enhance their performance.

## References

- [1] D. Bhattacharyya, M. N. Allen, and S. J. Mander, "Cryogenic Machining of Kevlar Composites," *Materials & Manufacturing Processes*, vol. 8, no. 6, pp. 631-651, 1993.
- [2] V. Dhand, G. Mittal, K. Y. Rhee, and D. Hui, "A Short Review on Basalt Fiber-Reinforced Polymer Composites," *Composites Part B*, vol. 73, pp. 166-180, 2015.
- [3] RangaKomanduri, "Machining Fiber-Reinforced Composites," *Mechanical engineering*, vol. 115, no. 4, pp. 58-64, 1993.
- [4] S. Madhu and M. Balasubramanian, "Inuence of Nozzle Design and Process Parameters on Surface Roughness of CFRP Machined By Abrasive Jet," *Materials and Manufacturing Processes*, vol. 32, no. 9, pp. 1011-1018, 2017.
- [5] R. Selvam, L. Karunamoorthy, and N. Arunkumar, "Investigation on Performance of Abrasive Water Jet in Machining Hybrid Composites," *Materials and Manufacturing Processes*, vol. 32, no. 6, pp. 700-706, 2017.
- [6] J. Meijer, "Laser Beam Machining ( LBM ) State of the Art and New Opportunities," *Journal of Materials Processing Technology*, vol. 149, pp. 2-17, 2004.
- [7] A. K. Dubey and V. Yadava, "Experimental Study of Nd: YAG Laser Beam Machining - An Overview," *Journal of Materials Processing Technology*, vol. 195, no. 1-3, pp. 15-26, 2008.
- [8] A. A. Cenna and P. Mathew, "Evaluation of Cut Quality of Fiber-Reinforced Plastics- A Review," *International Journal of Machine Tools & Manufacturing*, vol. 37, no. 6, pp. 723-736, 1997.
- [9] A. Dubey and V. Yadava, "Laser Beam Machining - A Review," *International Journal of Machine Tools and Manufacture*, vol. 48, pp. 609-628, 2008.
- [10] E. Carpene, D.Hoche and P. Schoaf, " Fundamentals of Laser Material Interaction," *Laser Materials Processing*, vol. 3, pp. 21-47, 2010.
- [11] H. Haken,"*Light-Laser Light Dynamics*". North Holland Physics Publishing, Amsterdam, vol. 2, 1985.
- [12] B. Hitz, J. J. Ewing, and J. Hecht, "Introduction to Laser Technology," IEEE press, ISBN: 0-7803-5373-0, 2001.
- [13] S. Martellucci, A. Chester, and A. Scheggi, "Laser Applications for Mechanical Industry," Dordrecht, Netherlands : Springer Science Business Media, B.V.ISBN: 94-010-4879-7, 1992.

- [14] P. Wirth, "Introduction to Industrial Laser Materials Processing," tech. rep. Ro n, 2004.
- [15] N. Dahotre and S. Harimkar, "Laser Fabrication And Machining of Materials," Springer, ISBN 978-0-387-72343-3, 2008.
- [16] A. Schawlow and C. Townes, "Infrared and Optical Masers," Physical Review, vol. 112 (6), pp. 1940-1949, 1957.
- [17] T. Maiman, "Simulated Optical Radiation in Ruby," Nature, vol. 187, pp. 493- 494, 1960.
- [18] A. Javan, W. Bennett, and D. Herriott, "Population Inversion And Continuous Optical Maser Oscillation in a Gas Discharge Containing a He-Ne Mixture," Physical Review Letters, vol. 6, no. 3, pp. 106-110, 1961.
- [19] W. Steen and J. Mazumder, "Laser Material Processing," Springer, ISBN: 978-1-84996-062-5, 2010.
- [20] C. Webb and J. Jones, "Handbook of Laser Technology and Applications," Tylor and Francis, vol.1, ISBN9780429183515, 2004.
- [21] W. Steen, "Laser Material Processing-An Overview," Journal of Optics A:Pureand Applied Optics, vol. 5, pp. S3-S7, 2003.
- [22] G. Chryssolouris, G. Tsoukantas, K. Salonitis, P. Stavropoulos, and S. Karagiannis, "Laser Machining Modelling and Experimentation-An Overview," Proceedings of SPIE, vol. 5131, pp. 158-168, 2003.
- [23] J. D. Majumdar and I. Manna, "Laser Processing of Materials," Sadhana, vol. 28, no. 34, pp. 495-562, 2003.
- [24] V. V. Antsiferov and G. I. Smirnov, "Physics of Solid-State Lasers," Cambridge International Science Publishing, vol. 1, ISBN: 9781898326175, 2005.
- [25] G. Chryssolouris, "Laser Machining Theory and Practice," Springer Science Business Media, LLC, 1991.
- [26] G. D. Gautam and A. K. Pandey, "Pulsed Nd: YAG Laser Beam Drilling: A Review," Optics and Laser Technology, vol. 100, pp. 183-215, 2018.
- [27] M. Gross, I. Black, and W. Muller, "Determination of the Lower Complexity Limit for Laser," Modelling and Simulation in Materials Science and Engineering, vol. 12, pp. 1237-1249, 2004.
- [28] M. Jawaid and H. P. Abdul Khalil," Cellulosic/Synthetic Fibre Reinforced Polymer Hybrid Composites: A Review," Carbohydrate Polymers, vol. 86, no. 1, pp. 1-18, 2011.

- [29] A. Batista, S. Tino, R. Fontes, S. Nobrega, and E. Aquino, "Anisotropy and Holes in Epoxy Composite Reinforced By Carbon/Glass and Carbon/Aramid Hybrid Fabrics: Experimental and Analytical Results," *Composites Part B: Engineering*, vol. 125, pp. 9-18, 2017.
- [30] F. Sarasini, J. Tirillo, M. Valente, T. Valente, S. Cio, S. Iannace, and S. Luigi, "Effect of Basalt Fiber Hybridization on the Impact Behaviour Under 173 low Impact Velocity of Glass / Basalt Woven Fabric / Epoxy Resin Composites," *Composites Part A*, vol. 47, pp. 109-123, 2013.
- [31] A. K. Bandaru, S. Patel, Y. Sachan, S. Ahmad, R. Alagirusamy, and N. Bhatnagar, "Mechanical Behaviour of Kevlar/Basalt Reinforced Polypropylene Composites," *Composites Part A: Applied Science and Manufacturing*, vol. 90, pp. 642-652, 2016.
- [32] J. Xu, Y. Ma, Q. Zhang, T. Sugahara, Y. Yang, and H. Hamada, "Crashworthiness of Carbon Fiber Hybrid Composite Tubes Moulded by Filament Winding," *Composite Structures*, vol. 139, pp. 130-140, 2016.
- [33] J. H. Song, "Pairing Effect and Tensile Properties of Laminated High-Performance Hybrid Composites Prepared Using Carbon/Glass and Carbon/Aramid Fibers ," *Composites Part B: Engineering*, vol. 79, pp. 61-66, 2015.
- [34] A. Caggiano, "Machining of Fibre Reinforced Plastic Composite Materials," *Materials*, vol. 11, pp. 442-461, 2018.
- [35] S. Tandon, V. K. Jain, P. Kumar, and K. Rajurkar, "Investigations into Machining of Composites," *Precision Engineering*, vol. 12(4), pp. 227-238, 1990.
- [36] V. Fiore, T. Scalici, G. D. Bella, and A. Valenza, "A Review on Basalt Fibre And Its Composites," *Composites Part B*, vol. 74, pp. 74-94, 2015.
- [37] A. Ross, "Basalt Fibers: Alternative to Glass?," *Composites Technology*, vol. 12(4), pp. 44-48, 2006.
- [38] V. Lopresto, C. Leone, and I. D. Iorio, "Mechanical Characterization of Basalt Fibre Reinforced Plastic," *Composites Part B*, vol. 42(4), pp. 717-723, 2011.
- [39] D. Pavlovski, B. Mislavsky, and A. Antonov, "CNG Cylinder Manufacturers Test Basalt Fibre," *Reinforced Plastics*, vol. 51(4), pp. 36-39, 2007.
- [40] S. Raj, V. R. Kumar, B. H. B. Kumar, S. Gopinath, and N. R. Iyer, "Flexural Studies on Basalt Fiber Reinforced Composite Sandwich Panel With Profile Sheet As Core," *Construction And Building Materials*, vol. 82, pp. 391-400, 2015.
- [41] S.O. Lee, K. Yop, and S.J. Park, "Influence of Chemical Surface Treatment of Basalt Fibers on Inter laminar Shear Strength and Fracture Toughness of Epoxy- Based

- Composites," *Journal of Industrial and Engineering Chemistry*, vol. 32, pp. 153-156, 2015.
- [42] C. Wang, W. Ming, Q. An, and M. Chen, "Machinability Characteristics Evolution of CFRP in a Continuum of Fiber Orientation Angles," *Materials and Manufacturing Processes*, vol. 32(9), pp. 1041-1050, 2017.
- [43] T. Srinivasan, K. Palanikumar, K. Rajagopal, and B. Latha, "Optimization of Delamination Factor in Drilling GFR-Polypropylene Composites," *Materials and Manufacturing Processes*, vol. 32(2), pp. 226-233, 2017.
- [44] R. Komanduri, "Machining of Fiber- Reinforced Composites," *Machining Science and Technology: An International Journal*, vol. 1(1), pp. 113-152, 1997.
- [45] H. Akshay, S. Dilpreet, K. Sagar, K. Dinesh, and G. Suhasini, "Machining Damage in FRPs Laser Versus Conventional Drilling," *Composites Part A*, vol. 82, pp. 42-52, 2015.
- [46] Ross. PJ., *Taguchi Techniques for Quality Engineering*. McGraw-Hill, New York, 1988.
- [47] Faisal N,Zindani D, Kumar K, Bhowmik S," Laser Micromachining of Engineering Materials—A Review," *Micro and Nano Machining of Engineering Materials: Recent Developments* , Springer , pp. 121–36.2019.
- [48] R.K. Roy," Design of experiments using the Taguchi approach: 16 steps to product and process improvement", New York: Wiley,2001.
- [49] Herzog. D, Jaeschke. P, Meier. O, Haferkamp. H," Investigations on The Thermal Effect Caused By Laser Cutting With Respect to Static Strength of CFRP," *International Journal of Machine Tool and Manufacture*, vol.48(12) , pp.1464–73,2008.
- [50] Li ZL, Zheng HY, Lim GC, Chu PL, Li L," Study on UV Laser Machining Quality of Carbon Fibre Reinforced Composites," *Composites Part A: Applied Science and Manufacturing* ,vol.41(10) ,pp.1403–8.2010.
- [51] Hejjaji.A, Singh.D, Kubher. S,Kalyanasundaram. D, Gururaja. S," Machining Damage In FRPs: Laser Versus Conventional Drilling," *Composites Part A: Applied Science and Manufacturing*, vol. 82, pp. 42–52, 2016.
- [52] Chan, C. and Mazumder," One-Dimensional Steady-State Model for Damage by Vaporization and Liquid Expulsion due To Laser-Material Interaction," *Journal of Applied Physics*, vol. 62, pp.4579, 1987.

- [53] C. F. Cheng, Y. C. Tsui, T. W. Clyne, “Application of A Three-Dimensional Heat Flow Model to Treat Laser Drilling Of Carbon Fiber”, *Composites, Acta Materialia*, vol. 46(12), pp.4273-4285, 1998
- [54] T.Young , D.O’ Driscoll, “Impact of Nd YAG laser drilled holes on the strength and stiffness of laminar flow Carbon Fiber Reinforced composite Panels”, *Composite: Part A*, vol.33, pp. 1-9.2009.
- [55] W.S.O. Rodden , S.S. Kudesia, D.P. Hand, J.D.C. Jones, “A Comprehensive Study of the Long Pulse Nd:YAG Laser Drilling of Multi-Layer Carbon Fiber Composites”, *Optics Communications*, vol. 210 , pp.319–328,2002
- [56] M. Dell’Erba, L.M. Galantucci and S. Miglietta,” An Experimental Study on Laser Drilling and Cutting of Composite Materials for The Aerospace Industry Using Excimer and CO<sub>2</sub> Sources,” *Composite Manufacturing*, vol.3(1), pp.14-19,1992.
- [57] E. Aoyama, H. Inoue, T. Hirogaki, H. Nobe, Y. Kitahara, T. Katayama, “Study on Small Diameter Drilling In GFRP”, *Composite Structures*, vol.32, pp.567-573.1995
- [58] T. Hirogaki, E. Aoyama, H. Inoue, K. Ogawa, S. Maeda, T. Katayama, “Laser Drilling Of Blind Via Holes in Aramid and Glass/Epoxy for Multilayer Printed Wiring Boards”, *Composite: Part A* , vol.32, pp.963-968,2001.
- [59] M. M. Noor, T. T. Mon, K. Kadirgama, M. R. M. Rejab, M. S. M. Sani, R. Rafizuan, W. A. W. Yusof, “ Drilling on Fibre-Glass Composite using CO<sub>2</sub> Laser ”, *International Conference on Advance Mechanical Engineering (ICAME09) Selangor*, 2009.
- [60] K. Ogawa, T. Hirogaki, E. Aoyama, K. Obata, T. Ayuzawa, “, Microvia Formation For Multi-Layer PWB By Laser Direct Drilling: Improvement of Hole Quality By Silica Fillers In Build-Up Layer”, *Proceedings of the ASME 2011 International Manufacturing Science and Engineering Conference* ,pp.1-10,2011.
- [61] K. Ogawa, T. Hirogaki, E. Aoyama, T. Ayuzawa ,” Microvia Formation For Multi-Layer PWB By Laser Direct Drilling: Improvement Of Drilled Hole Quality Of GFRP Plates”, *Proceedings of the ASME 2012 International Manufacturing Science and Engineering Conference*, pp. 1-6, 2012.
- [62] S. Nagesh, H. N. Narasimha Murthy , Ratna Pal, M. Krishna, B.S. Satyanarayana, “,Influence of Nano fillers On The Quality of CO<sub>2</sub> Laser Drilling in Vinylester / Glass Using Orthogonal Array Experiment Sand Grey Relational Analysis”, *Optics & Laser Technology*, vol.6, pp.23–33,2015.
- [63] Solati A, Hamedi M, Safarabadi M,” Combined GA-ANN Approach for Prediction of HAZ and Bearing Strength in Laser Drilling of GFRP Composite,” *Optics and Laser Technology*, vol.113,pp.104–15,2019.

- [64] T. Hirogaki, E. Aoyama, R. Minagi, K. Ogawa, T. Katayama, T. Matsuoka, H. Inoue, 2004, "Method for Cleaning Laser-Drilled Holes on Printed Wiring Boards by Plasma Treatment," *JSME International Journal, Series C*, vol.47(1), pp.105-110,2004.
- [65] E. Aoyama, T. Hirogaki, K. Ogawa, Nobuyuki DOI, R. Minagi, "Cu-Direct Via-Hole Drilling Of Aramid Fiber Reinforced Build-Up Layer By CO<sub>2</sub> Laser Beam", *Proceedings of IPACK2005, ASME Inter PACK '05*, July 17-22, San Francisco, California, USA, pp.1-8,2005.
- [66] K. Ogawa, T. Hirogaki, E. Aoyama, S. Maeda, H. Inoue, T. Katayama," Data Mining Of Factors Affecting Circuit Connection Reliability On Laser Drilled Micro Blind Via Holes In Multi-Layer PWBs", *JSME International Journal* ,vol.19(4), 522-528,2006.
- [67] Abrate S, "Machining of Composite Materials," *Composites Engineering Handbook*, vol 11, pp. 777–810, 1997.
- [68] Mathew J, Goswami G, Ramakrishnan N, Naik N.", *Parametric Studies on Pulsed Nd:YAG Laser Cutting of Carbon Fibre Reinforced Plastic Composites*",. *Journal of Materials Processing Technology*, pp. 198–203,1999.
- [69] Hocheng H, Tsao CC, "Comprehensive Analysis of Delamination In Drilling Of composite Materials with Various Drill Bits", *Journal of Material Processing Technology*,vol.140 (1), pp.335–9,2003.
- [70] Tsao CC, Hocheng H. " , Taguchi Analysis of Delamination Associated With Various Drill Bits In Drilling of Composite Material",. *International Journal of Machine Tool Manufacture*, vol. 44, 10, pp.90-1085,2004.
- [71] Davim JP, Rubio JC, Abrao AM. " , A Novel Approach Based on Digital Image Analysis to Evaluate the Delamination Factor after Drilling Composite Laminates", *Composites and Science Technology*, vol. 67(9), pp.1939–45,2007.
- [72] Gaugel S, Sripathy P, Haeger A, Meinhard D, Bernthaler T, Lissek F, "A Comparative Study on Tool Wears and Laminate Damage in Drilling of Carbon-Fiber Reinforced Polymers (CFRP)",*Composite Structures*,vol.155,pp.173–83,2016.
- [73] G.D. Gautam, D.R. Mishra, "Firefly Algorithm Based Optimization of Kerf Quality Characteristics in Pulsed Nd: YAG Laser Cutting of Basalt Fiber Reinforced Composite," *Composite. B*, vol.176, pp.1-15, 2019.
- [74] G.D. Gautam, D.R. Mishra, "Dimensional Accuracy Improvement by Parametric Optimization In Pulsed Nd: YAG Laser Cutting of Kevlar-29/Basalt Fiber reinforced

- Hybrid Composites”, *Journal of the Brazilian Society of Mechanical Sciences and Engineering*, vol. 41, pp. 284, 2019.
- [75] G. D. Gautam, D. R. Mishra,” Teaching Learning Algorithm Based Optimization of Kerf Deviations in Pulsed Nd:YAG Laser Cutting of Kevlar-29 Composite Laminates”, *FME Transactions*,vol.47, pp.560-575, 2019.
- [76] D. R. Mishra, G. D. Gautam, D. Prakash, A. Bajaj, A. Sharma, R. Bisht, S. Gupta,” Optimization of Kerf Deviations In Pulsed Nd:YAG Laser Cutting of Hybrid Composite Laminate Using GRA,” *FME Transactions*,vol.48, pp.109-116.2020.
- [77] G. D. Gautam, D. R. Mishra,” Parametric Investigation in Pulsed Nd:YAG Laser Cutting of Kevlar-Basalt Fiber Composite”, *Lasers in Manufacturing and Materials Processing*, Springer Nature, 2020.
- [78] K.K. Sharma, Y. Shrivastava, E. Neha, A. Jain, B Singh, “Evaluation of Flexural Strength of Hybrid FRP Composites Having Three Distinct Laminates,” *Materials Toady Proceedings*, vol.38, pp.418-422. 2021.
- [79] A. Jain, C.S. Kumar, Y. Shrivastava, “Fabrication and Machining of Fiber Matrix Composite through Electric Discharge Machining: A Short Review,” *Materials Toady Proceedings*,
- [80] A. Jain, B. Singh, Y. Shrivastava, “Reducing The Heat-Affected Zone During The Laser Beam Drilling of Basalt-Glass Hybrid Composite,” *Composite Part B: Engineering*, vol.176, no. 107294,2019
- [81] A. Jain, B. Singh, Y. Shrivastava, “Investigation of Kerf Deviations and Process Parameters During Laser Machining of Basalt Glass Hybrid Composite,” *Journal of Laser Applications*, vol.31, no. 032017-17, 2019.
- [82] A. Jain, B. Singh, Y. Shrivastava, “Heat-Affected Zone Investigation During The Laser Beam Drilling of Hybrid Composite Using Statistical Approach,” *Arabian Journal for Science and Engineering*, vol. 45 , pp.833–848, 2020.
- [83] A. Jain, B. Singh, Y. Shrivastava, “Analysis of Heat Affected Zone (HAZ) During Micro-Drilling of A New Hybrid Composite,” *Proceedings of The Institution of Mechanical Engineers, Part C: Journal of Mechanical Engineering Science*, pp. 1–15, 2019.
- [84] A. Jain, B. Singh, K. K. Sharma, Y. Shrivastava, “Fabrication, Testing and Machining of Hybrid Basalt-Glass Fiber Reinforced Plastic Composite,” *International Journal of Pure and Applied Physics*, vol. 59, pp.258–262, 2021.



- [85] R. Tewari, M.K. Singh, S. Zafar, S. Powar, "Parametric Optimization Of Laser Drilling Of Microwave-Processed Kenaf/HDPE Composite," *Polymers and Polymers Composite*, vol.29 (2021), pp. 176-187, 2021.
- [86] H. Jiang, C. Ma, M. Li, Z. Cao, "Femto Second Laser Drilling of Cylindrical Holes for Carbon Fiber-Reinforced Polymer (CFRP) Composites," *Molecules*, vol.26(10),pp.2953, 2021.
- [87] A.T. Erturk, E. Yarar, F. Vatansever, A.E. Sahin, M. Kiliçel, Y.O. Alpay, "A Comparative Study of Mechanical and Machining Performance of Polymer Hybrid and Carbon Fiber Epoxy Composite Materials," *Polymers and Polymers Composite*, vol. 29, pp.S655–S666, 2021
- [88] K. Giasin, M. Atif, Y. Ma, C. Jiang, U. Koklu, J. Sinke, "Machining GLARE Fibre Metal Laminates: A Comparative Study on Drilling Effect Between Conventional and Ultrasonic-Assisted Drilling," *International Journal of Advanced Manufacturing Technology*, vol.123, pp. 3657-3672, 2022.
- [89] P. Madhu, J. Praveenkumara, M.R. Sanjay, S. Siengchin, S. Gorbatyuk, "Introduction to Bio-Based Fibers and their Composites," *Advanced Bio-Based Fiber* , pp. 1-20, 2022.
- [90] Rampal , Gaurav Kumar , Sanjay Mavinkere Rangappa , Suchart Siengchin , Sunny Zafar , " A Review of Recent Advancements in Drilling of Fiber-Reinforced Polymer Composites, *Composites Part C: Vol.9*, pp. 100312,2022.

## List of Publication

1. Singh, K.P., Norkey, G., Gautam, G.D. (2021),” Parametric Optimization of Hole Quality in Laser Drilling Kevlar/Basalt Hybrid FRP Composite,” In: Parey, A., Kumar, R., Singh, M. (eds) Recent Trends in Engineering Design. Lecture Notes in Mechanical Engineering. Springer, Singapore. [https://doi.org/10.1007/978-981-16-1079-0\\_18](https://doi.org/10.1007/978-981-16-1079-0_18)
2. Singh, K.P.,Bahl.A, Norkey, G., Gautam, G.D. (2022),” Experimental investigation and parametric optimization of the hole-circularity and taper angle during laser drilling kevlar-29 fiber composite,” Materials Today Proceedings, Elsevier, Vol. 56, Part 6, pp.3325-3329, <https://doi.org/10.1016/j.matpr.2021.10.155>.
3. Singh, K.P.,Bahl.A,, Gautam, G.D., Norkey, G (2022),” Particle Swarm based Optimization of Hole Characteristics during Laser Drilling of BFRP,” NeuroQuantology,Vol.20(10),pp.32643276,<http://doi.org/10.14704/nq.2022.20.10.NQ55325>.

## **List of Conference**

1. International Conference on Advances in Sustainable Technologies (ICAST-2020) held on 6<sup>th</sup> to 7<sup>th</sup> November 2020 organized by School of Mechanical Engineering at Lovely Professional University, Jalandhar, Punjab.
2. 1<sup>st</sup> International Conference on Design and Materials (ICDM-2022) held on 27<sup>th</sup> to 30<sup>th</sup> January 2022organised at Delhi Technological University, Delhi, India.